AI Medicine
https://www.sciltp.com/journals/aim



Review

Research Progress on AI-Driven Biomarker Prediction in Non-Small Cell Lung Cancer

Baihua Zhang [1,2,*], Jing Teng [1,3] and Siyuan Lu [2]

[1] Research Institute for Medical and Biological Engineering, Ningbo University, Ningbo 315211, China
[2] School of Communications and Information Engineering, Nanjing University of Posts and Telecommunications, Nanjing 210003, China
[3] School of Basic Medical Sciences, Ningbo University, Ningbo 315211, China
*Correspondence: zhangbaihua@nbu.edu.cn

How To Cite: Zhang, B.; Teng, J.; Lu, S. Research Progress on AI-Driven Biomarker Prediction in Non-Small Cell Lung Cancer. *AI Medicine* **2026**, *3*(2), 11. https://doi.org/10.53941/aim.2026.100011

Received: 15 March 2026
Revised: 26 August 2026
Accepted: 22 September 2026
Published: 22 October 2026

Abstract: This study overviews the application of artificial intelligence (AI) in the prediction of biomarkers for non-small cell lung cancer (NSCLC). Different from recent reviews on AI-driven radiogenomics that adopt clinical or imaging-based classification, this work innovatively takes AI model architecture as the core classification framework. By analyzing multimodal data (mainly CT) and modeling paradigms (radiomics, deep learning and fusion models), it reveals the current research status centered on EGFR mutation prediction. In terms of technological evolution, prediction models are evolving from traditional radiomics to end-to-end learning, Transformer architecture and multimodal perception-driven deep learning paradigms. This study deeply analyzes the performance differences among different models, fills the application gaps in existing reviews, and provides an important benchmark reference for the clinical optimization of AI-assisted tools and the promotion of standardized precise diagnosis and treatment of NSCLC.

Keywords: NSCLC; artificial intelligence; epidermal growth factor receptor; radiomics; deep learning; PD-1

1. Introduction

Lung cancer is the most common malignant tumor worldwide, with a rapid upward trend in new cases in recent years, and has become the leading cause of cancer-related death globally. Up to now, the prevention and treatment of lung cancer still face enormous challenges. Most cases are diagnosed at an advanced stage, and the disease progresses rapidly after diagnosis, with a 5-year survival rate of only 17.8% for patients, significantly lower than that of other common malignant tumors [1]. Non-small cell lung cancer (NSCLC) is a common and highly aggressive lung cancer, accounting for 80–85% of the total incidence of lung cancer. It has an insidious onset and rapid progression, posing a serious threat to human life and health [2]. At present, targeted gene therapy guided by gene mutation detection has shown superior efficacy to traditional chemotherapy in lung cancer treatment due to its low side effects and good patient tolerance [3]. Meanwhile, immunotherapy, especially immune checkpoint inhibitors (ICIs), has revolutionized the treatment of NSCLC. In recent years, a variety of monoclonal antibodies targeting programmed death protein-1 (PD-1) and its ligand (PD-L1) have been approved for the treatment of advanced or locally advanced NSCLC [4].

In the current clinical setting, many biomarkers related to targeted therapy and immunotherapy have been widely used in the treatment of NSCLC. In terms of targeted therapy, targeted therapeutic drugs corresponding to gene mutations have been applied in clinical treatment of lung cancer, including epidermal growth factor receptor (EGFR), anaplastic lymphoma kinase (ALK), c-ros oncogene 1 (ROS1), Kirsten rat sarcoma viral oncogene homolog (KRAS), etc. For example, in lung adenocarcinoma, epidermal growth factor receptor - Tyrosine Kinase Inhibitors (EGFR-TKIs) have become important targeted drugs for the treatment of advanced lung

Copyright: © 2026 by the authors. This is an open access article under the terms and conditions of the Creative Commons Attribution (CC BY) license (https://creativecommons.org/licenses/by/4.0/).
Publisher's Note: Scilight stays neutral with regard to jurisdictional claims in published maps and institutional affiliations.

adenocarcinoma. Compared with standard platinum-based chemotherapy, patients treated with EGFR-TKIs exhibit better response rates and longer progression-free survival [5]. At the same time, immunotherapy has become a popular treatment for NSCLC. Increasing evidence shows that the use of immune checkpoint inhibitors (ICIs) in the treatment of NSCLC patients can effectively prolong the survival of patients with advanced and metastatic NSCLC [6]. Immunotherapy for NSCLC aims to utilize the immune system to recognize and eliminate cancer cells. Immune checkpoint markers are molecules expressed on the surface of both tumor cells and immune cells, which play a key role in regulating immune responses by promoting or inhibiting immune activity [7]. Immunotherapy has shown significant clinical efficacy in the cancer treatment of some NSCLC patients. The most extensively studied immune checkpoint markers include PD-1, PD-L1, CTLA-4, lymphocyte activation gene 3 (LAG-3), T-cell immunoglobulin and mucin domain-containing protein 3 (TIM-3) and B7 homologue 3 (B7-H3). These inhibitory signals suppress the ability of the immune system to recognize and attack cancer cells. Immune checkpoint inhibitors (such as anti-PD-1 and anti-PD-L1 antibody therapies) exert their effects by blocking these inhibitory signals. Tumor mutational burden (TMB) refers to the number of somatic mutations per coding region of the tumor genome. Studies have found that TMB can serve as an important predictive indicator for the efficacy of immune checkpoint inhibitors (ICIs) [7]. However, the clinical application of TMB is limited due to numerous challenges in detection. For both targeted therapy and immunotherapy, accurately and reliably determining the gene mutation status or immune checkpoint marker expression status of patients is crucial for achieving personalized precise treatment. For targeted therapy, precise diagnosis of the gene mutation status of lung cancer patients is a prerequisite for determining whether they can use relevant targeted therapeutic drugs. For immunotherapy, not all patients respond well to immunotherapy, and some patients may even experience severe toxic reactions. Therefore, identifying reliable predictive biomarkers is essential for optimizing patient selection and improving treatment outcomes. In particular, specific checkpoint markers can be used to guide therapies that enhance the immune system's ability to recognize and combat cancer cells. The accurate detection of core biomarkers (such as EGFR, PD-L1, ALK, TMB) is a prerequisite for realizing personalized precise treatment, directly guiding the selection of targeted therapy and immunotherapy regimens. However, the response rates of immunotherapy vary widely, highlighting the urgent need for predictive biomarkers to identify patients who are most likely to benefit from these therapies [8]. In clinical practice, the main clinical methods for measuring EGFR mutation status and PD-L1 expression currently rely on tissue samples obtained through surgical or needle biopsy, followed by the detection of different biomarkers via real-time fluorescence quantitative PCR (Polymerase Chain Reaction) and immunohistochemistry. This poses several problems: firstly, in clinical practice, multiple biopsies cause great pain to patients and may lead to tumor metastasis; meanwhile, extensive intratumoral heterogeneity and insufficient tumor tissue obtained from biopsy may reduce the accuracy of measuring EGFR status via biopsy [9]. The complex expression heterogeneity in the tumor microenvironment also limits the accuracy of comprehensively evaluating systemic PD-L1 expression using immunohistochemical methods [10]. In addition, tumors often progress or develop drug resistance in the advanced stage, requiring re-biopsy to dynamically assess tumor status [11]. Some patients may be ineligible for surgery, or unwilling to undergo multiple biopsies due to poor tolerance and high economic costs. Furthermore, the biopsy procedure itself may increase the potential risk of cancer metastasis [12].

Radiological imaging has long been an effective tool for monitoring NSCLC, including tumor progression and treatment response [13]. Computed tomography (CT), positron emission tomography (PET), pathological images, etc., are commonly used imaging modalities for NSCLC biomarker detection. CT images have high spatial resolution and can clearly display the anatomical structure of tumors, serving as the basis for clinical screening and feature extraction; pathological images can intuitively reflect the morphological and molecular characteristics of tumor cells, providing a direct basis for gene mutation detection; PET images can highlight the metabolic activity of tumors and assist in the evaluation of function-related biomarkers. With the help of advanced intelligent imaging technology, we can qualitatively or quantitatively analyze the correlation between patients' medical images and targeted gene mutations as well as immune checkpoints, and evaluate patients' prognosis and therapeutic efficacy [14]. Many studies have proven that information related to lung cancer gene mutations can be identified from extracted radiomic features, and the mutation status of lung cancer-related genes (such as EGFR) can be predicted based on these features [15]. Therefore, methods using intelligent tools to assist doctors in non-invasive gene mutation prediction are being widely studied. Meanwhile, some studies have confirmed a certain correlation between certain CT imaging features and gene mutation status. Genetic mutations in lung cancer are likely to be reflected in these morphological features [16]. For example, tumors presenting as mixed ground-glass opacity on CT are more prone to EGFR mutations, and significantly irregular tumor margins are likely associated with EGFR mutations. The fusion of different features helps improve prediction accuracy [17]. However, these studies used datasets with relatively small numbers of cases and lacked independent validation to confirm the reliability of the results. On the other hand, CT imaging can not only examine the macroscopic features of tumors

but also help explore the deeper implicit features of tumor cells [18]. The study by Liu et al. [19] showed that CT-based radiomic phenotypes can non-invasively identify lung adenocarcinomas (LUAD) with different molecular characteristics. The differences in PD-L1 expression and mutations in tumor protein p53 (TP53), epidermal growth factor receptor (EGFR), B-Raf proto-oncogene, serine/threonine kinase (BRAF), c-ros oncogene 1 (ROS1) and erb-b2 receptor tyrosine kinase 2 (ERBB2) among the four groups were statistically significant.

Although predictive biomarkers such as PD-L1 expression have been explored to guide treatment decisions for NSCLC, these biomarkers have limitations and cannot fully reflect the complex interaction between tumors and the immune system [20]. Artificial intelligence and machine learning technologies are increasingly widely used in the medical field due to their powerful data mining and pattern recognition capabilities. This has prompted the exploration of using artificial intelligence (AI) and machine learning (ML) technologies to integrate multiple biomarkers and clinical factors. AI and machine learning algorithms can be trained on various data sources, including genomic, radiomic and clinical data, to develop predictive models [21]. Biomedical images contain information that may reflect intrinsic pathophysiology, and quantitative image analysis may reveal the relationship between them, that is, imaging features are closely related to pathophysiological features. The process of transforming various digital medical images into mineable high-dimensional data is called radiomics. Compared with traditional imaging analysis, CT-based radiomics can extract a large number of quantitative imaging features from CT scans, which can capture tumor heterogeneity, serve as potential predictive biomarkers, stratify patients into different risk groups, and evaluate treatment response. Zhou et al. [22] explored the relationship between AI imaging features and EGFR gene mutations in lung adenocarcinoma based on CT images through feature correlation analysis, and found that gender, smoking history, pulmonary nodule morphology, cavitation sign, etc. were associated with EGFR mutations ($p < 0.05$). Therefore, CT-based radiomics has the potential to accurately predict treatment outcomes and guide treatment strategies. Both medical imaging and pathological tissue images, when combined with artificial intelligence, have shown great potential in assisting the diagnosis and treatment of NSCLC [23]. AI can automatically infer subtle heterogeneity hidden in medical images and identify potential semantics that are usually undetectable by the human eye [24], opening up new prospects for the treatment of NSCLC. However, in early radiomics, some studies required extensive expert manual annotation of data for model training, failing to fully exploit the potential of massive unannotated imaging data. In addition, with the widespread application of deep learning in this field, the "black-box" problem of deep neural networks has become increasingly prominent. Most high-performance deep learning models cannot clearly explain their decision-making logic, which makes it difficult for clinicians to trust the prediction results and severely hinders the clinical transformation of AI tools. Although a small number of recent studies have adopted explainable artificial intelligence (XAI) techniques such as Gradient-weighted Class Activation Mapping (Grad-CAM), SHapley Additive exPlanations (SHAP) and attention visualization to interpret model outputs, systematic sorting and comparative analysis of model interpretability across different AI architectures are still lacking in current reviews. Recently, with the development of deep learning technology, deep learning models have gradually replaced traditional machine learning models in biomarker prediction. By constructing multi-layer neural network models, deep learning technology can automatically extract deep implicit features from multimodal data, effectively overcoming the defects of traditional manual feature extraction methods. Deep learning models have achieved satisfactory results in many complex medical diagnoses [25]. Abundant achievements have also been made by deep learning models in predicting EGFR gene mutation status [26]. Wang et al. adopted the DenseNet121-FPN model to predict EGFR genotype in a large-scale study involving 18,232 lung cancer patients, and the model exhibited high predictive performance [15]. Meanwhile, some studies have combined deep learning methods with pathological tissue image analysis to directly predict the mutation status of genes such as EGFR from pathological images [27]. Jiang et al. proposed the JSSC-Net framework to explore the relationship between tumor microenvironment features and EGFR gene mutations [28]. Numerous achievements have also emerged in research on predicting immunotherapy-related biomarkers. Wang et al. [29] used 3D CNN to predict EGFR mutation and PD-L1 expression based on CT and clinical data. Subsequently, the researchers used a 3D ResNet model to predict PD-L1 expression and patient survival, achieving an AUC of 0.946 for predicting PD-L1 $\geq$ 50% [30]. These models enable more precise stratification of patients based on biomarkers, ultimately improving treatment outcomes.

This study provides a comprehensive overview of current diverse artificial intelligence technologies and their applications in NSCLC biomarker prediction. The study initially screened 487 scientific publications and selected 211 eligible research papers for in-depth review. The selected papers were classified according to imaging modalities (such as PET, CT, pathological images), types of deep learning models (such as DenseNet, ResNet) and the types of actual predicted biomarkers (such as EGFR, PD-1). The advantages and limitations of various AI models in predicting NSCLC-related biomarkers under different application scenarios and image modalities were emphatically analyzed, the shortcomings of current research were clarified, and future research directions in this

field were proposed. To the best of our knowledge, this is the first overview that comprehensively and systematically explores the impact of different model architectures on the predictive efficacy of NSCLC biomarkers. This study aims to provide a theoretical reference for the application of different AI technologies in the diagnosis and treatment of NSCLC; recommend optimal deep learning tools for specific application fields and provide a benchmark for future research; meanwhile, objectively examine the limitations of current research and discuss potential future development directions related to NSCLC biomarkers. The overall framework and distribution of the study are shown in Figure 1.

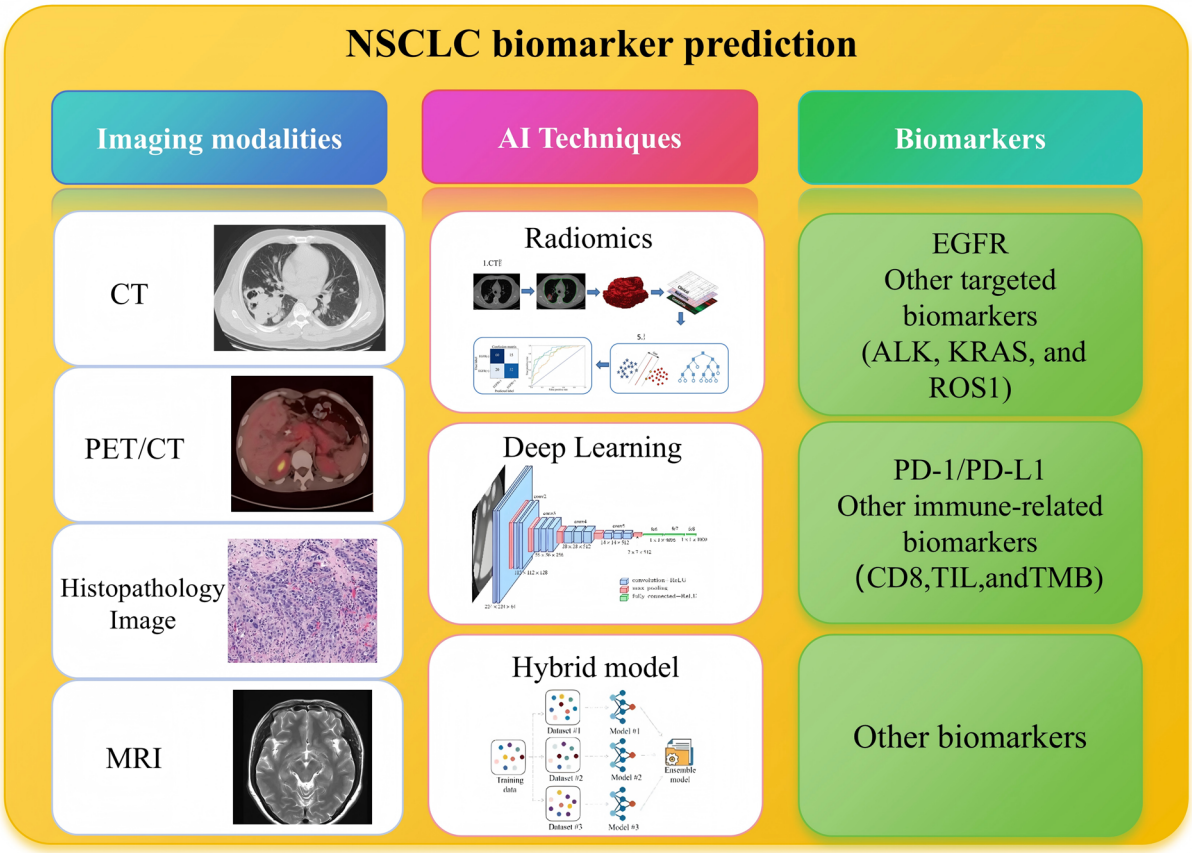


Figure 1. Diagram of the overall research.

The manuscript is organized as follows: Section 2 outlines the paper selection process, Section 3 discusses the results of the selected papers, Section 4 provides a discussion of the results, and finally Section 5 presents the conclusions.

2. Methods

2.1. Analysis of Existing Reviews

To clarify the research gaps of previous reviews, we first retrieved and analyzed published review papers related to NSCLC, AI, biomarker prediction, targeted therapy and immunotherapy from mainstream academic databases. After rigorous screening, 7 latest and representative review articles were finally included. By sorting out the research focus, advantages and limitations of these existing reviews, we further defined the research positioning and innovation of the present work.

In existing review studies, although each involves AI-assisted biomarker prediction, the focuses vary. Liao et al. [31] systematically reviewed the application of AI in precision cancer medicine, covering multi-source data such as genomics, transcriptomics and radiomics, and discussed biomarkers related to tumor screening, diagnosis, treatment and prognosis prediction; Chen et al. [32] focused on the application of radiomics and AI in precision lung cancer treatment, taking imaging data as the core and focusing on markers related to patient risk stratification, histological classification and clinical outcome prediction; Li et al. [33] looked forward to the development trend of NSCLC targeted therapy and immunotherapy, and analyzed targeted markers and immune markers based on clinical research data; Atmakuru et al. [34] systematically reviewed the application of deep learning and radiomics in lung cancer diagnosis, and conducted biomarker research such as lesion detection and survival prediction using multimodal imaging data; Zheng et al. [35] explored the application value of CT radiomics in the identification of

immune checkpoint markers and prediction of immunotherapy outcomes in NSCLC based on CT and PET/CT imaging data; Arango-Argoty et al. [36] introduced AI-driven methods for the discovery of immunotherapy predictive markers, and adopted a contrastive learning neural network framework for in-depth mining of CT imaging data; Bonci et al. [37] reviewed the application of AI in NSCLC diagnosis, prognosis and treatment optimization, and deeply analyzed markers related to diagnosis, treatment optimization and survival outcomes.

Previous review papers on AI-driven radiomics for NSCLC, including the 7 representative articles analyzed above, generally have three common limitations: first, most classify literature based on clinical biomarkers or single imaging modalities (CT/PET only), lacking systematic sorting from the perspective of AI technical iteration; second, most adopt descriptive narration and rarely carry out horizontal quantitative comparison of model performance across multiple dimensions; third, they pay less attention to cutting-edge architectures such as Transformer, multimodal large models and pathological AI technologies emerging in recent years. In contrast, we take AI modeling architectures as the primary classification standard for the first time, focusing on sorting the evolutionary logic of radiomics and traditional machine learning, CNN-based deep learning, Transformer and other advanced networks, as well as multimodal fusion models. This design makes the technical evolution and application differences of various AI solutions more intuitive, and effectively fills the gaps of recent radiomics reviews. The search strategy adopted in this review is described below.

2.2. Literature Search Strategy

Comprehensive literature retrieval was performed across three mainstream academic databases: PubMed, Web of Science Core Collection, and IEEE Xplore. The retrieval time was limited to the period from 1 January 2020 to 31 May 2025, and only full-text English academic papers were included. We adopted a combined retrieval strategy of subject words and free words, and grouped keywords into three categories: disease, research object and technical method. Disease keywords: non-small cell lung cancer, NSCLC, lung adenocarcinoma, lung cancer. Biomarker & therapy keywords: biomarker, EGFR, ALK, ROS1, KRAS, PD-1, PD-L1, TMB, targeted therapy, immunotherapy, immune checkpoint inhibitor. Technical keywords: artificial intelligence, deep learning, machine learning, radiomics, CNN, Transformer. The general retrieval string (PubMed format) was constructed as follows: ((non-small cell lung cancer) OR NSCLC OR lung cancer) AND (biomarker OR EGFR OR PD-L1 OR targeted therapy OR immunotherapy) AND (artificial intelligence OR deep learning OR machine learning OR radiomics) AND (CT OR PET OR PET/CT OR pathological images OR MRI).

After combined searches across the three databases, a total of 487 preliminary records were retrieved. The inclusion criteria were defined as follows: (1) original research articles (excluding letters, editorials and conference abstracts); (2) studies enrolling patients with pathologically confirmed non-small cell lung cancer; (3) research applying artificial intelligence, radiomics, machine learning or deep learning methods based on medical images (CT, PET/CT, MRI, pathological images) to predict NSCLC-related biomarkers; (4) articles published between January 2020 and May 2025; (5) full-text availability with complete research data, model results and experimental metrics fully reported. The exclusion criteria included: (1) review articles, case reports, conference abstracts and short communications without accessible full texts; (2) studies irrelevant to artificial intelligence techniques or biomarker prediction; (3) duplicate publications and studies with overlapping research datasets; (4) non-English articles; (5) studies with incomplete experimental data, ambiguous model design or unreported core evaluation metrics; (6) cell experiments, animal studies and purely theoretical research that contained no clinical imaging data. After rigorous screening, a total of 211 eligible original research articles were included for in-depth qualitative analysis. The literature search strategy is shown in Figure 2.

We assessed all 211 included studies, covering four domains: patient selection, index test, reference standard, flow and timing. For patient selection: 72.3% of studies used single-center retrospective cohorts without explicit exclusion criteria for repeated cases. For index test: Most AI/radiomics models lacked pre-specified threshold settings, and 31.0% did not report standardized image preprocessing. For reference standard: For mutation-status prediction tasks, most studies used pathological/genetic detection as the gold standard. For flow & timing: Only 17.8% conducted multi-center external validation; most studies lacked independent test sets. Overall, most studies had acceptable quality, but single-center retrospective design and insufficient external validation were the predominant limitations.

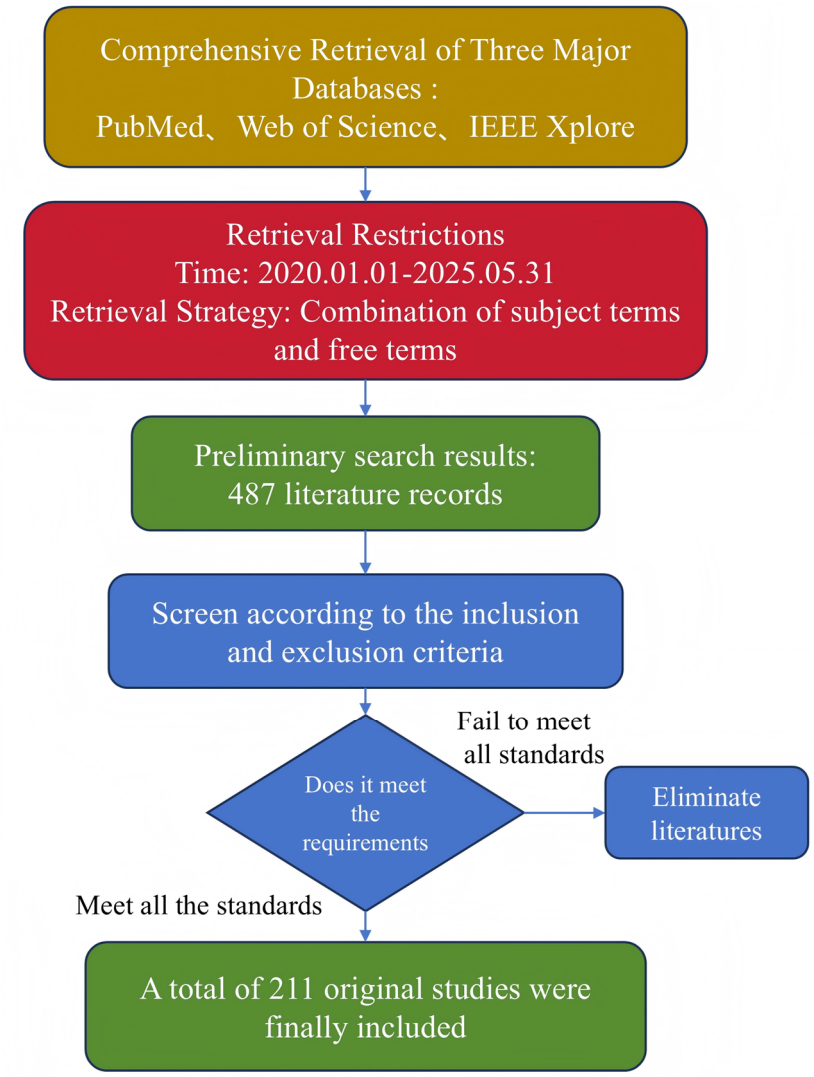


Figure 2. Literature search strategy.

2.3. Different Imaging Modalities

This review covers core imaging modalities such as CT, PET/CT, pathological images and MRI, aiming to ensure the inclusion of studies directly related to NSCLC biomarker detection. In terms of search strategy, the search formula designed in this study was limited to CT, PET, PET/CT, pathological images and MRI to accurately screen relevant work using these modalities and exclude studies using other irrelevant methods.

Each imaging modality exhibits unique clinical and scientific research value: CT images, with high spatial resolution, clear display of anatomical structures and extremely high clinical accessibility, serve as the basis for NSCLC screening and biomarker feature extraction, and can effectively identify structural changes caused by tumor lesions. Pathological images display the morphological features of tumor cells and offer morphological correlates that complement molecular assays for evaluating biomarkers such as gene mutations and PD-L1 expression. PET images can reflect the metabolic activity of tumors. The relationship between PET-derived metabolic features and biomarkers such as tumor mutational burden (TMB) remains investigational and has not been fully established. MRI images exhibit high soft tissue resolution, and have irreplaceable advantages especially in the detection of brain metastasis-related biomarkers. In addition, multimodal fusion data integrates multi-dimensional information such as anatomical, functional and molecular data, which can further significantly improve the accuracy and reliability of biomarker detection. Distribution of papers using different imaging modalities as shown in Figure 3.

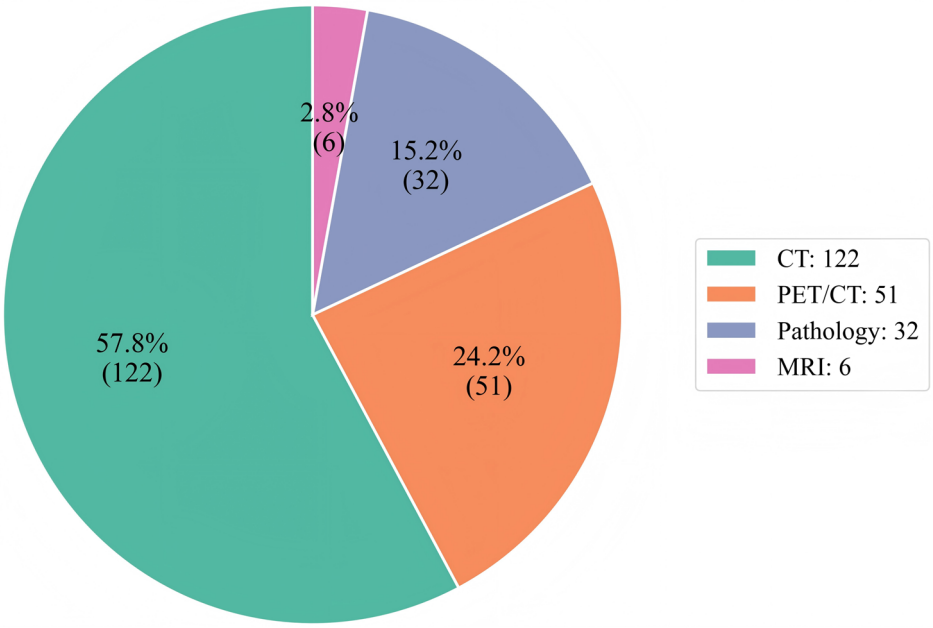


Figure 3. Distribution of papers using different imaging modalities.

2.4. Different Artificial Intelligence Methods

The AI models involved in this study are divided into three categories: radiomics and machine learning methods, deep learning methods, and hybrid models. In deep learning methods, they are further subdivided into classic deep learning algorithms dominated by convolutional neural networks (CNN) and emerging deep learning algorithms dominated by architectures such as Transformer. Different from single model methods, hybrid models include the fusion of different machine learning algorithms, the integration of different deep learning architectures, the combined application of machine learning and deep learning, and multimodal prediction models; in addition, this category also includes all studies in which deep learning models are used in at least one stage of the experimental process. Radiomics and machine learning methods mainly use traditional machine learning algorithms such as logistic regression, support vector machine (SVM), random forest (RF), and K-nearest neighbor (KNN) to achieve biomarker detection through manual extraction of radiomic features. Deep learning methods include CNN, deep neural network (DNN), Transformer, generative adversarial network (GAN), etc., which have the ability to automatically extract deep features of data. Hybrid models aim to achieve a significant improvement in predictive performance by integrating the advantages of multiple technologies. The quantitative distribution of studies in each category is as follows. Distribution of papers using different artificial intelligence methods as shown in Figure 4.

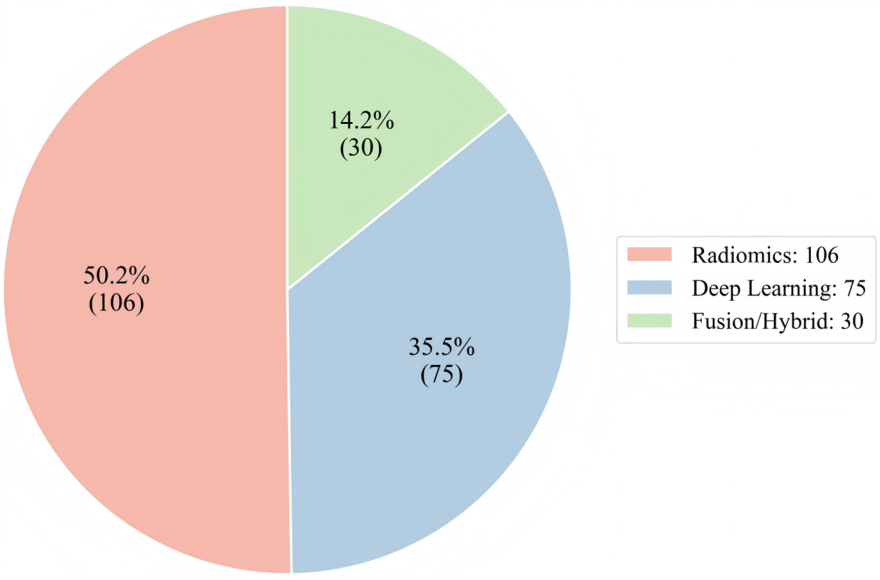


Figure 4. Distribution of papers using different artificial intelligence methods.

2.5. Different Biomarkers

According to the specific NSCLC-related tasks involved in the selected papers, this study divides biomarker prediction tasks into five subgroups: EGFR, other targeted biomarkers, PD-1/PD-L1, other immunotherapy biomarkers, and other related biomarkers. The detection of targeted therapy-related biomarkers mainly covers gene mutation detection such as EGFR, ALK, KRAS, ROS1, with a total of 136 related research papers; the detection of immunotherapy-related biomarkers mainly involves indicators such as PD-L1 expression, TMB, tumor-infiltrating lymphocytes (TILs) and cluster of differentiation 3 $(CD3)^+$/ cluster of differentiation 8 $(CD8)^+$ T cell expression, with a total of 61 related research papers; other related prediction tasks mainly include the prediction of clinical features such as overall survival (OS), with a total of 14 related research papers. The literature distribution of different research tasks is shown in Figure 5 below.

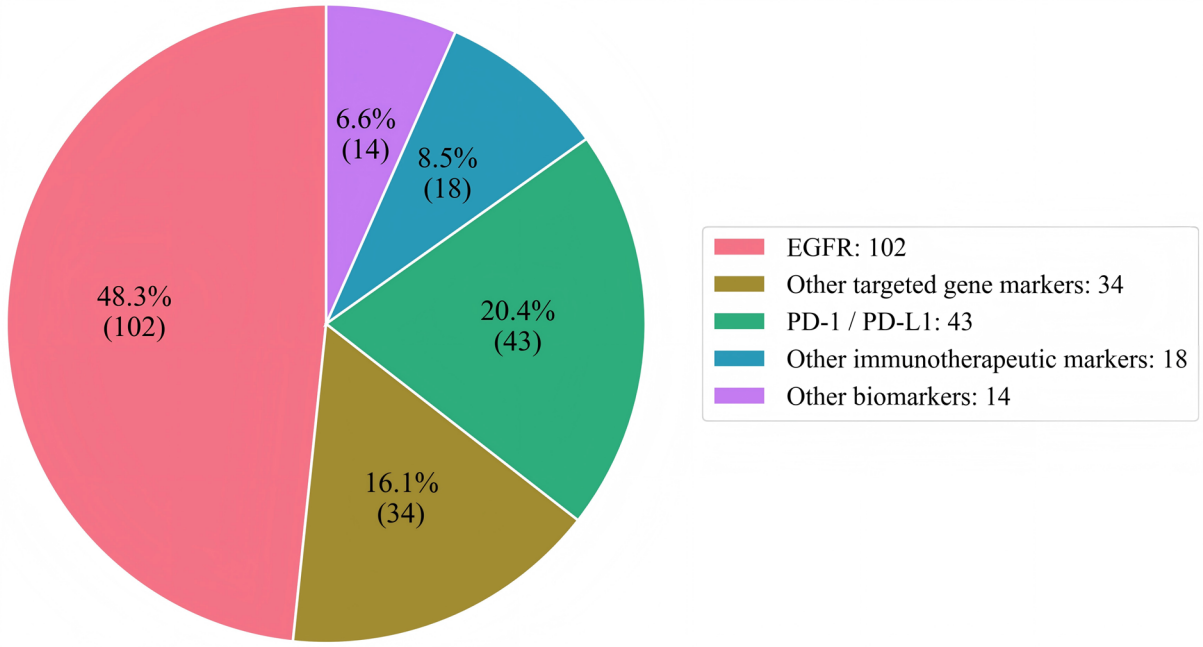


Figure 5. Distribution of papers predicting different biomarkers.

2.6. Public Datasets

This section summarizes public datasets utilized in the included studies. While some studies explicitly documented the use of public data sources, For the commonly used public datasets listed below, the trailing in-text citations refer to original studies that utilized the corresponding datasets, not references introducing the databases themselves: TCGA (The Cancer Genome Atlas) [38–44], TCIA (The Cancer Imaging Archive) [45,46], GEO (Gene Expression Omnibus) [47,48], and CPTAC (Clinical Proteomic Tumor Analysis Consortium) [49,50]. Single-center and multi-center clinical datasets established by individual research teams are also included.

First is TCGA, a program jointly launched by the National Cancer Institute (NCI) and the National Human Genome Research Institute of the United States, and one of the most influential cancer genomics platforms worldwide. It covers whole-exome sequencing, RNA sequencing, DNA methylation and clinical prognostic data, laying a molecular foundation for studying the correlation between gene mutations and imaging phenotypes. Complementary to it is TCIA, a database dedicated to hosting medical imaging data matched with TCGA samples. TCIA provides a large number of Digital Imaging and Communications in Medicine (DICOM) format images, including CT, PET/CT and MRI, enabling researchers to conduct radiomics research and explore the in-depth mapping between macroscopic imaging features and microscopic gene phenotypes. GEO is a public functional genomics data repository maintained by the National Center for Biotechnology Information of the United States, mainly collecting high-throughput gene chip and next-generation sequencing data. CPTAC further extends the research perspective to the protein level, revealing protein variations driving cancer development through large-scale proteogenomic analysis, providing a unique perspective for the discovery of novel protein biomarkers. DHMC is highly representative in pathological AI research, and its released lung cancer histology dataset contains digital whole-slide images annotated by multiple pathologists, which is widely used to train deep learning models for identifying lung adenocarcinoma subtypes. These datasets integrate key information such as patient demographic information, tumor characteristics, multimodal imaging data, pathological images, genomic data,

treatment regimens and clinical outcomes. Among them, TCGA provides rich NSCLC genomic and clinical data, TCIA provides corresponding imaging resources, and pathological-related data mainly comes from digital slice resources of TCGA and CPTAC, providing solid data support for the training and validation of deep learning models.

To standardize the analysis of model generalization ability, we categorized the validation strategies of all included AI models into three types in line with general specifications for medical artificial intelligence and radiomics research. Internal Cross-validation (ICV) randomly divides single-center datasets into training and validation sets, such as k-fold cross-validation; as the most basic validation method, it may not reflect how well a model adapts to external data. Single-center External Validation (SCEV) uses independent datasets from different patient cohorts at the same medical institution to preliminarily verify model stability within a single center. Multi-center External Validation (MCEV) adopts datasets from multiple independent medical institutions with different imaging devices, scanning protocols and patient populations, and is acknowledged as the gold standard for evaluating the clinical generalization and reproducibility of AI models. This review mainly analyzes the performance differences and performance attenuation between ICV and external validation (SCEV/MCEV).

3. Results

This section systematically introduces the predictive research of NSCLC biomarkers based on radiomics and machine learning methods, deep learning methods, and hybrid models under different imaging modalities. It focuses on discussing the similarities and differences of various AI models in related tasks, deeply analyzes the specific application scenarios of each technology, and conducts classified reviews of various related studies. When exploring AI technologies for biomarker predictive diagnosis, selecting an appropriate methodological architecture directly affects the construction of datasets and the selection of evaluation indicators. Whether it is a machine learning model, a deep learning model or a hybrid model, a dataset with sufficient depth and breadth is required to ensure the effectiveness of model training. In addition, the selected evaluation indicators must be highly consistent with the specific goals of model performance evaluation. For example, accuracy and area under the curve (AUC) are commonly used indicators to evaluate classification prediction tasks in deep learning research. In hybrid model research, the combined application of different model architectures can effectively improve the predictive performance of the model. At the same time, studies involving multimodal data put forward higher requirements for the integrity of datasets and methodological design. The integration of such multi-dimensional data enables the model to fully exert the synergistic advantages of various data types from radiological images to clinical records.

3.1. Radiomics and Machine Learning Methods

The process of transforming digital medical images into mineable high-dimensional quantitative data is called radiomics. This method has the advantages of strong feature interpretability and relatively low model training cost, and is widely used in NSCLC biomarker detection. By analyzing medical images collected from multiple parts and multiple follow-ups, radiomics can provide massive imaging biomarkers. Due to the early start of radiomics methods, a large number of mature studies have applied it to NSCLC-related biomarker prediction. In imaging data of different modalities such as CT, PET/CT and MRI, numerous works based on radiomics or machine learning architectures to predict targeted therapy and immunotherapy biomarkers have emerged. This section classifies and deeply analyzes predictive research according to different imaging modalities and biomarker types.

3.1.1. CT Related Studies

In the diagnosis and treatment pathway of lung cancer, especially NSCLC, CT images are commonly used for early screening and clinical staging, and can effectively reflect the macroscopic morphology and microscopic spatial structure of tumors. With extremely high spatial resolution, CT can clearly display the anatomical structure, location, size, shape, edge characteristics and other features of lesions. By mining these morphological features, researchers can establish the correlation between imaging phenotypes and targeted gene status as well as immune microenvironment, thereby realizing the analysis and prediction of relevant biomarkers.

In the detection research of targeted therapy biomarkers, many works focus on the prediction of EGFR mutation status and its subtypes, and have achieved good results. Zhang et al. [51] adopted a multivariate Logistic regression model to predict EGFR mutations, with a model AUC of 0.813; Liu et al. [52] compared the performance of models in CT-based EGFR mutation prediction, among which the random forest (RF) model achieved an AUC of up to 0.88 in the validation set. The superior performance of RF in this task is mainly attributed to its ability to handle the non-linear correlation between high-dimensional radiomic features and gene status, as well as its strong anti-overfitting capability for small and medium-sized datasets. Compared with invasive biopsy,

CT-based AI prediction can realize whole-tumor coverage sampling, effectively making up for the defect of local sampling bias caused by tumor spatial heterogeneity in puncture specimens. In NSCLC-related biomarker prediction research, studies targeting EGFR mutations are the most intensive, indicating that microscopic changes in tumors caused by gene mutations may lead to changes in macroscopic morphological features and be mapped on CT images. Table 1 summarizes the EGFR mutation prediction studies based on radiomics, machine learning methods and CT images. It can be seen from Table 1 that Least Absolute Shrinkage and Selection Operator (LASSO) regression dominates in feature screening, and many scholars have adopted LASSO for feature dimensionality reduction [53–55]. This may be because LASSO can compress the coefficients of unimportant features to zero, making it highly suitable for handling the high-dimensional problem of radiomic features. Logistic regression (LR) and support vector machine (SVM) are the most frequently used traditional machine learning models. For example, refs. [56,57] both adopted SVM models, proving their superior generalization ability in processing high-dimensional nonlinear data. In addition, the application proportion of nomograms has increased significantly in recent years. For example, Ref. [58] combined radiomic scores with independent clinical risk factors, and greatly improved the clinical interpretability and practicability of the model through nomograms. Nomograms convert complex model calculations into visual quantitative scales, which is more in line with the diagnostic habits of clinicians.

AUC (Area Under the Receiver Operating Characteristic Curve) is the gold standard for measuring the performance of binary classification models. In the studies listed in Table 1, the overall AUC of radiomics combined with machine learning models in EGFR prediction is at a moderate to high level. Njoto et al. [59] reported extremely high predictive efficacy, with a validation cohort AUC of 0.91. The ultra-high performance of this study is closely related to its single-center unified scanning protocol and relatively homogeneous patient population. In addition, Wu et al. [60] achieved an AUC of 0.9724 using enhanced CT combined with LASSO and logistic regression. Zhu et al. [61] achieved an AUC of 0.723 for EGFR mutation prediction in early lung adenocarcinoma, which is the relatively lowest value for the prediction of EGFR mutation status in the table; this may reflect that early lung cancer has fewer solid components and insufficiently exhibited tumor heterogeneity, resulting in relatively weak distinguishability of radiomic features for genotypes. Early-stage lesions are dominated by ground-glass opacity, with weak molecular phenotype expression, so the mapping relationship between imaging features and gene mutations is weakened.

Table 1. Prediction of EGFR gene mutations based on radiomics and machine learning methods and CT images.

Author	Year	Method	Data Type	Prediction Target	AUC Value
Zhang et al. [51]	2022	Multivariate Logistic Regression Model	Tumor Markers, CT Features	EGFR Mutation	0.813
Liu et al. [52]	2022	Logistic Regression, Decision Tree, Random Forest, SVM (RF Optimal)	CT Images	EGFR Mutation	Validation Set 0.88
Yang et al. [53]	2020	LASSO Regression	Venous Phase CT Radiomic Features	EGFR Mutation Status, TKI Sensitivity	0.8464
Chen et al. [56]	2021	Support Vector Machine (SVM) + Nomogram	Non-Enhanced CT, Clinicopathological Data	Rare EGFR Mutation	Training: 0.816, Validation: 0.795
Dang et al. [54]	2021	LASSO Logistic Regression + Nomogram	CT Images, Clinical Data	EGFR Mutation	0.894
Hou et al. [62]	2021	Clinicopathological + Conventional CT + CT Radiomics Combined Model	Clinicopathological, Conventional CT, CT Radiomics	EGFR T790M Mutation	Training Set 0.90, Validation Set 0.91
Ninomiya et al. [63]	2021	Support Vector Machine (SVM), Topological Invariant Betti Numbers	Contrast-Enhanced CT Images	EGFR Mutation	-
Rossi et al. [64]	2021	Machine Learning Model	CT Radiomics, Clinical Features (Gender, Smoking History)	EGFR Mutant/Wild Type	0.85
Weng et al. [65]	2021	mRMR + LASSO + Combined Model	Non-Enhanced CT, Clinical Features	EGFR Activating Mutation	Training Set 0.81, Validation Set 0.75
Zhang et al. [55]	2021	LASSO + Wilcoxon Test + Decision Tree/Logistic Regression/SVM	CT, Clinical Radiological Data	EGFR Mutation in Lung Adenocarcinoma	Development Set 0.849, Validation Set 0.835
Zhu et al. [66]	2021	Multi-Class Strategy + Ensemble Model	Enhanced CT, Clinical Data	EGFR/TP53 Co-Mutation in Advanced Lung Adenocarcinoma	EGFR(−) 0.857, EGFR(+)&TP53(+) 0.791

Table 1. *Cont.*

Author	Year	Method	Data Type	Prediction Target	AUC Value
Chen et al. [16]	2022	RF-BFE Feature Selection + Prediction Model	Original/Filtered CT, Clinicopathological Data	EGFR Mutation Status, Subtypes in Lung Adenocarcinoma	Mutation Status 0.765, Integrated Model 0.759
Cheng et al. [67]	2022	Gradient Boosting Decision Tree (GBDT)	CT, Clinicopathological Data	EGFR Mutation in Ground-Glass Opacity Lung Adenocarcinoma	External Validation Set 0.803
Dong et al. [58]	2022	Three-Stage Feature Selection + Radiomic Score + Nomogram	CT, Clinical Data	EGFR Mutation, Ki-67 Proliferation Index	Validation Set 0.798
Jiang et al. [57]	2022	Support Vector Machine (SVM)	CT, Clinical Data	EGFR Mutation Status,	Validation Set 0.7413
Chen et al. [68]	2025	TRANS Model (LASSO + Nomogram)	CT, Clinical Data, RNA Sequencing Data	NSCLC EGFR Mutation	0.84 ± 0.01
Hong et al. [69]	2020	LASSO + 6 Machine Learning Methods + Nomogram	Enhanced/Non-Enhanced CT	EGFR Mutation	Enhanced CT Validation Set 0.851
Lu et al. [70]	2020	LASSO + Logistic Regression + Nomogram	Non-Enhanced CT, Clinicopathological Data	EGFR Mutation	Test Set 0.894
Wu et al. [60]	2020	Pearson Correlation Coefficient + LASSO + Logistic Regression	Enhanced CT, Clinical Data	EGFR Mutation	0.9724
Lu et al. [71]	2022	Filter Method + 7 Machine Learning Models	CT, Clinical Data	EGFR Mutation in Lung Adenocarcinoma	0.86
Zhu et al. [61]	2022	LASSO Regression + Nomogram	CT, Clinical Data	EGFR Mutation in Early Lung Adenocarcinoma	0.723
Kawazoe et al. [72]	2023	Analysis of Variance + LASSO + Multiple Classifiers	CT, Clinical Data, Intratumoral/Peritumoral Radiomics	EGFR Mutation in Lung Adenocarcinoma	LR Test Set 0.783
Njoto et al. [59]	2023	Conditional Logistic Regression + Nomogram	Enhanced CT, Clinical Data	EGFR Mutation	Development Cohort 0.993, Validation Cohort 0.91
Omura et al. [73]	2023	Machine Learning Radiomics + Combined Model	Enhanced CT, Clinical Features (Gender, Smoking History)	EGFR Mutation in Early Lung Adenocarcinoma	Average 0.83
Shang et al. [74]	2023	t-Test + LASSO + mRMR + Radiomic Model	Thin-Section CT, Intratumoral/Peritumoral Radiomics	EGFR Mutation in Lung Adenocarcinoma	External Test Set 0.701
Chen et al. [75]	2024	mRMR + LASSO Logistic Regression + Stepwise Logistic Regression	CT, Clinical Data	NSCLC EGFR Mutation	External Validation Set 0.861
Ma et al. [76]	2024	7 Prediction Models + Nomogram	Dual-Energy CT, Conventional CT, Clinical Data	EGFR Mutation in Lung Adenocarcinoma	Training Set 0.86, Validation Set 0.83
Chen et al. [77]	2025	Multivariate Logistic Regression + Combined Model	CT Perfusion Imaging	NSCLC EGFR Mutation	0.956

In addition to binary classification prediction of EGFR mutation status, some studies have deeply explored the prediction of EGFR mutation subtypes [78,79], the most common of which are exon 19 deletion mutation (19Del) and exon 21 L858R point mutation. Accurate differentiation of these two subtypes helps clinicians predict the difference in therapeutic efficacy of different subtypes. From a clinical perspective, 19Del and L858R have distinct sensitivity to different generations of EGFR-TKIs, so subtype prediction has direct guiding value for individualized medication. Compared with the simple binary classification task of mutant type versus wild type, the difficulty of distinguishing EGFR mutation subtypes increases significantly. Kawazoe Y (2023) [80] used machine learning, achieving an AUC of 0.85 for L858R prediction and 0.77 for 19Del prediction. The combined prediction model developed by Huo JW (2022) [81] achieved AUCs of 0.847 and 0.806 for 19Del and L858R, respectively. Overall, subtype prediction AUCs generally face the challenge of breaking through the 0.9 bottleneck. The underlying reason is that the imaging phenotype differences between different EGFR subtypes are far smaller than those between mutant and wild-type genes, resulting in weaker feature discrimination.

At the same time, numerous achievements have emerged in predictive research targeting other key targeted gene mutations, as shown in Table 2. ALK rearrangement is often present as solid masses with pleural retraction

on CT images. KRAS mutations are more common in patients with a smoking history, and their imaging prediction has attracted much attention. T790M mutation is the main molecular mechanism of drug resistance in patients after treatment with first-generation or second-generation EGFR-TKIs. Although the incidence of ALK rearrangement is low, machine learning has shown significant potential in predicting this target. Hao P. (2022) [82] used SVM, achieving high AUCs of 0.914 in the validation set on non-contrast CT. This is because ALK-mutated tumors have highly characteristic CT manifestations, forming a strong radiogenomic correlation. In recent years, radiomics studies on T790M resistance mutation have increased rapidly. Xiong W. (2024) [83] adopted models such as random forest (RF), with a training set AUC as high as 0.961. In terms of feature engineering, the mRMR algorithm is frequently used to filter redundant features [84]. Compared with LASSO, mRMR focuses on both feature correlation and redundancy, and is more suitable for multi-target joint prediction scenarios. In addition, ensemble learning algorithms such as XGBoost have performed well in handling nonlinear mapping tasks of genomic features by virtue of their strong regularization ability. Le NQK (2021) [85] combined genetic algorithm with XGBoost to analyze low-dose CT, achieving an accuracy of 0.86 in predicting KRAS mutation. Meanwhile, the multi-scale radiomics model proposed by Zhang X (2024) [86] can simultaneously predict ALK and ROS1, with AUCs of 0.902 and 0.900 respectively. Multi-scale radiomics can capture lesion features of different sizes and textures, and is more adaptable to the morphological heterogeneity of rare mutant tumors.

Table 2. Prediction of EGFR subtypes and other targeted gene mutations based on radiomics, machine learning and CT images.

Author	Year	Method	Data Type	Prediction Target	Accuracy	AUC Value
Li et al. [78]	2020	LASSO Logistic Regression + 5 Machine Learning Methods	CT Images, Clinical Data	EGFR Mutation, 19Del/L858R Subtypes		0.79 for EGFR, 0.74 for subtypes
Liu et al. [79]	2020	Logistic Regression Model	3D Radiomics Features	EGFR Mutation and Subtypes in Lung Adenocarcinoma	Highest Accuracy = 75.5%	-
Huo et al. [81]	2022	Combined Prediction Model	CT-Clinical Radiomics Features	EGFR Subtypes (19Del/L858R) in Lung Adenocarcinoma		0.847 for 19Del, 0.806 for L858R
Kawazoe et al. [80]	2023	Analysis of Variance + LASSO + Machine Learning + Nomogram	Non-contrast CT, Clinical Data	EGFR Mutation and Subtypes in Lung Adenocarcinoma		0.85 for L858R, 0.77 for 19Del
Ninomiya et al. [87]	2023	Support Vector Machine (SVM) + 3D Betti Numbers (3DBN)	CT, Clinical Data (Gender, Smoking History)	EGFR Del19/L858R Subtypes	Accuracy = 0.810	-
Ma et al. [88]	2020	Pearson Correlation Coefficient + ANOVA/Recursive feature elimination + SVM	Contrast/Non-contrast CT	ALK Rearrangement in Solid Lung Adenocarcinoma		0.8285 for test set
Song et al. [89]	2020	F-test + DBSCAN + RFE + Soft Voting Classifier	Non-contrast CT, Clinical Data	ALK Rearrangement in Lung Adenocarcinoma		0.88 for test set
Hao et al. [82]	2022	SVM + LASSO	Non-contrast CT, Clinical Data	ALK Rearrangement		0.965 for training set, 0.914 for validation set
Choe et al. [90]	2021	Two-step Binary Radiomics Classification Model	CT Images	ALK Rearrangement, EGFR Mutation in Lung Adenocarcinoma		0.77 for ALK development set, 0.68 for validation set
Le et al. [85]	2021	Genetic Algorithm + XGBoost	Low-dose CT	EGFR, KRAS Mutation	KRAS Prediction Accuracy = 0.86	-
Yang et al. [84]	2022	mRMR + LASSO + Nomogram	Contrast CT, Clinical Data	Acquired T790M Mutation, Osimertinib Prognosis		0.76 for validation set
Li et al. [91]	2023	Multivariate Logistic Regression + Radiomics + Nomogram	Non-contrast CT, Clinical Data	T790M Mutation in Lung Adenocarcinoma		0.841 for test set
Lu et al. [92]	2024	LASSO + 7 Machine Learning Models	CT, Clinical Data	Acquired EGFR T790M Mutation in NSCLC		0.86
Xiong et al. [83]	2024	RF, LR, SVM + Nomogram	CT, Clinical Data	Acquired T790M Mutation in NSCLC		0.961 for RF training set
Zhang et al. [86]	2024	Multi-scale Radiomics Model	CT, Clinical Data	Multiple Targeted Mutations in NSCLC (ALK, ROS1)		0.902 for ALK, 0.900 for ROS1
Li et al. [93]	2025	Multidimensional Model (Random Forest)	CT, Molecular Data	EGFR/TP53 Co-mutation in NSCLC, TKI Resistance		0.843 for test set
Zhang et al. [94]	2021	LASSO + Machine Learning Models	Contrast-enhanced CT, Clinical Data	EGFR, KRAS, ERBB2, TP53 Mutation		0.87 for ERBB, 0.84 for TP53, 0.78 for EGFR, 0.81 for KRAS

In addition to the prediction of targeted therapy biomarkers, radiomics and machine learning methods have also been widely used in the detection of immunotherapy biomarkers. Jiang et al. [95] adopted ridge regression recursive feature elimination combined with Logistic regression model to predict PD-L1 expression, achieving an AUC of 0.96 in the main cohort; Wen et al. [96] used Logistic regression model to integrate CT imaging features and clinicopathological features to predict PD-L1 expression, with an AUC of 0.839; Bracci et al. [97] adopted binary Logistic regression model to predict PD-L1 expression, achieving a validation set AUC of 0.789. Traditional machine learning methods can effectively process high-dimensional texture features extracted from CT images, aiming to capture intratumoral heterogeneity and the interaction state between tumor edges and the host immune system. Table 3 reflects the studies on immunotherapy biomarker prediction based on radiomics, machine learning and CT images. Most studies set the prediction target as PD-L1 expression status [97,98].

Meanwhile, predictive studies targeting CD8+ tumor-infiltrating lymphocytes (TILs) [99] and TMB [96] also occupy an important position. This may reflect the urgent clinical need for comprehensive evaluation of the tumor immune microenvironment (TIME) rather than a single target. In terms of machine learning algorithm selection, LASSO regression combined with multivariate Logistic regression is the current mainstream paradigm [96,100], and its popularity is mainly attributed to the strong model interpretability of this architecture. Immunotherapy-related models need to be recognized by clinicians. Although the imaging prediction of immune markers is universally recognized as more difficult than targeted gene mutations, Jiang et al. [95] achieved an AUC as high as 0.96 in the main cohort, and still maintained a high level of 0.85 in the external cohort. The decline in external validation performance is a common problem in single-center studies, which is caused by differences in patient populations and CT scanning standards across medical institutions. In contrast, the CD8 radiomics feature model constructed by Sun et al. [100] only achieved an AUC of 0.63; this may be attributed to the high spatial heterogeneity of CD8+ cell distribution in tumor tissues, and it is often difficult to fully characterize their microscopic distribution relying solely on macroscopic imaging features. For immunotherapy-related biomarkers (PD-L1, CD8+ TILs, TMB), external validation performance shows greater fluctuations. Jiang et al. achieved an ICV AUC of 0.96 for PD-L1 prediction, while the SCEV AUC fell to 0.85.

Table 3. Prediction of immunotherapy biomarkers based on radiomics, machine learning and CT images.

Author	Year	Method	Data Type	Prediction Target	AUC Value
Jiang et al. [95]	2021	Ridge Regression Recursive Feature Elimination + Logistic Regression	CT Images, Clinical Data	PD-L1 Expression	0.96 for main cohort, 0.85 for external cohort
Wen et al. [96]	2021	LASSO + Logistic Regression	CT Images, Clinicopathological Features	PD-L1 Expression, TMB	0.839
Bracci et al. [97]	2021	Binary Logistic Regression, CT Texture Analysis	Contrast-enhanced CT	PD-L1 Expression (≥50%)	0.789 for validation set
Sun et al. [101]	2020	LASSO Regression + Multivariate Logistic Regression	CT Images, Clinicopathological Data	PD-L1 Expression	0.829 for training set, 0.848 for validation set
Yoon et al. [102]	2020	Multivariate Logistic Regression	CT, Clinical Data	PD-L1 Expression in Advanced Lung Adenocarcinoma	c = 0.646
Liu et al. [103]	2023	CNN + Deep Learning Radiomics Model (DLRM)	Contrast-enhanced Chest CT, Clinicopathological Data	PD-L1 Expression	0.804 for both training and validation sets
Fu et al. [104]	2023	Multi-scale Feature Extraction + Multilayer Perceptron (MLP)	Chest CT Radiomics	PD-L1 Expression in NSCLC	Accuray: 76.57%
Sun et al. [100]	2020	CD8 Radiomics Feature Model	Contrast CT	Outcome of Immunoradiotherapy, Abscopal Effect	0.63
Chen et al. [99]	2023	LASSO Regression + Radiomics Score	CT	Abundance of CD8 + TILs in NSCLC	0.83 for training set, 0.68 for test set
Montoya et al. [105]	2023	NLR + Radiomics Feature Model	CT, Laboratory Data	Immunotherapy Response, OS in NSCLC	0.75
Iwatate et al. [106]	2020	Machine Learning Model	CT	p53 Status, PD-L1 Expression in Pancreatic Cancer	0.795 for p53, 0.683 for PD-L1
Park et al. [107]	2022	LASSO Model	CT, Pathological H&E Sections	Tumor Infiltrating Lymphocytes (TIL)	-
Shiinoki et al. [98]	2022	Null Importance + LASSO + LightGBM	Intratumoral + Peritumoral Radiomics of CT	PD-L1 Expression in NSCLC (≥1%, ≥50%)	0.74 for ≥1%; 0.83 for ≥50%
Chen et al. [108]	2023	Composite Radiomics Features (LCI-RPV)	Contrast-enhanced CT, CD274 RNA	PD-L1 Positivity, Immunotherapy Response in NSCLC	0.70 for test set

In addition, some studies have used radiomics and machine learning methods to predict immunotherapy response and prognosis of NSCLC. Wu et al. [109] integrated radiomics features and clinical features to predict immunotherapy response, achieving AUCs of 0.75 in the validation sets. Yolchuyeva et al. [110] adopted the XGBoost model to predict overall survival (OS) of NSCLC after immunotherapy, with a validation set accuracy of 0.62. Subsequently, Yolchuyeva et al. [111] further used multiple machine learning algorithms to construct a multi-institutional prognostic model to predict the survival outcome of first-line immunotherapy for NSCLC, among which the best model for progression-free survival (PFS) prediction yielded an AUC of 0.604. In addition, Wu et al. [112] adopted machine learning models combined with gene expression profiles and experimental data to identify succinylation-related biomarkers in lung adenocarcinoma, with an AUC as high as 0.912. The above studies indicate that radiomics and machine learning methods show significant clinical application value in predicting immunotherapy response and survival benefit of NSCLC.

82% of included studies only adopted ICV, with AUC ranging from 0.723 to 0.993 for primary prediction tasks assessed in the development cohort; only 18% conducted SCEV, and none completed standardized MCEV. A universal performance attenuation trend is observed: the average AUC drops by 0.06–0.12 from ICV to SCEV. From the perspective of research reproducibility, most CT-based radiomics and machine learning studies in this field are built on single-center private datasets with only internal validation. Even if some models achieve ultra-high AUC values, their performance drops sharply in external validation cohorts, which is closely related to inconsistent CT scanning parameters, reconstruction algorithms and manual tumor segmentation standards across different medical centers. In addition, traditional radiomics relies heavily on manual feature screening. Different feature filtering thresholds and region-of-interest delineation rules may lead to inconsistent final model results, further reducing the reproducibility of such studies. Meanwhile, studies combining clinical features and radiomic nomograms have slightly better replicability.

3.1.2. PET/CT Related Studies

Different from single CT focusing on anatomical features, PET/CT integrates anatomical and metabolic information. Therefore, PET/CT has been widely used in the field of predicting targeted therapy and immunotherapy biomarkers for non-small cell lung cancer. From the perspective of radiogenomics, gene mutations will rewire tumor metabolic pathways, so PET metabolic parameters have a more direct coupling relationship with molecular phenotypes. In terms of biomarker prediction, PET/CT has significant advantages over single CT: firstly, it breaks through the limitation of traditional CT that only relies on tumor diameter to evaluate efficacy; secondly, PET/CT can non-invasively correlate key biomarkers such as tumor gene mutation status, PD-L1 expression and tumor mutation burden (TMB), providing a scientific basis for population screening and regimen formulation of targeted therapy. PET/CT can effectively distinguish true progression from pseudo progression through differences in metabolic activity. Meanwhile, PET/CT relies on functional metabolic parameters to accurately evaluate the tumor immune microenvironment (TIME). PET/CT represents multi-modal fusion of anatomy and metabolism, and its most commonly used tracer is fluorodeoxyglucose, which reflects the degree of glucose metabolism activity of tumor cells. Applying radiomics to PET/CT means that the algorithm not only analyzes the morphological features provided by CT, but also mines the metabolic spatial distribution features brought by PET. Combined with machine learning models, accurate prediction of relevant biomarkers can be achieved.

In terms of targeted therapy biomarker detection, PET/CT is often used to evaluate systemic metastasis of advanced lung cancer, and researchers can accelerate patients into the precision treatment process by utilizing this feature. At present, a number of studies have been carried out on targeted therapy biomarker prediction based on radiomics, machine learning and PET/CT images, as shown in Table 4. Zhang et al. [113] predicted EGFR mutation based on ^{18}F-FDG PET/CT images, achieving a validation set AUC of 0.87 after combining clinical variables; Yang et al. [114] used the random forest (RF) model to predict EGFR mutation and prognosis, with a validation set AUC of 0.71; Shiri et al. [115] adopted multiple classifiers and integrated multi-modal imaging data to predict EGFR and KRAS mutations, with the best AUC of 0.82 for EGFR prediction.

Many studies tend to integrate PET metabolic features, CT anatomical features and clinical data for combined prediction. Notably, random forest (RF) and support vector machine (SVM) are extremely frequently used in such multi-modal studies [114,116,117]. This is because PET and CT features often belong to numerical distributions of different dimensions, and nonlinear classifiers have strong robustness in processing heterogeneous and cross-scale features. Li et al. [116] achieved an amazing AUC of 0.94877 by comparing ^{18}F-MPG with conventional ^{18}F-FDG PET/CT, combined with SVM. The radiomics analysis pipeline proposed by Liu et al. [118] even achieved an AUC of 0.960 for the PET path. However, Koyasu et al. [119] used the Bayesian-optimized XGBoost model, and its AUC for predicting EGFR mutation was only 0.659; Agüloğlu et al. [120] used the naive Bayes model to

predict ALK mutation, with an AUC of 0.682. This suggests that failure to effectively handle the complex feature correlation of multi-modal images will lead to reduced model generalization. From the perspective of reproducibility, PET/CT research faces more prominent challenges than single CT research: the radioactivity calibration, scanning time window and reconstruction parameters of PET equipment varies greatly among institutions. Meanwhile, most PET/CT studies also use single-center data and lack multi-center joint verification. In addition, research is extending from single mutation prediction to co-mutation fields, for example, Li et al. [121] successfully predicted EGFR-TP53 co-mutation in lung adenocarcinoma using correlation analysis and GBDT model, with a validation set AUC of 0.794.

Table 4. Prediction of targeted therapy biomarkers based on radiomics, machine learning and PET/CT images.

Author	Year	Method	Data Type	Prediction Target	AUC Value	Accuracy
Zhang et al. [113]	2020	LASSO + Radiomics Signature Model	F-18-FDG PET/CT, Clinical Variables	EGFR Mutation	0.87 for validation set	-
Yang et al. [114]	2020	Random Forest (RF)	PET/CT Radiomics Features	EGFR Mutation, Prognosis	0.71 for validation set	-
Shiri et al. [115]	2022	6 Feature Selection + 12 Classifiers	Multi-modal Imaging (Including PET)	EGFR, KRAS Mutation	0.82 for Best EGFR	-
Zhang et al. [122]	2020	Multi-step Feature Selection + Radiomics Model	^{18}F-FDG PET/CT, Gender	EGFR Mutation, Subtypes in NSCLC	0.827 for Combined Model; 0.661 for Subtypes	75.29%
Agüloğlu et al. [120]	2022	Naive Bayes	^{18}F-FDG PET/CT, Clinical Data	EGFR, ALK Mutation in NSCLC	0.751 for EGFR; 0.682 for ALK	71.4% for EGFR; 77.4% for ALK
Aide et al. [123]	2022	LASSO Regression (100-fold Cross Validation)	^{18}F-FDG PET, Clinical Data	Targetable Molecular Alterations in Lung Adenocarcinoma	0.866 for training set	-
Li et al. [124]	2022	PET/CT Radiomics + Clinical Features	^{18}F-FDG PET/CT, Clinical Features	EGFR Mutation, Subtypes	0.837 for test set; 0.652 for subtypes	74.1%; 56.7% for subtypes
Zhao et al. [125]	2022	Multi-model Comparison + Nomogram	^{18}F-FDG PET/CT, Clinical Data	EGFR Mutation in Lung Adenocarcinoma	0.864 for Combined Model	-
Gao et al. [126]	2023	LR, RF, SVM + Combined Model	^{18}F-FDG PET/CT, Clinical Data	EGFR Mutation in Lung Adenocarcinoma	0.797 for Stage I–II; 0.723 for Stage III–IV	-
Koyasu et al. [119]	2020	RF, XGB + Bayesian Optimization	^{18}F-FDG PET/CT	EGFR Mutation in NSCLC	0.659 for XGB Model	-
Liu et al. [127]	2020	Random Forest + Logistic Regression + Xgboost	^{18}F-FDG PET/CT	EGFR Subtypes in Lung Adenocarcinoma	0.77 for 19Del; 0.92 for L858R	-
Chang et al. [128]	2021	Multivariate Logistic Regression + Nomogram	PET/CT, Clinical Features	EGFR Mutation in Lung Adenocarcinoma	0.84	-
Li et al. [116]	2021	LASSO + SVM	^{18}F-MPG PET, ^{18}F-FDG PET	EGFR Mutation in Lung Cancer	0.94877	90%
Nair et al. [129]	2021	Multivariate Logistic Regression	CT, PET-CT	EGFR Mutation	0.87 for PET Model	-
Tan et al. [130]	2023	Wilcoxon + LASSO Regression + Prediction Model	^{18}F-FDG PET/CT	EGFR Mutation in Lung Adenocarcinoma	0.90 for training set; 0.79 for test set	-
Zhang et al. [131]	2023	Data Dimensionality Reduction + 4 Classifiers	^{18}F-FDG PET	EGFR Mutation in Lung Adenocarcinoma	0.843 for Logistic Regression	-
Ruan et al. [132]	2024	LASSO Logistic Regression, SVM	^{18}F-FDG PET/CT, Clinical Data	EGFR Mutation in NSCLC	0.741 for SVM validation set	-
Wang et al. [117]	2024	Multivariate Logistic Regression	^{18}F-FDG PET/CT, Clinical Data	EGFR Mutation in Stage IV Lung Adenocarcinoma	0.897	-
Wang et al. [133]	2024	SVM, Logistic Regression	^{18}F-FDG PET/CT, Clinical Data	EGFR Mutation in Solid Lung Adenocarcinoma	0.768 for test set	-
Li et al. [121]	2025	Correlation Analysis + GBDT + Composite Model	^{18}F-FDG PET/CT, Clinical Data	EGFR-TP53 Co-mutation in Lung Adenocarcinoma	0.794 for validation set	
Chang et al. [134]	2021	mRMR + LASSO + Machine Learning	PET/CT, Clinical Data	ALK Rearrangement in Lung Adenocarcinoma	Training Set 0.87; Test Set 0.88	-
Wang et al. [135]	2022	Radiomics Score + Composite Model	CT, PET/CT, EGFR Data	KRAS Mutation	0.921	0.910
Zhang et al. [136]	2023	Mann-Whitney U + Spearman + RFE + LR + Nomogram	^{18}F-FDG PET, Smoking History	KRAS Mutation in Lung Adenocarcinoma	Test Set 0.750	-
Hinzpeter et al. [137]	2024	Correlation Analysis + Prediction Model	^{18}F-FDG PET/CT, NGS	Driver Gene Mutations in NSCLC (TP53, KRAS)	-	-
Liu et al. [118]	2023	Radiomics Analysis Pipeline	^{18}F-FDG PET/CT	EGFR Mutation	CT Path 0.917, PET Path 0.960	

Meanwhile, PET/CT combined with radiomics and machine learning methods has also been widely applied in the prediction of immunotherapeutic biomarkers. By mining the dual information of PET metabolic features and CT texture features through machine learning algorithms, it can identify the advantageous beneficiary

population of immunotherapy more accurately. As shown in Table 5, the multi-model fusion strategy is frequently adopted in current research, and the integration of clinical information, PET metabolic parameters and CT anatomical features has become the standard configuration. For example, Li et al. [138] adopted a multivariate Logistic regression model to evaluate PD-L1 expression based on PET/CT radiomics and clinicopathological features, achieving an AUC of 0.814 in predicting PD-L1; Zhang et al. [139] adopted univariate analysis combined with multivariate Logistic regression model to predict PD-L1 expression status based on ^{18}F-FDG PET/CT and clinicopathological data. Consistent research results indicate that the comprehensive model integrating PET metabolic parameters and clinical information has significantly better predictive performance than single-modal models. In the modeling stage after feature screening, LASSO regression combined with Logistic regression remains the mainstream framework at present [140,141]. In addition, tree-based classifiers and ensemble learning algorithms have been gradually introduced [142,143]. Jiang et al. [140] adopted automatic relevance determination combined with LASSO model in their research to evaluate PD-L1 expression in NSCLC based on PET/CT, with both the single CT path and PET/CT fusion path achieving an AUC of 0.97. In the study by Lim et al. [143], the optimal naive Bayes model after comparing multiple algorithms only achieved an AUC of 0.712. This further confirms that model performance is highly dependent on dataset homogeneity, PET image reconstruction parameters, uniformity of feature extraction standards, and algorithm selection. The research results in Table 5 demonstrate that machine learning radiomics based on PET/CT multimodal metabolic-anatomical information has exhibited high diagnostic efficacy in the auxiliary screening of key immunotherapeutic targets such as PD-L1.

Table 5. Prediction of immunotherapeutic biomarkers based on radiomics, machine learning and PET/CT imaging.

Author	Year	Methodology	Data Type	Prediction Target	AUC Value
Li et al. [138]	2021	LASSO Regression + Multivariate Logistic Regression	PET/CT Radiomics, Clinicopathological Features	PD-L1 Expression (≥50%)	0.814
Lim et al. [143]	2022	Multiple Machine Learning Algorithms (Naive Bayes Optimal)	PET/CT Radiomics	PD-L1 Expression	0.712
Wang et al. [144]	2023	5 Machine Learning Classifiers	PET/CT Images	PD-L1 Status	Test Set 0.813
Wang et al. [145]	2020	Correlation Analysis	^{18}F-FDG PET/CT	NSCLC Immunomarkers (CD8 TILs, PD-L1)	-
Wu et al. [146]	2022	Correlation Analysis, ROC Analysis	^{18}F-RGD PET/CT, Molecular Data	NSCLC PD-L1 Expression	-
Jiang et al. [140]	2020	Automatic Relevance Determination + LASSO Model	PET/CT	NSCLC PD-L1 Expression (SP142 ≥ 1%)	CT Model 0.97, PET/CT Model 0.97
Wang et al. [147]	2020	Prediction Model for Modeling and Validation Cohorts	^{18}F-FDG PET/CT	PD-L1 Expression in Advanced NSCLC	Accruary: 84.8%
Zhang et al. [139]	2022	Univariate Analysis + Multivariate Logistic Regression	^{18}F-FDG PET/CT, Clinicopathological Data	PD-L1 Expression in Untreated NSCLC	-
Ji et al. [142]	2025	Otsu Method + Extra Trees Classifier	^{18}F-FDG PET/CT, TCGA Gene Expression Data	PD-L1 Expression in LA-NSCLC	Training Set 0.833, Test Set 0.786
Kiss et al. [141]	2025	Mann-Whitney U Test + LASSO Regression + Logistic Regression	^{18}F-FDG PET/CT Radiomics	NSCLC PD-L1 Expression	Optimal Model 0.783
Zhou et al. [148]	2021	Composite Metabolic Features + Combined Model	Dual-phase ^{18}F-FDG PET/CT, Molecular Data	Immune Type of Tumor Microenvironment in NSCLC (TMIT-I)	0.818
Cui et al. [149]	2022	Logistic Regression Model	Baseline/Preoperative ^{18}F-FDG PET/CT	Pathological Response to Neoadjuvant Immunochemotherapy in Stage III NSCLC	-
Yang et al. [150]	2024	LASSO Regression + Radiomics Model	^{18}F-FDG PET/CT	Pathological Complete Response to Neoadjuvant Immunochemotherapy in NSCLC	Validation Set 0.818

3.1.3. MRI Related Studies

In addition to the three common modalities mentioned above, some studies have explored the use of MRI images to predict biomarkers in non-small cell lung cancer (NSCLC). Ahn et al. [151] adopted machine learning algorithms, combined with contrast-enhanced T1-weighted MRI image features to detect EGFR mutations, with

the RF classifier achieving an AUC of 0.868; Meissner AK et al. [152] used a random forest classifier to predict PD-L1 expression in NSCLC patients with brain metastasis based on preoperative enhanced T1-weighted MRI, achieving a test set AUC of 0.84; Hu et al. [153] adopted LASSO regression to construct a radiomics signature extracted from chest CT and enhanced MRI, which significantly improved the predictive performance for EGFR status, with the combined model (RS-BM-Com) achieving an AUC of 0.882 in the external validation set. The above studies indicate that machine learning-based methods can effectively mine deep features in MRI images and achieve reliable prediction of key NSCLC biomarkers such as EGFR and PD-L1. Most MRI-related studies in this field only adopted ICV. Combined with external validation analysis, MRI models have the worst generalization potential among all imaging modalities. Even if the ICV performance is good, it is difficult to guarantee stable performance in external independent cohorts. Large-sample multi-center external validation is urgently needed for MRI-based biomarker prediction models.

3.2. Deep Learning Methods

Deep Neural Networks (DNN) realize end-to-end automatic feature learning from raw images, overcoming the limitations of manual feature engineering in traditional radiomics. At present, mainstream deep learning architectures applied to NSCLC biomarker prediction mainly include CNN, Transformer and generative models, as well as emerging foundation models. Convolutional Neural Networks extract features based on local receptive fields, with outstanding advantages in capturing local texture and morphological information of lesions. Transformer relies on the self-attention mechanism to establish long-distance feature associations across the whole image, which is more suitable for analyzing tumors with high spatial heterogeneity. Generative AI such as GAN and diffusion models are mainly used for medical data augmentation to solve the problem of insufficient samples for rare mutations. Vision and pathology foundation models have strong cross-task migration capabilities, but are restricted by high computing power requirements. Traditional radiomics only extracts predefined features based on expert experience, while deep learning can mine high-order hidden features related to tumor molecular phenotypes. Given the high cost of medical image acquisition and scarcity of annotated samples, transfer learning technology based on pre-trained weights from large natural image datasets has been widely adopted. Transfer learning alleviates the problem of insufficient medical labeled data and reduces the risk of model overfitting. In addition, advanced architectures such as Squeeze-and-Excitation attention module and EfficientNet have been widely used in relevant studies to endow the model with stronger lesion focusing ability and improve parameter efficiency. From the perspective of model interpretability, traditional end-to-end deep learning belongs to typical black-box models. Its feature extraction and decision-making processes are implicit and uninterpretable. At present, Grad-CAM, class activation mapping and other visual interpretation tools are the most commonly used XAI techniques for deep learning in this field, which can roughly locate the image regions that the model focuses on for prediction.

3.2.1. Convolutional Neural Network Related Studies

In the prediction of targeted gene biomarkers for NSCLC, the non-invasive, real-time and dynamic prediction using deep learning models based on CT or PET/CT images is regarded as an effective way to overcome the intratumoral heterogeneity of biopsy specimens. Macroscopic signs in CT images such as lobulation, spiculation, pleural indentation and ground-glass opacity components, after being extracted by deep neural networks, can establish a strong mapping relationship with underlying genomics, making it possible to predict targeted biomarkers through CT images.

As shown in Table 6, the vast majority of targeted therapy-related studies focus on EGFR mutation prediction, which is consistent with the clinical epidemiological characteristics of the high EGFR mutation rate (approximately 40–50%) among East Asian patients with lung adenocarcinoma. Current research is not only limited to the binary classification of mutation status [47,154], but also moving towards refined mutation subtype classification [155] and direct prediction of survival benefits from TKI targeted therapy [156,157]. In addition to EGFR, a few studies also cover KRAS mutations [158] and ALK rearrangements [159]. In terms of algorithm architecture, the most frequent keywords are 3D CNN and its residual network variants, such as ResNet34 adopted by Jia et al. [47] and the 18-layer CNN developed by Song et al. [155]. Meanwhile, lightweight and high-efficiency network architectures are increasingly favored, such as EfficientNetV2 [157,160] and SE-CNN with attention mechanism [161]. The multi-channel multi-task deep learning model adopted by Dong et al. [158] realized the simultaneous prediction of EGFR and KRAS, indicating that researchers are attempting to use the shared weight mechanism of network architecture to capture potential exclusive or synergistic imaging features between different mutations. In terms of predictive performance, the highest performance comes from the 3D CNN model developed

by Zhang et al. [162], which achieved an AUC as high as 0.947 for predicting EGFR mutations. However, some studies showed a decline in performance in external validation or multi-center testing. For example, Shao et al. [163] used 3D CNN combined with transfer learning to predict EGFR mutations in lung adenocarcinoma, with a test set AUC of 0.730; Wang et al. [29] also achieved a test set AUC of 0.73 for predicting EGFR. This reflects that differences in CT image parameters and equipment heterogeneity among different institutions are still the main challenges affecting the cross-center generalization ability of deep learning models. Statistical results from Table 6 show that CNN-based deep learning models have more significant performance attenuation in external validation than traditional machine learning models: the average AUC drops by 0.13–0.20 from ICV to SCEV. In terms of interpretability, most CNN studies adopt Grad-CAM to generate heat maps to visualize the model's attention areas on CT or pathological images. This method can intuitively display which tumor regions drive the prediction results, but it can only provide shallow visual explanation. Only a few studies combined Grad-CAM results with pathological analysis to explore the pathological basis of model decision-making.

Table 6. Prediction of targeted therapy biomarkers based on deep learning methods.

Author	Year	Methodology	Data Type	Prediction Target	AUC Value	Accuracy
Jia et al. [47]	2023	ResNet34 + Hybrid Loss Function	CT Images	EGFR Mutation	0.8861	81.58%
Zhang et al. [161]	2020	SE-CNN (Squeeze-and-Excitation Convolutional Neural Network)	CT, Clinical Data	EGFR Mutation in Lung Adenocarcinoma	Internal 0.910, External 0.841	-
Dong et al. [158]	2021	Multi-channel Multi-task Deep Learning (MMDL)	CT, Clinical Data	EGFR, KRAS Mutation	-	Training 79.43%, Validation 75.06%
Yoon et al. [164]	2022	Deep Learning + Clinical Factors	CT Images	EGFR Mutation in Pure Ground-glass Nodule Lung Adenocarcinoma	Test Set 0.85	-
Huang et al. [165]	2022	Resnet-101, LightGBM, LR + Fusion Model	CT, Clinical, Radiomics	EGFR Mutation	0.751	-
Wang et al. [15]	2022	Fully Automatic AI System (FAIS)	CT, Clinical Data	Lung Cancer EGFR Genotype, TKI Response	0.748–0.813	-
Deng et al. [156]	2022	EfficientNetV2-based ESBP System	CT Images	Survival Benefit from TKI/ICI in Stage IV NSCLC	-	-
Song et al. [155]	2021	18-layer CNN + Grad-CAM	CT Images	EGFR Mutation Subtype in Lung Adenocarcinoma	Micro-average 0.78, Macro-average 0.79	-
Song et al. [159]	2021	Deep Learning Model (DLM)	CT, Clinicopathological Data	ALK Fusion, TKI Response	Validation Set 0.8481	-
Mahajan et al. [166]	2024	3D CNN (Automatic Segmentation + Feature Extraction)	CT, Clinical Semantic Features	EGFR Mutation	0.88 ± 0.03	-
Zhang et al. [162]	2024	3D CNN Model	CT Images	EGFR Mutation	0.947	-
Xiao et al. [160]	2023	EfficientNet-V2 + PET/CT Fusion	PET/CT Images	NSCLC EGFR Mutation	-	81.92%
Shao et al. [163]	2024	3D CNN + Transfer Learning (TS_TL)	PET/CT, Clinical Data	EGFR Mutation in Lung Adenocarcinoma	Test Set 0.730	-
Yin et al. [167]	2021	Squeeze-and-Excitation ResNet + Stacked Generalization	PET/CT Images	EGFR Mutation	Stacked Model 0.84	-
Mu et al. [26]	2020	EGFR-DLS Deep Learning Model	^{18}F-FDG PET/CT	NSCLC EGFR Mutation	-	High
Xu et al. [157]	2024	EfficientNetV2-L	CT Images, RNA Sequencing	EGFR Mutation, TKI Prognosis	Test Set 0.907	-
Silva et al. [168]	2021	Deep Transfer Learning + Model Stacking	CT Images	NSCLC EGFR Mutation	0.98	

Meanwhile, deep learning methods based on CT and PET/CT images have been widely applied in the prediction of immunotherapeutic biomarkers, as shown in Table 7. Current research directions are mainly divided into two categories: one is dedicated to predicting PD-L1 expression thresholds, such as the classification study on high PD-L1 expression (≥50%) by Tian et al. [169]; the other is to directly predict clinical endpoint indicators of immunotherapy, such as the prediction of immunotherapy response in advanced NSCLC by He et al. [170] and

early treatment response in unresectable NSCLC by Yuan et al. [171]. In terms of model architecture, 3D DenseNet is a highly frequently used and deep network architecture. Zhu et al. [172] applied 3D DenseNet to predict PD-L1 expression status in advanced lung adenocarcinoma; Liang et al. [173] also adopted the 3D DenseNet121 model and achieved an AUC of 0.96. In contrast, Tian et al. [169] achieved a test set AUC of 0.76 for predicting PD-L1, which to a certain extent implies that single modality may have a performance upper limit in characterizing complex immune microenvironment features.

Table 7. Prediction of PD-L1 expression and immunotherapeutic biomarkers based on deep learning methods and CT/PET/CT imaging.

Author	Year	Methodology	Data Type	Prediction Target	AUC Value
Wang et al. [29]	2021	3D CNN + Prognostic Model	CT Images, Clinical Data	EGFR Mutation, PD-L1 Expression	0.73 for EGFR in Test Set
Tian et al. [169]	2021	3D Convolutional Neural Network	CT Images	PD-L1 Expression (≥50%), Immunotherapy Response	0.76 in Test Set
He et al. [170]	2020	3D-Densenet + TMB Radiomic Signature	CT Images	Immunotherapy Response in Advanced NSCLC	0.81 in Test Set
Zhu et al. [172]	2020	3D DenseNet	Enhanced Thin-Slice CT	PD-L1 Expression in Advanced Lung Adenocarcinoma	>0.750
Saad et al. [174]	2023	Ensemble Deep Learning (Deep-CT)	CT Images, Clinicopathological Data	ICI Benefit in NSCLC	OS C-index 0.75
Yuan et al. [171]	2025	DenseNet121 + SIINI Combined Model	CT Images, Laboratory Data	Early Immunotherapy Response in Unresectable NSCLC	0.865 in Internal Validation
Liang et al. [173]	2024	3D DenseNet121 + Structured Data Embedding	PET/CT Images, Clinical Features	PD-L1 Expression	0.96
Mu et al. [175]	2021	SResCNN + Deep Learning Score (DLS)	^{18}F-FDG PET/CT	PD-L1 Status, Immunotherapy Response	≥0.82 in External Test Set
Huang et al. [176]	2025	Habitat Analysis + Multiple Instance Deep Learning (DenseNet121+K-means+Extra-Trees)	CT Images, Clinical Data	Efficacy of PD-1/PD-L1 Immunotherapy in NSCLC	0.906 in Training Set, 0.889 in Validation Set, 0.831 in Test Set

Deep learning methods can also automatically mine relevant biomarkers for NSCLC from pathological images. As the gold standard for clinical diagnosis, pathological images directly reflect the downstream phenotypic evolution of gene mutations through the size, shape and the heterogeneity of tissue structure. With powerful feature extraction and pattern recognition capabilities, deep learning can effectively handle gigapixel image analysis tasks and realize automated and accurate prediction of relevant biomarkers. It can independently mine shallow details such as cell morphology and deep implicit features directly from pathological sections, thereby capturing complex pathological patterns closely related to key biomarkers.

At present, numerous studies on targeted gene mutation prediction based on deep learning and pathological images have emerged, covering EGFR [49,177–180], ALK rearrangement [181], KRAS and even TP53 mutations [44], as shown in Table 8. Some cutting-edge studies have begun to explore multi-task learning and the construction of underlying foundation models. For example, Wang et al. [182] proposed CHIEF, which is capable of processing whole slides from 19 anatomical sites. In terms of immunotherapy biomarker prediction, most studies focus on PD-L1 expression [183,184] and tumor mutation burden (TMB) assessment [185,186]. In the process of algorithm evolution, early studies mostly adopted classic CNN models such as ResNet, DenseNet, Visual Geometry Group 16 (VGG16) and Inception-ResNet-v2 for feature analysis; subsequently, more powerful architectures such as multi-resolution deep learning [185] were introduced successively. Among these studies, several models have demonstrated outstanding performance: Mayer et al. [187] used advanced CNN to directly identify ALK and ROS1 fusions from H&E-stained sections, with both detection sensitivity and specificity reaching 100%; Yong et al. [50] adopted in-domain transfer learning for cancer detection, achieving an accuracy of up to 99.78%. Translating morphological features into genetic codes is an extremely challenging task, yet AI has delivered strong performance. When predicting highly difficult EGFR mutation subtypes, Zhang et al. [180] achieved an extremely high AUC of 0.927 in a surgical specimen cohort by combining contrastive learning and deep learning model. Jain and Massoud [185] utilized multi-resolution deep learning to predict TMB, with an average precision (AP) of 0.89. However, not all models can achieve satisfactory predictive performance. Niu et al. [188] obtained a 5-fold cross-validation AUC of only 0.64 for TMB prediction in the TCGA cohort; Dammak et al. [189] used VGG16 for TMB prediction, achieving an external test AUC of merely 0.65. In summary, Table 8 depicts the transformative potential

of deep learning in pathological image analysis. Computational pathology is rapidly evolving from a traditional auxiliary tool into a critical means for exploring potential biomarkers in precise NSCLC diagnosis and treatment.

Table 8. Prediction of biomarkers based on deep learning and pathological images.

Author	Year	Methodology	Data Type	Prediction Target	AUC Value	Accuracy
Ishii et al. [190]	2022	Neural Network Model	Microscopic Images of Lung Cancer Cytological Samples	ALK Fusion, EGFR Mutation, KRAS Mutation	-	≈0.95 for EGFR/KRAS
Mayer et al. [187]	2022	Advanced Convolutional Neural Network (CNN)	H&E-Stained Sections	ALK, ROS1 Fusion	-	100% Sensitivity, 100% Specificity
Zhao et al. [178]	2023	ResNet-50	Pathological Images	EGFR Mutation	0.82 in Test Set	-
Hondelink et al. [191]	2022	Supervised Deep Learning	PD-L1-Stained Whole Slides	Automatic TPS Assessment	-	79% Concordance
Choi et al. [192]	2022	AI-powered TPS Analyzer	PD-L1-Stained Whole Slides	PD-L1 Expression (Reducing Observer Variability)	-	90.2% Concordance
Liu et al. [193]	2021	Automated Tumor Proportion Scoring System	PD-L1-Stained Sections	TPS Assessment	-	PCC = 0.9436
Tomita et al. [49]	2022	Weakly Supervised CNN	H&E-Stained FFPE Whole Slides of Lung Adenocarcinoma	EGFR Mutation	0.799 in DHMC Cohort	-
Pao et al. [177]	2023	Attention Mechanism-Based Deep Learning	H&E Sections of Advanced Lung Adenocarcinoma	EGFR Mutation	0.870	-
Zhao et al. [194]	2025	DeepGEM Multiple Instance Learning	Lung Cancer Biopsy Sections, NGS Data	Lung Cancer Gene Mutations	0.80–0.91 for Resection Biopsy	-
Zanoletti et al. [179]	2025	Two-Stage CNN (InceptionResNet-V2) + Grad-CAM	H&E Whole Slides of NSCLC	EGFR Mutation	0.77	76.67%
Terada et al. [181]	2022	DenseNet	Virtual H&E Sections of NSCLC	ALK Rearrangement	0.73 at 1.0 μm/pixel Resolution	-
Noorbakhsh et al. [40]	2020	CNN	TCGA H&E Sections	TP53 Mutation	0.65–0.80	-
Morel et al. [44]	2023	CNN	H&E Sections of Lung/Breast/Colorectal Cancer	Driver Mutations Including KRAS, EGFR, TP53	positive predictive: 90.6%	-
Raczkowska et al. [42]	2022	ARA-CNN + Machine Learning	H&E Sections of NSCLC	PDGFRB Mutation	0.735	-
Jain et al. [185]	2020	Image2TMB Multi-Resolution Deep Learning	H&E Sections of Lung Adenocarcinoma	TMB	0.92 in Precision-Recall Curve	0.89 Average Precision
Sadhwani et al. [186]	2021	CNN + Clinical Integration Model	H&E Whole Slides of Lung Adenocarcinoma + Clinical Data	TMB	0.71	-
Niu et al. [188]	2022	Deep Learning	TCGA H&E Sections of Lung Adenocarcinoma	TMB	0.64 in 5-Fold Cross-Validation	-
Dammak et al. [189]	2023	VGG16 Transfer Learning	H&E Sections of Multi-Center Lung Squamous Cell Carcinoma	TMB	0.65 in External Test	-
Wang et al. [195]	2021	Dual-Scale Classification Deep Learning	PD-L1 Immunohistochemical Images	PD-L1 Expression	-	88% Concordance with Pathologists
Cheng et al. [183]	2022	3 Deep Learning AI Models	PD-L1 22C3/SP263 Sections	PD-L1 Expression in Lung Cancer	-	96.4% for M2/M3 in SP263
Wu et al. [184]	2022	Deep Learning Tumor Detection + AI System	PD-L1 22c3/SP263 Whole Slides	PD-L1 Expression	-	R = 0.9429–0.9787 for TPS Concordance
Ligero et al. [196]	2024	Weakly Supervised Deep Learning	PD-L1 IHC Sections	Immunotherapy Response in Solid Tumors	0.88 ± 0.06 in NSCLC Cohort	-

Table 8. *Cont.*

Author	Year	Methodology	Data Type	Prediction Target	AUC Value	Accuracy
Fu et al. [39]	2020	Deep Transfer Learning	Pathological Images, Genomic Data	Pan-Cancer Mutation, Prognosis, Tumor Classification	-	Accurately classify cancer types
Kather et al. [197]	2020	Deep Learning	Pan-Cancer Pathological Images	Clinically Actionable Genetic Alterations	-	consistently infer a wide range of genetic mutations
Lu et al. [198]	2021	TOAD Deep Learning	Routine H&E Sections	Tumor Origin of Cancer of Unknown Primary	-	0.83 for Top-1
Wang et al. [199]	2021	HEAL Deep Learning Framework	H&E Sections of Lung/Colorectal Cancer	Multi-Task Pathological Analysis	AUC value of 0.732	-
Chen et al. [43]	2023	Unsupervised Clustering Multiple Instance Deep Learning	H&E Sections of Three Cancer Types	Optimization of Gene Mutation Prediction	0.631–0.747	-
Lu et al. [46]	2024	PathChat Vision-Language Model	Pathological Sections + Text Data	Auxiliary Diagnosis of Lung Cancer Pathology	-	78.5%
Wang et al. [182]	2024	CHIEF Pathological Foundation Model	Whole Slides of 19 Anatomical Sites	Cancer Cell Detection, Tumor Origin	-	Optimal Performance in 32 Datasets
Yong et al. [50]	2024	Transfer Learning + Ensemble Learning	Pathological Images	Cancer Detection	-	99.78% in GasHisSDB
Huang et al. [200]	2022	Aitrox AI Segmentation Model	PD-L1-Stained Whole Slides	PD-L1 Expression Scoring	-	Strong Correlation with Gold Standard
Zhang et al. [180]	2024	CNN (Contrastive Learning) + Vision Transformer	H&E-Stained Whole Slides	EGFR Mutation Subtype	0.927 in USTC Surgical Specimen Cohort	-
Campanella et al. [201]	2025	Fine-Tuned Open-Source Foundation Model	Pathological Images	EGFR Mutation	0.870 in External Validation	-
Huang et al. [41]	2021	DeepIMLH (CNN + ResNet + Deep Convolutional Gaussian Mixture Model)	H&E-Stained Sections of Lung Cancer	Lung Cancer Gene Mutations, Targeted Drug Efficacy	-	Favorable
Sun et al. [27]	2024	Transformer Aggregation Model	Pathological Images	Gene Mutations Including TP53, CSMD3	4% Increase in Average AUC	-

Meanwhile, some studies have applied deep learning methods to MRI models to predict the mutation status of biomarkers. Given that patients with EGFR mutations have a significantly higher probability of brain metastasis, deriving the genetic status of primary lung cancer by mining imaging features from multi-sequence MRI has become a highly innovative research direction. Li et al. [202] proposed a radiomics combined with graph convolutional network architecture (Radio-GCN) model, which predicted EGFR mutation subtypes based on multi-sequence MRI, achieving an astonishing AUC of 0.996 in the lesion-level test set. You et al. [203] developed the EGFR-TKI System, which accurately predicts EGFR genotypes and TKI treatment response in metastatic NSCLC based on brain MRI images. In addition, Cao et al. [204] adopted ResNet34 and deep learning radiomics models to predict EGFR mutation status in lung adenocarcinoma patients with brain metastasis based on multi-sequence MRI, with the fusion model achieving an AUC of 0.936 in the validation set. The above studies suggest that deep learning can effectively capture specific imaging phenotypes in the microenvironment of brain metastases.

3.2.2. Research on Other Deep Learning Models

In the past few years, the field of deep learning has witnessed leapfrog development, with more advanced architectures such as Transformer and generative artificial intelligence emerging. Transformer initially occupied a core position in natural language processing. It relies on the self-attention mechanism to calculate the association

weights between any two patches in an image. This enables the model to simultaneously capture spatial interaction features between the tumor core, peritumoral region, and even the distal lung parenchyma. At the same time, generative adversarial networks (GAN) can synthesize high-quality simulated medical images by learning the data distribution of real samples, effectively alleviating the class imbalance and small-sample problems. For Transformer and CNN-Transformer fusion models, most current research is still in the internal validation stage. A small number of SCEV results show that the global feature capture advantage of Transformer cannot completely offset equipment heterogeneity, with an average AUC attenuation of 0.11–0.17 in external cohorts. In terms of interpretability, Transformer relies on self-attention mechanism, and researchers can visualize the attention weight distribution between image patches to explain the model's global feature association logic. In contrast, the GAN exhibits poor interpretability. Its data generation and discrimination procedures are largely implicit.

At present, Transformer has been widely applied in feature extraction and prediction of NSCLC biomarkers, as shown in Table 9. Zhao et al. [48] proposed GMILT network designed for medical images, achieving an AUC of 0.856 in predicting EGFR mutation status; Fang et al. [205] developed the TransMIEL model combining multiple instance reinforcement learning; in addition, fusion architectures of CNN and Transformer have also demonstrated strong performance potential. In addition to the classic EGFR mutation status prediction [48,205], researchers are using new technologies to tackle more challenging clinical tasks. For example, the MUSK model proposed by Xiang et al. [206] marks the entry of this field into the era of large models, constructing a multimodal Transformer architecture capable of processing digital pathological images and text data simultaneously. The multi-label multi-task system developed by Shao et al. [207] can simultaneously predict 8 key gene mutations and PD-L1 expression in NSCLC, with an average AUC of 0.862. With their global vision and powerful feature representation capabilities, models such as Transformer have significantly improved the robustness and generalization ability of models. Beyond lightweight task-specific deep learning architectures, large vision foundation models and advanced generative AI have gradually become pivotal driving forces for the innovation of NSCLC radiogenomics research. Pre-trained foundation models break the limitation that traditional deep networks rely on small-scale labeled clinical data. In current research, pathology foundation models, multi-modal vision-language foundation models are increasingly adopted for NSCLC biomarker prediction: these models greatly improve the model adaptability for low-sample clinical scenarios. Foundation models can integrate multi-type imaging and clinical text information, and deliver more stable predictive performance across different cohorts. Meanwhile, foundation models also facilitate high-throughput mining of implicit correlations between imaging phenotypes and molecular biomarkers, accelerating the discovery of novel radiomic signatures. Modern generative AI represented by diffusion models has further expanded the application boundary of generative technology in this field. Song et al. [208] used GAN models to directly predict the risk of disease progression during EGFR-TKI targeted therapy. Unlike traditional GANs, which are prone to mode collapse, diffusion models generate high-fidelity medical images with more stable quality. They are used for data augmentation to address the scarcity of labeled samples for rare mutations.

Table 9. Prediction of biomarkers based on advanced deep learning methods.

Author	Year	Methodology	Data Type	Prediction Target	AUC Value	Accuracy
Zhao et al. [48]	2024	GMILT Transformer Network	CT Images	EGFR Mutation Status	0.856 in TCIA Test Set	-
Fang et al. [205]	2025	TransMIEL Model (Transformer Multiple Instance Reinforcement Learning)	-	EGFR Mutation	Outperforms Existing Methods	-
Xiang et al. [206]	2025	MUSK Model (Multimodal Transformer)	Pathological Images, Text Data	Lung Cancer Immunotherapy Response	Optimal Performance in 23 Benchmarks	-
Zhao et al. [209]	2024	Denseformer Framework (CNN + Transformer Fusion)	3D Lung CT	EGFR Mutation	Outperforms Single-Modal CT Models	-
Song et al. [208]	2020	Bidirectional Generative Adversarial Network (GAN)	CT Images	Risk of Disease Progression during EGFR-TKI Therapy	-	-
Dehkharghanian et al. [38]	2023	DenseNet121, KimiaNet	TCGA Pathological Images	Image Acquisition Site	-	Over 86% for KimiaNet
Shao et al. [207]	2022	Multi-Label Multi-Task Deep Learning (MMDL)	CT Images, Molecular Data	8 Gene Mutations and PD-L1 Expression in NSCLC	0.862	-
Gui et al. [210]	2022	Multi-Task Learning Model (AIRNet)	CT Images	EGFR Mutation in NSCLC	-	-

3.3. Hybrid Models

Hybrid models enhance the performance of single tasks by combining multiple models or technologies, fully integrating the core advantages of machine learning and deep learning. They compensate for the shortcomings of single models in feature extraction, generalization adaptation, and other aspects, thereby strengthening the performance of the core task of predicting NSCLC-related biomarkers.

3.3.1. Fusion of Heterogeneous Models

Single models often inevitably suffer from bias or high variance. Heterogeneous model fusion draws on the advantages of different models. Specifically, combining completely different algorithms such as LR, SVM and RF can effectively break through the limitations of single models, making the prediction model more stable. Table 10 displays studies on biomarker prediction using multi-model fusion. It can be seen that model stacking and parallel multi-classifiers are the mainstream approaches. Feng et al. [211] adopted a complex combination of LR, SVM, RF and XGBoost combined with SMOTE. Meanwhile, stacking different deep learning models can also yield high prediction results. Chen et al. [212] used a stacked deep learning model to predict EGFR mutations based on PET/CT images and clinical data, achieving an AUC of 0.85 ± 0.09. Some studies also stacked different deep learning models: Qin et al. [213] adopted a Convolutional Neural Network–Long Short-Term Memory (CNN-LSTM) hybrid DNN model to detect EGFR mutations, integrating the advantages of both CNN and LSTM. On the premise of sufficient computing power, replacing single models with heterogeneous stacking is a choice to pursue higher prediction accuracy with limited medical sample sets.

Table 10. Studies on biomarker prediction based on heterogeneous model fusion.

Author	Year	Method Adopted	Data Type	Prediction Target	AUC Value	Accuracy
Feng et al. [211]	2022	LR + SVM + RF + XGBoost + SMOTE	CT Images	EGFR Mutation	Test Set 0.8654	-
Prelaj et al. [214]	2022	CatBoost, LR, NN, RF, SVM + SHAP	Real-World Data	NSCLC Immunotherapy Efficacy	-	OS6 0.83
Benfares et al. [215]	2025	Random Forest	Clinical + CT Morphology + Radiomics	EGFR Mutation	5-Fold 0.91	-
Qin et al. [216]	2020	Artificial Neural Network (ANN), Logistic Regression	Clinical + CT + Serum Markers	EGFR Mutation	Model2 0.882 Model1 0.909	-
Shiinoki et al. [98]	2022	Null Importance + LASSO + LightGBM	Intratumoral + Peritumoral Radiomics of CT	NSCLC PD-L1 Expression	0.83	-
Wang et al. [217]	2022	10 Machine Learning Classifiers	Molecular Data	Durable Response to Immunotherapy	SVM_poly 0.77–0.78	-
Chen et al. [212]	2022	Stacked Deep Learning (PET/CT + ResNet + SVM)	PET/CT + Clinical	EGFR Mutation	0.85 ± 0.09	-
Qin et al. [213]	2020	CNN + LSTM Hybrid DNN	CT + Clinical	EGFR Mutation	0.78	75%

3.3.2. Heterogeneous ML-DL Ensemble Model

Compared with independently constructed deep learning models, the ML-DL ensemble model integrating machine learning and deep learning can make up for the application shortcomings of single deep learning models in the task of non-small cell lung cancer biomarker prediction. It not only relies on deep learning to extract high-dimensional visual features and implicit pathological patterns, but also uses classical machine learning algorithms to process structured clinical data and realize efficient fusion of multimodal information. The ML-DL ensemble model balances model accuracy and interpretability, retaining the high-precision advantage of deep learning while clarifying feature contribution through the machine learning module.

Table 11 presents studies on biomarker prediction based on heterogeneous ML-DL ensemble models. The splicing of deep learning and machine learning greatly enhances model performance. For example, the ResNet + PyRadiomics (version 2.2.0) + SVM architecture proposed by Yao et al. [218] perfectly complements different features, achieving an AUC of 0.94 for EGFR prediction. Peng et al. [219] adopted CNN combined with three traditional machine learning algorithms and a nomogram model to evaluate durable clinical benefit and prognosis in NSCLC patients, with the model achieving a high AUC of 0.959. Zhang et al. [220] employed the Deep-RadScore model with an external test set AUC of 0.884 for EGFR prediction. The combination of XGBoost and deep learning is extremely common, such as the XGBoost + 3D ConvNeXt model constructed by Hao et al. [221].

These studies indicate that deep learning networks can achieve satisfactory predictive performance when well-integrated with multi-dimensional evaluation tools at the level of underlying logic. Although heterogeneous models perform well in internal cohorts, their performance often regresses to a realistic level when faced with external test sets. The multi-task deep neural network proposed by Gong et al. [222] achieved an external validation set AUC of 0.80 ± 0.05 for EGFR mutation prediction; the fused nomogram by Wu et al. [223] obtained an external test set AUC of 0.809. These values reflect the most authentic and robust cross-center generalization capability at present. In terms of reproducibility, hybrid models have intermediate performance between traditional machine learning and pure deep learning. At present, there is a lack of unified standard frameworks for hybrid model construction in this field, and the combination modes of different algorithms vary greatly among studies. Compared with pure deep learning models, hybrid models integrate interpretable radiomic features, which plays a certain role in suppressing the interference of equipment noise.

Table 11. Studies on biomarker prediction based on heterogeneous ML-DL ensemble models.

Author	Year	Hybrid Method	Data Type	Prediction Target	AUC Value
Vanguri et al. [224]	2022	Expert-Guided Feature Extraction + Integrated Model	CT, Pathological Images, Genome	PD-(L)1 Treatment Response	0.80 (95% CI 0.74–0.86)
Hao et al. [221]	2024	XGBoost + 3D ConvNeXt + Radiomics + Multi-Model Fusion	CT Images	EGFR Mutation Subtype	Fusion Model 0.801
Kim et al. [225]	2024	CNN + Radiomics + Clinical Data Fusion	Contrast-Enhanced CT	EGFR Mutation	Internal Cohort ≈ 0.81
Gong et al. [222]	2023	Multi-Task Deep Neural Network DNN + Radiomics + Feature Fusion	CT Images	NSCLC EGFR Mutation	External Validation 0.80 ± 0.05
Huang et al. [176]	2025	DenseNet121 + K-means + Extra-Trees + Multi-Instance Deep Learning	CT, Clinical Data	NSCLC PD-1/PD-L1 Efficacy	High Performance in Each Dataset
Peng et al. [219]	2022	CNN + 3 Traditional Machine Learning + Nomogram	Molecular Data	NSCLC Immunotherapy Durable clinical benefit (DCB)	CNN DCB 0.959–0.965
Huang et al. [226]	2022	Radiomics RM, Deep Learning DLM, Hybrid Model HM	PET/CT, Clinical	NSCLC EGFR Mutation	Hybrid Model Validation Set 0.85
Zhang et al. [220]	2024	Deep-RadScore (Radiomics + Deep Learning Feature Fusion)	CT, Molecular Data	NSCLC EGFR Mutation	External Test 0.884
Zuo et al. [227]	2023	LightGBM/XGBoost + SHAP/LIME + Cox	^{18}F-FDG PET/CT, Clinical	Lung Adenocarcinoma EGFR Mutation, Prognosis	Prognostic C-Index 0.863
Zuo et al. [228]	2024	11 Feature Selection + 7 Classifiers + XAI Explainable AI	^{18}F-FDG PET/CT, Clinical	Lung Adenocarcinoma EGFR Mutation	Optimal External Test 0.81
Wu et al. [223]	2024	Habitat Radiomics, Deep Learning, Fused Nomogram	CT, Clinical Data	Stage I NSCLC EGFR Mutation	Fused External Test 0.809
Yao et al. [218]	2024	ResNet + PyRadiomics + SVM	PET/CT	EGFR Sensitive Mutation	0.94

3.4. Multimodal Prediction Model

Tumors represent an extremely complex three-dimensional spatiotemporal evolutionary ecosystem. Single-modal imaging data can reflect density differences, morphological changes, and metabolic characteristics of tumors, whereas genomic data alone can reveal underlying molecular mutations. Multimodal data can integrate information from different dimensions: medical imaging (CT/PET) reflects macroscopic structure, whole-slide pathological images reflect microscopic cell morphology, peripheral blood serum tumor markers reflect systemic immune status, and clinical medical records reflect patients' real conditions. Through cross-modal alignment technology, these heterogeneous data achieve information complementation in the same high-dimensional latent space, enabling a more comprehensive judgment of biomarker status. AI-driven extraction of radiomic features from medical images, combined with weighted fusion of genomic, textual and other data, may enable improved estimation of target gene status and tumor immune microenvironment status.

Multimodal frameworks endow models with the ability to handle clinical tasks, and present multi-task parallel studies. The LUCID framework proposed by Lu et al. [229] simultaneously predicts EGFR mutation and survival time; the multi-task AI system of Wang et al. [230] synchronously predicts EGFR and PD-L1 status; Wang et al. [231] even challenges the co-mutation prediction of EGFR and TP53. Many studies combine diverse

modalities to predict biomarkers from a more multivariate perspective. For example, the TRANS model by Chen et al. [68] fuses CT imaging, clinical data and RNA sequencing data to predict NSCLC EGFR mutation, achieving an AUC of 0.84. Tan et al. [232] adopted a stacked ensemble model to predict EGFR/ALK mutations and rare EGFR mutations based on clinical, pathological and serum tumor marker data, with an AUC of 0.883 for EGFR prediction. In Table 12, the multi-task AI system of Wang et al. [230] achieves the best prediction performance. This system predicts EGFR and PD-L1 status, with a combined prediction AUC of 0.928. This confirms that clinical features may have a strong supplementary and corrective effect on single imaging features. For multimodal fusion models, interpretability becomes more complex due to the superposition of multi-source data. Current studies mostly use partitioned interpretation: using feature importance for clinical data, Grad-CAM for imaging data, and SHAP values to calculate the overall contribution of each modality.

Table 12. Studies on biomarker prediction based on multimodal data.

Author	Year	Method Adopted	Prediction Target	AUC Value	Involved Modalities
Lu et al. [229]	2025	LUCID Multimodal Integration Framework	EGFR Mutation, Survival Time	0.851–0.881	CT, Clinical Data
Ji et al. [233]	2025	3D CNN + Weak Supervision + Multi-Instance Learning + Nomogram	EGFR Mutation and Subtype	External Test 0.850	CT, Pathological Images, Clinical Data
Ai et al. [234]	2024	Multimodal Integration Model (bTMB + ctDNA + RECIST)	NSCLC Immunotherapy DCB	Validation Set 0.887	Clinical Molecular Data, Imaging Evaluation
Qin et al. [216]	2020	Artificial Neural Network (ANN)	Lung Cancer EGFR Mutation	Model2 0.882, Model1 0.909	Clinical Data, CT Images, Serum Tumor Markers
Chen et al. [68]	2025	TRANS Model (LASSO + Nomogram)	NSCLC EGFR Mutation	0.84 ± 0.01	CT Images, Clinical Data, RNA Sequencing
Chen et al. [108]	2023	Composite Radiomics LCI-RPV	NSCLC Immunotherapy Response, Pulmonary Toxicity	Test Set 0.70	Contrast-Enhanced CT, CD274 RNA Expression
Mitra et al. [235]	2025	Machine Learning + Graph Structure Learning + LLM	NSCLC Immunotherapy Response	Test Set 0.83	CT, Clinical Pathological Data
Trivizakis et al. [236]	2021	Deep Feature + Transcriptomics Fusion	NSCLC Molecular/Histological Subtype	Molecular Subtype 0.831 ± 0.09	CT, Molecular Transcriptomic Data
Tan et al. [232]	2022	Stacked Ensemble Model (Deep Learning + Machine Learning)	NSCLC EGFR/ALK Mutation	EGFR Test Set 0.883	Clinical, Pathological, Serum Tumor Markers
Wang et al. [230]	2022	ML-DL ensemble models	EGFR, PD-L1 Status	Combined Prediction 0.928	CT, Clinical Data
Wang et al. [231]	2025	Progressive Binary Classification Model	EGFR/TP53 Co-Mutation	TP53 0.811	Non-Contrast CT, Clinical Data
Shao et al. [237]	2023	Radiomics/Pathomics + Multimodal Fusion	Gene Mutation	—	Imaging, Pathology, Genome
Shao et al. [238]	2024	Multimodal Integration MMI System	Lung Cancer/Pulmonary Infection Differentiation	Internal Test 0.910	CT Images, Clinical Text
Jiang et al. [28]	2023	JSSC-Net	EGFR Mutation and Subtype	0.7778	Pathological Images + Clinical
Liu et al. [239]	2022	XGBoost	NSCLC Immunotherapy Benefit	—	Molecular + Clinical Data

3.5. Comparative Studies

Comparative studies are crucial for understanding problems in different systems, testing hypotheses, and evaluating the performance of one model compared with others under similar conditions. This section conducts an in-depth analysis from multiple dimensions, including image preprocessing and equipment versatility, imaging modalities, model types and structures, feature dimensions and regional fusion, biomarkers and prediction targets, to assess their performance in predicting NSCLC-related biomarkers from different levels.

In terms of image preprocessing and equipment versatility, data heterogeneity is the biggest obstacle to model generalization in the field of medical imaging AI. Shiri et al. [240] deeply explored the impact of feature harmonization on prediction of EGFR and KRAS mutations. The results showed that after harmonization processing, the AUC for EGFR prediction reached 0.94 and that for KRAS prediction reached 0.93, significantly better than the untreated group. This indicates that harmonization can effectively eliminate non-biological noise caused by equipment differences. Meanwhile, Wang et al. [241] compared the performance of same-equipment

and cross-equipment PET radiomics in predicting EGFR mutations. The study found that the AUC ranged from 0.72 to 0.78 under the same equipment, but dropped to 0.63–0.74 across equipment. The significant decline in cross-equipment performance suggests that to ensure model robustness, large-scale cross-equipment and cross-dataset research should be carried out in future model development. For the comparison of imaging modalities, Yang et al. [150] innovatively compared the performance of the novel imaging agent ^{18}F-MPG PET and traditional ^{18}F-FDG PET in predicting EGFR mutations. The results showed that MPG PET achieved a prediction accuracy of 90%, comprehensively outperforming FDG PET. Yang et al. [242] compared the value of contrast-enhanced CT and unenhanced CT in predicting EGFR mutations, finding that the AUC of contrast-enhanced CT was slightly better than unenhanced CT. These studies demonstrate that imaging modalities exert substantial influences on model predictive outcomes. Some modalities yield notable performance improvements.

In the comparison of model types and structures, the evolution of algorithms has directly driven the improvement of prediction efficiency. In a study on CT-based EGFR mutation prediction, Zhang et al. [162] proved that the AUC of 3D CNN reached 94.7%, significantly better than the 72.4% of the traditional radiomics model. The research by Liu et al. [243] also supports this trend. In this study, deep learning achieved an AUC of 0.84, which was superior to the 0.78 obtained by machine-learning radiomics. Deep learning can automatically extract high-order abstract and non-linear spatial features that cannot be captured by traditional texture algorithms, helping to improve model performance. Meanwhile, Li et al. [244] compared multiple structures for PD-L1 expression prediction and found that the Radiomics-deep learning fusion models achieved a high AUC of 0.910, far ahead of single radiomics with an AUC of 0.785 and single deep-learning with an AUC of 0.867. The study by Huang et al. [226] also confirmed that the hybrid model achieved an AUC of 0.85 for EGFR prediction, better than pure radiomics and deep learning models. These studies indicate that hybrid models can analyze biomarker-related content from more perspectives, with greater advantages in accuracy and robustness than single models.

Regarding the comparison of feature dimensions and regional fusion, Yamazaki et al. [245] compared the performance of single intratumoral features and features combining intratumoral and peritumoral in EGFR prediction, finding that the AUC of combined features increased to 0.774, better than the 0.730 of single intratumoral features. This shows that the selection of image regions is also a critical part of biomarker prediction. Cheng et al. [246] compared the ability of primary lesion combined with bone metastasis and single radiomics in EGFR prediction, finding that the combined model performed AUC of 0.812, suggesting that integrating features may yield better EGFR prediction results. Wang et al. [135] integrated patients' EGFR status information when predicting KRAS mutations, boosting the AUC from 0.834 to 0.921. This indicates that clinical prior knowledge and even other known gene mutation statuses are extremely important information that can potentially improve model performance. For the comparison of biomarkers and prediction targets, different gene mutations and immune markers show huge differences in imaging manifestations. Rinaldi et al. [247] compared the prediction difficulty of three core driver genes in the same study. EGFR yielded the best performance with an AUC of 0.86, whereas KRAS achieved an AUC of 0.61 and ALK attained an AUC of 0.65. When predicting multiple mutations simultaneously, Zhang et al. [94] found that ERBB2 had the optimal prediction effect, followed by EGFR. Yang et al. [248] developed a CNN-based DeepLRHE framework to predict multiple mutant genes; among them, TP53 achieved the highest AUC (0.87), while EGFR, DNMT3A, PBRM1, and STK11 yielded AUCs ranging from 0.71 to 0.84. Compared with well-predicted gene types such as EGFR, KRAS and ALK have more heterogeneous imaging features, making them more difficult to predict. In the comparison of efficacy prediction and clinical strategies, Hashimoto et al. [249] conducted a strategic comparison: evaluating the performance of the clinical-radiomics model and traditional biopsy in predicting PD-L1 expression. The results showed that the AI model achieved an accuracy of 0.74, comprehensively outperforming traditional biopsy. These studies suggest that AI-based models provide a whole-tumor-level global perspective and may serve as an adjunct triage aid in selected high-risk patients pending prospective validation, rather than replacing certain high-risk invasive biopsies. Biopsy remains the reference standard for diagnosis.

In addition to numerical comparison, this section explores the possible factors contributing to the observed performance differences. Multiple factors jointly determine model efficacy. Inconsistent scanning parameters, equipment differences and lack of unified preprocessing give rise to cross-center data heterogeneity, which may lead to performance decline. In terms of imaging modalities, PET/CT integrates anatomical and metabolic information, so it achieves higher accuracy for immune biomarkers like PD-L1 and TMB than single CT. For datasets, single-center retrospective cohorts easily cause overfitting, lowering model recognition ability for minority samples. Most studies lack multi-center external validation, which severely restricts the real-world generalizability of existing models. Hybrid and multimodal models outperform single models because they fuse different features, compensating for the limitations of single feature types. Comparative studies in biomarker prediction research.as shown in Table 13.

Table 13. Comparative studies in biomarker prediction research.

Author	Year	Category of Comparative Study	Specific Comparative Content	Key Results
Shiri et al. [240]	2020	Image Preprocessing Comparison	Impact of feature harmonization on PET/CT-based prediction of EGFR/KRAS mutations	After harmonization: EGFR AUC = 0.94, KRAS AUC = 0.93; superior to non-harmonized data (AUC = 0.87–0.90)
Li et al. [244]	2024	Model Structure Comparison	Radiomics, deep learning, and fusion models for PD-L1 expression prediction based on PET/CT	Fusion model AUC = 0.910, outperforming radiomics (0.785) and deep learning (0.867)
Yang et al. [248]	2021	Prediction Target Comparison	CNN-based DeepLRHE framework for predicting TP53 EGFR, DNMT3A, PBRM1, STK11.	TP53 yielded the highest AUC of 0.87; AUC values for EGFR, DNMT3A, PBRM1, STK11 ranged from 0.71 to 0.84.
Chen et al. [250]	2023	Prediction Target Comparison	Different radiomics models for predicting CD3/CD8 T cell expression	CD3: AUC = 0.943, accuracy 93%; superior to CD8: AUC = 0.837, accuracy 80%
Zhang et al. [162]	2024	Model Type Comparison	3D CNN vs. radiomics model for EGFR mutation prediction based on CT	CNN AUC = 94.7%, significantly better than radiomics (72.4%, $p < 0.05$)
Yang et al. [150]	2021	Imaging Modality Comparison	^{18}F-MPG PET vs. ^{18}F-FDG PET for EGFR mutation prediction	MPG PET: accuracy 90%, AUC = 0.94877; superior to FDG PET (76%, 0.87374)
Zhao et al. [178]	2023	Model Structure Comparison	ResNet50 vs. other models for EGFR mutation prediction	ResNet50: AUC = 0.82, sensitivity 76%, specificity 74%
Liu et al. [243]	2025	Model Type Comparison	Machine learning-based radiomics vs. deep learning model for EGFR mutation prediction	Internal validation: machine learning AUC = 0.78, deep learning AUC = 0.84; external validation: both ≈ 0.77
Huang et al. [226]	2022	Model Structure Comparison	Radiomics model (RM), deep learning model (DLM), and hybrid model (HM) for EGFR mutation prediction	Hybrid model AUC = 0.85, outperforming RM (0.68) and DLM (0.79)
Dang et al. [54]	2021	Feature Dimension Comparison	Single radiomics/imaging/clinical features vs. combined model for EGFR mutation prediction	Combined model AUC = 0.894, significantly optimal
Yamazaki et al. [245]	2022	Feature Region Comparison	Intratumoral features alone vs. intratumoral + peritumoral features for EGFR mutation prediction	Combined features AUC = 0.774, superior to single intratumoral features (0.730, $p < 0.001$)
Wang et al. [241]	2024	Device Universality Comparison	Same-device vs. cross-device PET radiomics for EGFR mutation prediction	Same-device AUC = 0.72–0.78; cross-device AUC = 0.63–0.74
Rinaldi et al. [247]	2023	Biomarker Comparison	Predictive performance for EGFR/KRAS/ALK mutations and survival	EGFR AUC = 0.86, KRAS = 0.61, ALK = 0.65; survival C-index = 0.80
Fuster-Matanzo et al. [251]	2025	Biomarker Comparison	Sensitivity of AI-based prediction for different driver mutations in NSCLC	Sensitivity for both EGFR/ALK = 0.754
Parra-Medina et al. [252]	2025	Biomarker Comparison	Deep learning-based prediction performance for lung cancer driver mutations	EGFR: sensitivity 80%/specificity 77%; ALK: 84%/85%
Zheng et al. [253]	2025	Biomarker Comparison	Machine learning-based predictive performance at different PD-L1 thresholds	PD-L1 ≥ 1%: C = 0.806; ≥50%: C = 0.826
Wang et al. [254]	2023	Efficacy Prediction Comparison	Radiomics-based prediction of PFS under EGFR-TKI treatment	Pooled HR = 2.80, C-index = 0.71
Yolchuyeva et al. [110]	2023	Efficacy Prediction Comparison	XGBoost-based prediction of OS under immunotherapy	Discovery cohort accuracy = 0.63, validation cohort = 0.62
He et al. [170]	2020	Efficacy Prediction Comparison	TMB radiomics biomarker for predicting immunotherapy response	AUC = 0.81, significant differences in OS/PFS
Mu et al. [175]	2021	Efficacy Prediction Comparison	PD-L1 DLS for predicting DCB under immunotherapy	C-index = 0.70–0.87
Zhang et al. [94]	2021	Biomarker Comparison	Simultaneous prediction of EGFR/KRAS/ERBB2/TP53 mutations	ERBB2 AUC = 0.87 (optimal), EGFR AUC = 0.78
Hashimoto et al. [249]	2024	Strategy Comparison	Clinical + radiomics model vs. preoperative biopsy for PD-L1 prediction	Model AUC = 0.83, accuracy = 0.74; superior to biopsy (0.34–0.68)
Cheng et al. [246]	2023	Lesion/Modality Comparison	Primary lesion + bone metastasis (CT + MRI) vs. single radiomics for EGFR prediction	Combined model AUC = 0.812, optimal
Zhang et al. [113]	2020	Model/Feature Comparison	PET/CT radiomics vs. clinical model; integration with clinical variables	Radiomics AUC = 0.85, increased to 0.87 after clinical variable integration
Wang et al. [135]	2022	Feature Fusion Comparison	PET/CT model vs. EGFR information-integrated model for KRAS mutation prediction	Integrated model AUC = 0.921, accuracy = 0.910; superior to original model (0.834)
Yang et al. [242]	2022	Imaging Modality Comparison	Contrast-enhanced CT vs. non-contrast CT for EGFR mutation prediction	Contrast-enhanced CT AUC = 0.842, non-contrast CT = 0.833

To further intuitively summarize the quantitative performance of different AI models, imaging modalities and biomarker prediction tasks, we sorted out representative quantitative indicators of mainstream models from the included studies, including AUC and accuracy. As summarized in Table 14, regarding overall predictive performance, multimodal fusion models and PET/CT-based deep learning models attain the highest AUC values (up to 0.97), followed by hybrid models and machine learning methods. Single-modal CT-based basic CNN models deliver moderate performance and are more vulnerable to imaging equipment. In terms of adaptability to different biomarkers, most models achieve satisfactory results for common biomarkers including EGFR and PD-L1. For rare mutations such as ALK, ROS1 and T790M, ensemble learning and GAN-based data augmentation

strategies exhibit distinct advantages. When it comes to immune markers like TMB and CD8+ TILs, PET/CT multimodal models outperform single-modal CT models. In terms of cost and application thresholds, traditional radiomics combined with machine learning features low computational cost and minimal data requirements. By contrast, Transformer-based models and fully multimodal models demand powerful computing resources and complete multi-source datasets.

Table 14. Comprehensive quantitative comparison of mainstream AI models for NSCLC biomarker prediction.

Model Category	Specific Algorithm	Imaging Modality	Predicted Biomarker	Core Metrics (AUC/Accuracy)
Radiomics + Traditional Machine Learning (RM + ML)	Logistic Regression (LR)	CT	EGFR mutation	0.723–0.972 (AUC)
	Random Forest (RF)	CT/PET/CT	EGFR, ALK	0.88 (AUC, CT); 0.71 (AUC, PET/CT)
	Support Vector Machine (SVM)	CT/PET/CT	EGFR, ALK, PD-L1	0.741–0.953 (AUC)
	LASSO + Nomogram	CT	EGFR mutation/subtype	0.701–0.993 (AUC)
	Random Forest (RF)	CT	KRAS, T790M	0.86 (Accuracy, KRAS); 0.961 (AUC, T790M)
Deep Learning (DL)	2D/3D CNN	CT/PET/CT	EGFR, PD-L1	0.730–0.947 (AUC)
	ResNet/DenseNet	CT/PET/CT/Pathology	PD-L1, EGFR	0.750–0.960 (AUC)
	Transformer (GMILT/Denseformer)	CT/Pathology	EGFR, multiple genes	0.856 (AUC)
	GAN	CT	EGFR-TKI drug resistance	-
Hybrid Models (ML + DL/Ensemble)	CNN + SVM/RF	PET/CT	EGFR	0.85 ± 0.09 (AUC)
	Radiomics + 3D ConvNeXt	CT	EGFR subtype	0.801 (AUC)
	Multiple Classifier Fusion	CT	PD-L1, immunotherapy response	0.75–0.87 (AUC)
Multimodal Fusion Models	CT + Clinical Data	CT + Clinical	EGFR, PD-L1	0.84–0.928 (AUC)
	CT + Pathology + RNA	Multimodal	EGFR	0.84 ± 0.01 (AUC)
	PET + CT + Metabolic Features	PET/CT	PD-L1, TMB	0.783–0.97 (AUC)

To intuitively illustrate the architectures of different frameworks, we summarize four major categories of biomarker prediction frameworks: radiomics combined with traditional machine learning, deep learning-based models, ML-DL ensemble models, and multimodal fusion models. Radiomics combined with traditional machine learning extracts handcrafted imaging features for prediction, featuring low computational demands. Deep learning-based models automatically learn hierarchical features from raw images. ML-DL ensemble models integrate multiple algorithms to may help improve overall performance and robustness. Multimodal fusion models combine multi-source imaging data, which may enable improved estimation by fusing complementary information across different modalities.

4. Discussion

This study systematically and comprehensively reviews the application of various artificial intelligence technologies in the field of NSCLC biomarker prediction. The literature was classified according to imaging modalities, types of deep learning models, and categories of predicted biomarkers. Through in-depth analysis, we identified several potential findings regarding AI-driven biomarker prediction in non-small cell lung cancer. Traditional radiomics method is stable and interpretable but limited by manual features; single deep learning has high accuracy but poor interpretability and cross-center robustness; hybrid and multimodal models integrate the advantages of multiple technologies and become the mainstream development direction at this stage. This paper focuses on analyzing the advantages and disadvantages of different AI models in various clinical scenarios, clarifying the shortcomings of existing research. As one of the few reviews to dissect the impact of model differences on NSCLC biomarker prediction, this study aims to sort out the application achievements of AI in NSCLC diagnosis and treatment, provide references for the optimization of suitable deep learning tools in subfields and follow-up research.

Firstly, this study categorized and sorted the screened literature data meeting the research criteria. In terms of imaging modalities, the included studies mainly covered four categories: CT-related, PET/CT-related, pathology-related, and MRI-related. Statistical results showed that CT-related studies accounted for an absolute

majority, while MRI-related studies were the fewest. This finding fully confirms the core status of CT modality in the field of AI-based NSCLC biomarker prediction. The underlying reasons are mainly attributed to the advantages of CT examination, including non-invasiveness, rapidity, high spatial resolution, and wide clinical popularity, which can clearly display the morphology, density, and peripheral tissue invasion characteristics of lung cancer. Meanwhile, based on modeling methods, the studies were divided into three categories: radiomics, deep learning, and fusion models, among which radiomics-related studies were the most frequent. This phenomenon is largely related to its early development and relatively low requirements for data volume. In the prediction research of various targeted biomarkers, studies on EGFR mutation ranked far ahead, which is highly consistent with clinical practice. Among East Asian patients with lung adenocarcinoma, EGFR mutation is one of the prevalent gene alterations. EGFR-mutant lesions may exhibit classic and relatively distinguishable imaging phenotypes on CT images. The correlation between such imaging features and gene mutations has been widely recognized and verified clinically, thus promoting the large-scale development of EGFR-related prediction research.

Subsequently, this study systematically sorted out and deeply discussed the evolution trajectory and application potential of different AI methods in NSCLC biomarker prediction, covering traditional radiomics and machine learning, basic deep learning models, advanced deep learning architectures, multi-model fusion strategies, and multi-modal joint analysis. In the field of radiomics and traditional machine learning, existing studies have fully confirmed that this approach can accurately and quantitatively predict core gene mutations for targeted therapy and key biomarkers for immunotherapy, achieving particularly strong results in the identification of EGFR mutations and PD-L1 expression status. With the widespread application of basic deep learning models, the biomarker prediction paradigm has realized a leap to automatic feature extraction, with substantial improvement in overall predictive performance. This technical dividend is particularly prominent in pathological image analysis. On this basis, advanced deep learning architectures represented by Transformer have been innovatively introduced, relying on the powerful attention mechanism to enable more sensitive capture of complex intratumoral heterogeneity and global spatial dependencies. However, in response to the inherent defects inevitable in single algorithm architectures, fusion model strategies have emerged. The robustness and predictive stability of fusion models in coping with multi-center heterogeneous data have been significantly improved. Finally, the rise of multi-modal models marks the progression of the prediction system to a new dimension. Through overall coordinated analysis of multi-dimensional heterogeneous data such as imaging, pathology, and clinical prior knowledge, models can analyze tumor biological characteristics from the most macroscopic and comprehensive perspective. In the comparative research, this study compared the predictive efficacy of NSCLC biomarkers from multiple dimensions. In terms of image preprocessing, feature harmonization technology significantly improved model robustness; in terms of imaging modalities, specific molecular probe PET was superior to traditional imaging; in terms of model structure, deep learning and fusion models outperformed single radiomics; in terms of feature dimensions, integrating peritumoral information and clinical variables could optimize prediction results. AI technology has achieved accurate prediction of targeted and immunotherapy-related biomarkers for NSCLC from multi-source imaging modalities. In cross-study quantitative comparison, individual studies adopt distinct feature screening algorithms, model frameworks and hyperparameter settings. Even for the same prediction task, these factors will lead to divergent performance results. Therefore, conclusions drawn from cross-study comparison should be interpreted prudently. Standardized datasets, unified validation protocols and uniform evaluation criteria are urgently needed in this field to realize more credible large-scale meta-analysis and cross-literature comparison in the future.

Dataset imbalance, model overfitting and insufficient generalizability are three interrelated prevalent defects across most AI models for NSCLC biomarker prediction, and they severely restrict the reliability and clinical value of relevant research. In terms of dataset imbalance, most included studies face obvious class distribution bias: on the one hand, rare driver genes such as ALK, ROS1 and T790M drug-resistant mutations have far fewer patient samples compared with common EGFR mutations; on the other hand, the number of patients with different PD-L1 expression levels and diverse tumor stages also varies greatly. Severe class imbalance will cause models to tend to predict majority categories blindly. In such a context, overfitting becomes extremely common, especially for deep learning architectures. Most models achieve extremely high performance on internal training and validation cohorts, but their predictive indicators drop sharply on external independent datasets. Small sample sizes, excessive model parameters relative to limited annotated data, and single-center homogeneous cohorts are the main triggers of overfitting. Even if a model performs well in a single research institution, it often fails to maintain stable efficacy when applied to datasets from other hospitals. To relieve these problems, current researchers have adopted multiple solutions: using generative AI such as GAN and diffusion models to augment minority samples, applying class-weighted loss functions and synthetic minority oversampling technique (SMOTE) to balance data distribution and feature harmonization to enhance the generalization ability of models.

We further conduct an in-depth analysis of multimodal AI integration for NSCLC biomarker prediction in clinical oncology. Current multimodal frameworks mainly combine CT, PET/CT, pathological slides, clinical metadata and omics data, and adopt different fusion strategies to break the information limitations of single-modal models. However, the practical application of multimodal AI in real clinical settings still faces prominent technical and clinical obstacles. First, data heterogeneity and matching difficulty are core constraints: different modalities have inconsistent data formats, spatial resolutions and value distributions, and complete paired imaging, pathological and genetic data are extremely scarce in routine clinical practice. Second, most existing studies rely on simple feature splicing or weighted fusion, making it difficult to fully mine the inherent association between different types of data. In addition, complex multimodal models usually require high computing power and strict deployment environments. From the perspective of clinical application value, existing studies prove multimodal fusion can improve prediction performance. At present, it has achieved promising results in partial cohorts, while universal, fully accurate multi-biomarker prediction remains a future research goal pending further validation, showing unique advantages in guiding combined targeted therapy and immunotherapy.

Despite the great potential of deep learning tools in predicting NSCLC targeted and immune biomarkers, multiple severe challenges need to be overcome before their clinical translation. Firstly, data heterogeneity and instability are the primary bottlenecks restricting model reliability. Significant differences exist in scanning parameters, image reconstruction algorithms, and equipment noise among different medical institutions, leading to drastic fluctuations in predictive efficacy of non-standardized data, which seriously affects the reproducibility of results. Secondly, although prediction models for common clinical targets such as EGFR mutation and PD-L1 expression are well-established biomarkers with strong clinical utility, for rare and low-frequency mutations such as ALK and ROS1, the overall prediction accuracy is not ideal. Finally, the attribute of deep learning models leads to a lack of transparency in feature correlation and decision-making logic. This lack of interpretability makes it difficult for clinicians to fully trust the prediction results given by AI.

Apart from the inherent technical defects of AI models, the large-scale deployment and popularization of current AI-driven NSCLC biomarker prediction systems also face prominent practical challenges in real oncology clinical scenarios. These barriers involve clinical workflow, medical data management, clinical personnel, medical equipment, economic cost, regulatory policies and doctor-patient acceptance, which together hinder the transition from laboratory research to routine clinical application. Prospective clinical trials and large-scale prospective validation studies are urgently required to further verify the clinical value and practical performance of existing AI-driven biomarker prediction models for NSCLC. At present, the vast majority of included studies are designed as single-center retrospective analyses based on historical imaging and clinical datasets. Although retrospective research can preliminarily verify model efficacy, it cannot truly reflect the stability and applicability of AI tools in real continuous clinical workflows. Different from retrospective research, prospective trials enroll patients consecutively according to unified inclusion and exclusion criteria, adopt standardized imaging acquisition, image preprocessing and model application protocols, and conduct dynamic follow-up and outcome assessment. In addition, multi-center prospective validation across different tiers of medical institutions is particularly critical, as it can fully test the adaptability of models to diverse imaging devices, scanning parameters and patient populations, and make up for the limitations of single-center research.

From the perspective of ethics, law and patient privacy, the large-scale application of AI radiogenomics models in NSCLC diagnosis and treatment also faces prominent practical challenges. All AI biomarker prediction systems rely heavily on high-volume multimodal medical data including imaging scans, pathological slides, genetic sequencing results and personal clinical information. Such sensitive patient health data involves strict privacy protection requirements. At present, most existing studies adopt single-center private datasets, and cross-institutional data sharing for model training and external validation is greatly restricted by regional laws and patient informed consent rules. Meanwhile, there is still a lack of unified industry ethical guidelines and standardized legal supervision rules specifically for radiomics AI in oncology. To resolve these issues, future research and clinical promotion should strictly follow the principle of informed consent, adopt privacy-preserving technologies such as federated learning to realize model training without accessing raw patient data, ensuring safe and ethical implementation of AI technologies in routine oncology practice.

In the future, AI-based NSCLC biomarker prediction will present a development trend of in-depth integration. Firstly, algorithm architectures will undergo transformation. Advanced models are gradually replacing traditional convolutional neural networks with their strong global feature modeling capabilities, and the addition of generative models will effectively solve the problem of scarce medical imaging samples. Secondly, the standardization and normalization of datasets will become an industry consensus, and cross-center and multi-equipment image harmonization technologies will eliminate heterogeneous noise; thirdly, the prediction dimension will expand from single imaging to more modal data such as pathomics and liquid biopsy, constructing a comprehensive tumor portrait.

At present, some large models have been applied in cancer diagnosis and other related work [198,255–257]. These multi-modal vision-language models and AI Agents will intervene in biomarker prediction, deeply linking cumbersome clinical text medical records with visual images to achieve end-to-end automated diagnostic decision-making. More importantly, with the breakthrough of interpretable technologies such as class activation mapping (CAM), the transparency of prediction logic will greatly enhance clinical trust. Coupled with the application of data security technologies such as federated learning, AI prediction will be closely integrated with clinical surgical planning and efficacy monitoring by deepening the dynamic correlation with patients' clinical information. Current evidence verifies the technical feasibility of AI biomarker prediction. As supporting technologies improve, these tools are expected to gradually integrate into clinical workflows and serve as auxiliary references for precise diagnosis and treatment; large-scale real-time clinical application still requires long-term verification.

5. Conclusions

This study presents a comprehensive overview of the application of artificial intelligence technologies in NSCLC biomarker prediction. Through in-depth analysis of core literatures, covering various imaging modalities including CT, PET, MRI, and pathological images, and focusing on key biomarkers such as EGFR, PD-L1, and TMB, the research systematically sorts out the technological evolution of radiomics, machine learning, deep learning, and fusion models. Through horizontal comparative studies, the performance differences under different algorithms, biomarkers, and imaging modalities are clarified. This review summarizes current empirical findings and existing limitations. It can provide practical references for follow-up research. Whether it can substantially improve patient outcomes needs more prospective clinical trials to confirm.

Author Contributions

B.Z.: Conceptualization, methodology, data curation, formal analysis, investigation, writing—original draft; J.T.: Methodology, data curation, formal analysis, investigation; S.L.: Methodology, formal analysis, writing—review and editing. All authors have read and agreed to the published version of the manuscript.

Funding

This research was funded by General Program of Zhejiang Provincial Department of Education (Grant No. Y202559701), Innovation Team Project of the Ningbo Yongjiang Talent Program (Grant No. ZX2025000419) and National Natural Science Foundation of China (Grant No. 62501295).

Institutional Review Board Statement

Not applicable.

Informed Consent Statement

Not applicable.

Data Availability Statement

Not applicable.

Conflicts of Interest

The authors declare no conflict of interest. Given the role as Associate Editor, Siyuan Lu had no involvement in the peer review of this paper and had no access to information regarding its peer-review process. Full responsibility for the editorial process of this paper was delegated to another editor of the journal.

Use of AI and AI-Assisted Technologies

During the preparation of this work, the authors used DeepSeek to understand technical concepts and polish the language. After using this tool, the authors reviewed and edited the content as needed and take full responsibility for the content of the published article.

References

1. Siegel, R.L.; Miller, K.D.; Wagle, N.S.; et al. Cancer statistics, 2023. *CA Cancer J. Clin.* **2023**, *73*, 17–48. https://doi.org/10.3322/caac.21763.
2. Global Burden of Disease Cancer Collaboration; Fitzmaurice, C.; Akinyemiju, T.F.; et al. Global, Regional, and National Cancer Incidence, Mortality, Years of Life Lost, Years Lived with Disability, and Disability-Adjusted Life-Years for 29 Cancer Groups, 1990 to 2016: A Systematic Analysis for the Global Burden of Disease Study. *JAMA Oncol.* **2018**, *4*, 1553–1568. https://doi.org/10.1001/jamaoncol.2018.2706.
3. Liu, X.; Jiang, G.; Sun, X.; et al. Relationship between driver gene mutations and clinical pathological characteristics in older lung adenocarcinoma. *Front. Oncol.* **2023**, *13*, 1275575. https://doi.org/10.3389/fonc.2023.1275575.
4. Keegan, A.; Ricciuti, B.; Garden, P.; et al. Plasma IL-6 changes correlate to PD-1 inhibitor responses in NSCLC. *J. Immunother. Cancer* **2020**, *8*, e000678. https://doi.org/10.1136/jitc-2020-000678.
5. Choi, C.M.; Kim, M.Y.; Hwang, H.J.; et al. Advanced adenocarcinoma of the lung: Comparison of CT characteristics of patients with anaplastic lymphoma kinase gene rearrangement and those with epidermal growth factor receptor mutation. *Radiology* **2015**, *275*, 272–279. https://doi.org/10.1148/radiol.14140848.
6. Cao, D.; Xu, H.; Xu, X.; et al. A reliable and feasible way to predict the benefits of Nivolumab in patients with non-small cell lung cancer: A pooled analysis of 14 retrospective studies. *Oncoimmunology* **2018**, *7*, e1507262. https://doi.org/10.1080/2162402x.2018.1507262.
7. Kurose, K.; Sakaeda, K.; Fukuda, M.; et al. Immune checkpoint therapy and response biomarkers in non-small-cell lung cancer: Serum NY-ESO-1 and XAGE1 antibody as predictive and monitoring markers. *Adv. Clin. Chem.* **2023**, *112*, 155–204. https://doi.org/10.1016/bs.acc.2022.09.004.
8. Ni, S.; Liang, Q.; Jiang, X.; et al. Prognostic models for immunotherapy in non-small cell lung cancer: A comprehensive review. *Heliyon* **2024**, *10*, e29840. https://doi.org/10.1016/j.heliyon.2024.e29840.
9. Sacher, A.G.; Dahlberg, S.E.; Heng, J.; et al. Association between Younger Age and Targetable Genomic Alterations and Prognosis in Non-Small-Cell Lung Cancer. *JAMA Oncol.* **2016**, *2*, 313–320. https://doi.org/10.1001/jamaoncol.2015.4482.
10. Alfranca, Y.L.; Garcia, M.E.O.; Rueda, A.G.; et al. Blood Biomarkers of Response to Immune Checkpoint Inhibitors in Non-Small Cell Lung Cancer. *J. Clin. Med.* **2022**, *11*, 3245. https://doi.org/10.3390/jcm11113245.
11. Imyanitov, E.N.; Iyevleva, A.G.; Levchenko, E.V. Molecular testing and targeted therapy for non-small cell lung cancer: Current status and perspectives. *Crit. Rev. Oncol. Hematol.* **2021**, *157*, 103194. https://doi.org/10.1016/j.critrevonc.2020.103194.
12. Liu, Y.; Kim, J.; Qu, F.; et al. CT Features Associated with Epidermal Growth Factor Receptor Mutation Status in Patients with Lung Adenocarcinoma. *Radiology* **2016**, *280*, 271–280. https://doi.org/10.1148/radiol.2016151455.
13. Rivière, A.; Lecuyer, A.I.; Laurent, E.; et al. 1-year mortality in lung cancer in France according to key timepoints of care pathways. *ERJ Open Res.* **2022**, *8*, 00157-2022. https://doi.org/10.1183/23120541.00157-2022.
14. Onimaru, R.; Onishi, H.; Ogawa, G.; et al. Final report of survival and late toxicities in the Phase I study of stereotactic body radiation therapy for peripheral T2N0M0 non-small cell lung cancer (JCOG0702). *Jpn. J. Clin. Oncol.* **2018**, *48*, 1076–1082. https://doi.org/10.1093/jjco/hyy141.
15. Wang, S.; Yu, H.; Gan, Y.; et al. Mining whole-lung information by artificial intelligence for predicting EGFR genotype and targeted therapy response in lung cancer: A multicohort study. *Lancet Digit. Health* **2022**, *4*, e309–e319. https://doi.org/10.1016/s2589-7500(22)00024-3.
16. Chen, Q.; Li, Y.; Cheng, Q.; et al. EGFR Mutation Status and Subtypes Predicted by CT-Based 3D Radiomic Features in Lung Adenocarcinoma. *Onco Targets Ther.* **2022**, *15*, 597–608. https://doi.org/10.2147/ott.s352619.
17. Sleeman, W.C.; Kapoor, R.; Ghosh, P. Multimodal classification: Current landscape, taxonomy and future directions. *ACM Comput. Surv.* **2023**, *55*, 1–31. https://doi.org/10.1145/3543848.
18. HajiEsmailPoor, Z.; Tabnak, P.; Baradaran, B.; et al. Diagnostic performance of CT scan–based radiomics for prediction of lymph node metastasis in gastric cancer: A systematic review and meta-analysis. *Front. Oncol.* **2023**, *13*, 1185663. https://doi.org/10.3389/fonc.2023.1185663.
19. Liu, X.; Xu, T.; Wang, S.; et al. CT-based radiomic phenotypes of lung adenocarcinoma: A preliminary comparative analysis with targeted next-generation sequencing. *Front. Med.* **2023**, *10*, 1191019. https://doi.org/10.3389/fmed.2023.1191019.
20. Mino-Kenudson, M.; Schalper, K.; Cooper, W.; et al. Predictive Biomarkers for Immunotherapy in Lung Cancer: Perspective from the International Association for the Study of Lung Cancer Pathology Committee. *J. Thorac. Oncol.* **2022**, *17*, 1335–1354. https://doi.org/10.1016/j.jtho.2022.09.109.
21. Gao, Q.; Yang, L.; Lu, M.; et al. The artificial intelligence and machine learning in lung cancer immunotherapy. *J. Hematol. Oncol.* **2023**, *16*, 55. https://doi.org/10.1186/s13045-023-01456-y.
22. Zhou, G.; Xu, S.; Liu, X.; et al. Relationship between the image characteristics of artificial intelligence and EGFR gene mutation in lung adenocarcinoma. *Front. Genet.* **2023**, *13*, 1090180. https://doi.org/10.3389/fgene.2022.1090180.

23. She, Y.; Jin, Z.; Wu, J.; et al. Development and Validation of a Deep Learning Model for Non–Small Cell Lung Cancer Survival. *JAMA Netw. Open* **2020**, *3*, e205842. https://doi.org/10.1001/jamanetworkopen.2020.5842.
24. Lai, Y.H.; Chen, W.N.; Hsu, T.C.; et al. Overall survival prediction of non-small cell lung cancer by integrating microarray and clinical data with deep learning. *Sci. Rep.* **2020**, *10*, 4679. https://doi.org/10.1038/s41598-020-61588-w.
25. De Fauw, J.; Ledsam, J.R.; Romera-Paredes, B.; et al. Clinically applicable deep learning for diagnosis and referral in retinal disease. *Nat. Med.* **2018**, *24*, 1342–1350. https://doi.org/10.1038/s41591-018-0107-6.
26. Mu, W.; Jiang, L.; Zhang, J.; et al. Non-invasive decision support for NSCLC treatment using PET/CT radiomics. *Nat. Commun.* **2020**, *11*, 5228. https://doi.org/10.1038/s41467-020-19116-x.
27. Sun, K.; Zheng, Y.; Yang, X.; et al. A novel transformer-based aggregation model for predicting gene mutations in lung adenocarcinoma. *Med. Biol. Eng. Comput.* **2024**, *62*, 1427–1440. https://doi.org/10.1007/s11517-023-03004-9.
28. Jiang, Y.; Ma, S.; Xiao, W.; et al. Predicting EGFR gene mutation status in lung adenocarcinoma based on multifeature fusion. *Biomed. Signal Process. Control.* **2023**, *84*, 104786. https://doi.org/10.1016/j.bspc.2023.104786.
29. Wang, C.; Xu, X.; Shao, J.; et al. Deep Learning to Predict EGFR Mutation and PD-L1 Expression Status in Non-Small-Cell Lung Cancer on Computed Tomography Images. *J. Oncol.* **2021**, *2021*, 5499385. https://doi.org/10.1155/2021/5499385.
30. Wang, C.; Ma, J.; Shao, J.; et al. Non-Invasive Measurement Using Deep Learning Algorithm Based on Multi-Source Features Fusion to Predict PD-L1 Expression and Survival in NSCLC. *Front. Immunol.* **2022**, *13*, 828560. https://doi.org/10.3389/fimmu.2022.828560.
31. Liao, J.; Li, X.; Gan, Y.; et al. Artificial intelligence assists precision medicine in cancer treatment. *Front. Oncol.* **2023**, *12*, 998222. https://doi.org/10.3389/fonc.2022.998222.
32. Chen, M.; Copley, S.J.; Viola, P.; et al. Radiomics and artificial intelligence for precision medicine in lung cancer treatment. *Semin. Cancer Biol.* **2023**, *93*, 97–113. https://doi.org/10.1016/j.semcancer.2023.05.004.
33. Li, M.S.C.; Mok, K.K.S.; Mok, T.S.K. Developments in targeted therapy & immunotherapy—How non-small cell lung cancer management will change in the next decade: A narrative review. *Ann. Transl. Med.* **2023**, *11*, 358. https://doi.org/10.21037/atm-22-4444.
34. Atmakuru, A.; Chakraborty, S.; Faust, O.; et al. Deep learning in radiology for lung cancer diagnostics: A systematic review of classification, segmentation, and predictive modeling techniques. *Expert Syst. Appl.* **2024**, *255*, 124665. https://doi.org/10.1016/j.eswa.2024.124665.
35. Zheng, J.; Xu, S.; Wang, G.; et al. Applications of CT-based radiomics for the prediction of immune checkpoint markers and immunotherapeutic outcomes in non-small cell lung cancer. *Front. Immunol.* **2024**, *15*, 1434171. https://doi.org/10.3389/fimmu.2024.1434171.
36. Arango-Argoty, G.; Bikiel, D.E.; Sun, G.J.; et al. AI-driven predictive biomarker discovery with contrastive learning to improve clinical trial outcomes. *Cancer Cell* **2025**, *43*, 875–890.e8. https://doi.org/10.1016/j.ccell.2025.03.029.
37. Bonci, E.A.; Bandura, A.; Dooley, A.; et al. Artificial intelligence in NSCLC management for revolutionizing diagnosis, prognosis, and treatment optimization: A systematic review. *Crit. Rev. Oncol. Hematol.* **2025**, *216*, 104929. https://doi.org/10.1016/j.critrevonc.2025.104929.
38. Dehkharghanian, T.; Bidgoli, A.A.; Riasatian, A.; et al. Biased data, biased AI: Deep networks predict the acquisition site of TCGA images. *Diagn. Pathol.* **2023**, *18*, 67. https://doi.org/10.1186/s13000-023-01355-3.
39. Fu, Y.; Jung, A.W.; Torne, R.V.; et al. Pan-cancer computational histopathology reveals mutations, tumor composition and prognosis. *Nat. Cancer* **2020**, *1*, 800–810. https://doi.org/10.1038/s43018-020-0085-8.
40. Noorbakhsh, J.; Farahmand, S.; Foroughi pour, A.; et al. Deep learning-based cross-classifications reveal conserved spatial behaviors within tumor histological images. *Nat. Commun.* **2020**, *11*, 6367. https://doi.org/10.1038/s41467-020-20030-5.
41. Huang, K.; Mo, Z.; Zhu, W.; et al. Prediction of Target-Drug Therapy by Identifying Gene Mutations in Lung Cancer With Histopathological Stained Image and Deep Learning Techniques. *Front. Oncol.* **2021**, *11*, 642945. https://doi.org/10.3389/fonc.2021.642945.
42. Rączkowska, A.; Paśnik, I.; Kukiełka, M.; et al. Deep learning-based tumor microenvironment segmentation is predictive of tumor mutations and patient survival in non-small-cell lung cancer. *BMC Cancer* **2022**, *22*, 1001. https://doi.org/10.1186/s12885-022-10081-w.
43. Chen, Z.; Li, X.; Yang, M.; et al. Optimization of deep learning models for the prediction of gene mutations using unsupervised clustering. *J. Pathol. Clin. Res.* **2023**, *9*, 3–17. https://doi.org/10.1002/cjp2.302.
44. Morel, L.O.; Derangère, V.; Arnould, L.; et al. Preliminary evaluation of deep learning for first-line diagnostic prediction of tumor mutational status. *Sci. Rep.* **2023**, *13*, 6927. https://doi.org/10.1038/s41598-023-34016-y.
45. Chen, Y.; Zhou, C.; Zhang, X.; et al. Construction of a novel radioresistance-related signature for prediction of prognosis, immune microenvironment and anti-tumour drug sensitivity in non-small cell lung cancer. *Ann. Med.* **2025**, *57*, 2447930. https://doi.org/10.1080/07853890.2024.2447930.

46. Lu, M.Y.; Chen, B.; Williamson, D.F.K.; et al. A multimodal generative AI copilot for human pathology. *Nature* **2024**, *634*, 466–473. https://doi.org/10.1038/s41586-024-07618-3.
47. Jia, L.; Wu, W.; Hou, G.; et al. Residual neural network with mixed loss based on batch training technique for identification of EGFR mutation status in lung cancer. *Multimed. Tools Appl.* **2023**, *82*, 33443–33463. https://doi.org/10.1007/s11042-023-14876-2.
48. Zhao, W.; Chen, W.; Li, G.; et al. GMILT: A Novel Transformer Network That Can Noninvasively Predict EGFR Mutation Status. *IEEE Trans. Neural Netw. Learn. Syst.* **2024**, *35*, 7324–7338. https://doi.org/10.1109/tnnls.2022.3190671.
49. Tomita, N.; Tafe, L.J.; Suriawinata, A.A.; et al. Predicting oncogene mutations of lung cancer using deep learning and histopathologic features on whole-slide images. *Transl. Oncol.* **2022**, *24*, 101494. https://doi.org/10.1016/j.tranon.2022.101494.
50. Yong, M.P.; Hum, Y.C.; Lai, K.W.; et al. Histopathological Cancer Detection Using Intra-Domain Transfer Learning and Ensemble Learning. *IEEE Access* **2024**, *12*, 1434–1457. https://doi.org/10.1109/access.2023.3343465.
51. Zhang, H.; He, M.; Wan, R.A.; et al. Establishment and Evaluation of EGFR Mutation Prediction Model Based on Tumor Markers and CT Features in NSCLC. *J. Healthc. Eng.* **2022**, *2022*, 8089750. https://doi.org/10.1155/2022/8089750.
52. Liu, Y.; Zhou, J.; Wu, J.; et al. Development and Validation of Machine Learning Models to Predict Epidermal Growth Factor Receptor Mutation in Non-Small Cell Lung Cancer: A Multi-Center Retrospective Radiomics Study. *Cancer Control* **2022**, *29*, 10732748221092926. https://doi.org/10.1177/10732748221092926.
53. Yang, C.; Chen, W.; Gong, G.; et al. Application of CT radiomics features to predict the EGFR mutation status and therapeutic sensitivity to TKIs of advanced lung adenocarcinoma. *Transl. Cancer Res.* **2020**, *9*, 6683–6690. https://doi.org/10.21037/tcr-20-1216.
54. Dang, Y.; Wang, R.; Qian, K.; et al. Clinical and radiological predictors of epidermal growth factor receptor mutation in nonsmall cell lung cancer. *J. Appl. Clin. Med. Phys.* **2021**, *22*, 271–280. https://doi.org/10.1002/acm2.13107.
55. Zhang, G.; Cao, Y.; Zhang, J.; et al. Predicting EGFR mutation status in lung adenocarcinoma: Development and validation of a computed tomography-based radiomics signature. *Am. J. Cancer Res.* **2021**, *11*, 546–560.
56. Chen, W.; Hua, Y.; Mao, D.; et al. A Computed Tomography-Derived Radiomics Approach for Predicting Uncommon EGFR Mutation in Patients With NSCLC. *Front. Oncol.* **2021**, *11*, 722106. https://doi.org/10.3389/fonc.2021.722106.
57. Jiang, M.; Yang, P.; Li, J.; et al. Computed tomography-based radiomics quantification predicts epidermal growth factor receptor mutation status and efficacy of first-line targeted therapy in lung adenocarcinoma. *Front. Oncol.* **2022**, *12*, 985284. https://doi.org/10.3389/fonc.2022.985284.
58. Dong, Y.; Jiang, Z.; Li, C.; et al. Development and validation of novel radiomics-based nomograms for the prediction of EGFR mutations and Ki-67 proliferation index in non-small cell lung cancer. *Quant. Imaging Med. Surg.* **2022**, *12*, 2658–2671. https://doi.org/10.21037/qims-21-980.
59. Njoto, E.N.; Jasminarti Dwi Kusumawardani, I.A.; Rai, I.B.N. Predicting EGFR Mutation in Lung Adenocarcinoma: Development and Validation of the EGFR Mutation Predictive Score (EMPS) in Bali, Indonesia. *Asian Pac. J. Cancer Prev.* **2023**, *24*, 2903–2910. https://doi.org/10.31557/apjcp.2023.24.8.2903.
60. Wu, S.; Shen, G.; Mao, J.; et al. CT Radiomics in Predicting EGFR Mutation in Non-small Cell Lung Cancer: A Single Institutional Study. *Front. Oncol.* **2020**, *10*, 542957. https://doi.org/10.3389/fonc.2020.542957.
61. Zhu, H.; Song, Y.; Huang, Z.; et al. Accurate prediction of epidermal growth factor receptor mutation status in early-stage lung adenocarcinoma, using radiomics and clinical features. *Asia-Pac. J. Clin. Oncol.* **2022**, *18*, 586–594. https://doi.org/10.1111/ajco.13641.
62. Hou, D.; Li, W.; Wang, S.; et al. Different Clinicopathologic and Computed Tomography Imaging Characteristics of Primary and Acquired EGFR T790M Mutations in Patients with Non-Small-Cell Lung Cancer. *Cancer Manag. Res.* **2021**, *13*, 6389–6401. https://doi.org/10.2147/cmar.s323972.
63. Ninomiya, K.; Arimura, H.; Chan, W.Y.; et al. Robust radiogenomics approach to the identification of EGFR mutations among patients with NSCLC from three different countries using topologically invariant Betti numbers. *PLoS ONE* **2021**, *16*, e0244354. Correction in: *PLoS ONE* **2024**, *19*, e0316496. https://doi.org/10.1371/journal.pone.0244354.
64. Rossi, G.; Barabino, E.; Fedeli, A.; et al. Radiomic Detection of EGFR Mutations in NSCLC. *Cancer Res.* **2021**, *81*, 724–731. https://doi.org/10.1158/0008-5472.can-20-0999.
65. Weng, Q.; Hui, J.; Wang, H.; et al. Radiomic Feature-Based Nomogram: A Novel Technique to Predict EGFR-Activating Mutations for EGFR Tyrosine Kinase Inhibitor Therapy. *Front. Oncol.* **2021**, *11*, 590937. https://doi.org/10.3389/fonc.2021.590937.
66. Zhu, Y.; Guo, Y.B.; Xu, D.; et al. A computed tomography (CT)-derived radiomics approach for predicting primary co-mutations involving TP53 and epidermal growth factor receptor (EGFR) in patients with advanced lung adenocarcinomas (LUAD). *Ann. Transl. Med.* **2021**, *9*, 545. https://doi.org/10.21037/atm-20-6473.
67. Cheng, B.; Deng, H.; Zhao, Y.; et al. Predicting EGFR mutation status in lung adenocarcinoma presenting as ground-glass opacity: Utilizing radiomics model in clinical translation. *Eur. Radiol.* **2022**, *32*, 5869–5879. https://doi.org/10.1007/s00330-022-08673-y.

68. Chen, Z.; Lu, H.; Liu, A.; et al. TRANS: A prediction model for EGFR mutation status in NSCLC based on radiomics and clinical features. *Respir. Res.* **2025**, *26*, 211. https://doi.org/10.1186/s12931-025-03287-6.
69. Hong, D.; Xu, K.; Zhang, L.; et al. Radiomics Signature as a Predictive Factor for EGFR Mutations in Advanced Lung Adenocarcinoma. *Front. Oncol.* **2020**, *10*, 28. https://doi.org/10.3389/fonc.2020.00028.
70. Lu, X.; Li, M.; Zhang, H.; et al. A novel radiomic nomogram for predicting epidermal growth factor receptor mutation in peripheral lung adenocarcinoma. *Phys. Med. Biol.* **2020**, *65*, 055012. https://doi.org/10.1088/1361-6560/ab6f98.
71. Lu, J.; Ji, X.; Wang, L.; et al. Machine Learning-Based Radiomics for Prediction of Epidermal Growth Factor Receptor Mutations in Lung Adenocarcinoma. *Dis. Markers* **2022**, *2022*, 2056837. https://doi.org/10.1155/2022/2056837.
72. Kawazoe, Y.; Shiinoki, T.; Fujimoto, K.; et al. Investigation of the combination of intratumoral and peritumoral radiomic signatures for predicting epidermal growth factor receptor mutation in lung adenocarcinoma. *J. Appl. Clin. Med. Phys.* **2023**, *24*, e13980. https://doi.org/10.1002/acm2.13980.
73. Omura, K.; Murakami, Y.; Hashimoto, K.; et al. Detection of EGFR mutations in early-stage lung adenocarcinoma by machine learning-based radiomics. *Transl. Cancer Res.* **2023**, *12*, 837–847. https://doi.org/10.21037/tcr-22-2683.
74. Shang, Y.; Chen, W.; Li, G.; et al. Computed Tomography-derived intratumoral and peritumoral radiomics in predicting EGFR mutation in lung adenocarcinoma. *Radiol. Med.* **2023**, *128*, 1483–1496. https://doi.org/10.1007/s11547-023-01722-6.
75. Chen, Z.; Gao, S.; Ding, C.; et al. CT-based non-invasive identification of the most common gene mutation status in patients with non-small cell lung cancer. *Med. Phys.* **2024**, *51*, 1872–1882. https://doi.org/10.1002/mp.16744.
76. Ma, J.W.; Jiang, X.; Wang, Y.M.; et al. Dual-energy CT-based radiomics in predicting EGFR mutation status non-invasively in lung adenocarcinoma. *Heliyon* **2024**, *10*, e24372. https://doi.org/10.1016/j.heliyon.2024.e24372.
77. Chen, C.; Liu, X.; Li, A.; et al. Non-invasive prediction of EGFR gene mutations in non-small cell lung cancer by multi-parameter CT perfusion imaging. *Front. Med.* **2025**, *12*, 1660923. https://doi.org/10.3389/fmed.2025.1660923.
78. Li, S.; Luo, T.; Ding, C.; et al. Detailed identification of epidermal growth factor receptor mutations in lung adenocarcinoma: Combining radiomics with machine learning. *Med. Phys.* **2020**, *47*, 3458–3466. https://doi.org/10.1002/mp.14238.
79. Liu, G.; Xu, Z.; Ge, Y.; et al. 3D radiomics predicts EGFR mutation, exon-19 deletion and exon-21 L858R mutation in lung adenocarcinoma. *Transl. Lung Cancer Res.* **2020**, *9*, 1212–1224. https://doi.org/10.21037/tlcr-20-122.
80. Kawazoe, Y.; Shiinoki, T.; Fujimoto, K.; et al. Comparison of the radiomics-based predictive models using machine learning and nomogram for epidermal growth factor receptor mutation status and subtypes in lung adenocarcinoma. *Phys. Eng. Sci. Med.* **2023**, *46*, 395–403. https://doi.org/10.1007/s13246-023-01232-9.
81. Huo, J.W.; Luo, T.Y.; Diao, L.; et al. Using combined CT-clinical radiomics models to identify epidermal growth factor receptor mutation subtypes in lung adenocarcinoma. *Front. Oncol.* **2022**, *12*, 846589. https://doi.org/10.3389/fonc.2022.846589.
82. Hao, P.; Deng, B.Y.; Huang, C.T.; et al. Predicting anaplastic lymphoma kinase rearrangement status in patients with non-small cell lung cancer using a machine learning algorithm that combines clinical features and CT images. *Front. Oncol.* **2022**, *12*, 994285. https://doi.org/10.3389/fonc.2022.994285.
83. Xiong, W.; Yu, X.; Zhou, T.; et al. A Radiomics-clinical Nomogram based on CT Radiomics to Predict Acquired T790M Mutation Status in Non-small Cell Lung Cancer Patients. *Curr. Med. Imaging* **2024**, *20*, e15734056283623. https://doi.org/10.2174/0115734056283623240215102037.
84. Yang, X.; Fang, C.; Li, C.; et al. Can CT Radiomics Detect Acquired T790M Mutation and Predict Prognosis in Advanced Lung Adenocarcinoma with Progression After First- or Second-Generation EGFR TKIs? *Front. Oncol.* **2022**, *12*, 904983. https://doi.org/10.3389/fonc.2022.904983.
85. Le, N.Q.K.; Kha, Q.H.; Nguyen, V.H.; et al. Machine Learning-Based Radiomics Signatures for EGFR and KRAS Mutations Prediction in Non-Small-Cell Lung Cancer. *Int. J. Mol. Sci.* **2021**, *22*, 9254. https://doi.org/10.3390/ijms22179254.
86. Zhang, X.; Zhang, G.; Qiu, X.; et al. Non-invasive decision support for clinical treatment of non-small cell lung cancer using a multiscale radiomics approach. *Radiother. Oncol.* **2024**, *191*, 110082. https://doi.org/10.1016/j.radonc.2024.110082.
87. Ninomiya, K.; Arimura, H.; Tanaka, K.; et al. Three-dimensional topological radiogenomics of epidermal growth factor receptor Del19 and L858R mutation subtypes on computed tomography images of lung cancer patients. *Comput. Methods Programs Biomed.* **2023**, *236*, 107544. https://doi.org/10.1016/j.cmpb.2023.107544.
88. Ma, D.N.; Gao, X.Y.; Dan, Y.B.; et al. Evaluating Solid Lung Adenocarcinoma Anaplastic Lymphoma Kinase Gene Rearrangement Using Noninvasive Radiomics Biomarkers. *Onco Targets Ther.* **2020**, *13*, 6927–6935. https://doi.org/10.2147/OTT.S257798.
89. Song, L.; Zhu, Z.; Mao, L.; et al. Clinical, Conventional CT and Radiomic Feature-Based Machine Learning Models for Predicting ALK Rearrangement Status in Lung Adenocarcinoma Patients. *Front. Oncol.* **2020**, *10*, 369. https://doi.org/10.3389/fonc.2020.00369.
90. Choe, J.; Lee, S.M.; Kim, W.; et al. CT radiomics-based prediction of anaplastic lymphoma kinase and epidermal growth factor receptor mutations in lung adenocarcinoma. *Eur. J. Radiol.* **2021**, *139*, 109710. https://doi.org/10.1016/j.ejrad.2021.109710.

91. Li, X.; Chen, J.; Zhang, C.; et al. Application value of CT radiomic nomogram in predicting T790M mutation of lung adenocarcinoma. *BMC Pulm. Med.* **2023**, *23*, 339. https://doi.org/10.1186/s12890-023-02609-y.
92. Lu, J.; Ji, X.; Liu, X.; et al. Machine learning-based radiomics strategy for prediction of acquired EGFR T790M mutation following treatment with EGFR-TKI in NSCLC. *Sci. Rep.* **2024**, *14*, 446. https://doi.org/10.1038/s41598-023-50984-7.
93. Li, J.; Xu, R.; Wang, D.; et al. Non-invasive identification of TKI-resistant NSCLC: A multi-model AI approach for predicting EGFR/TP53 co-mutations. *BMC Pulm. Med.* **2025**, *25*, 336. https://doi.org/10.1186/s12890-025-03805-8.
94. Zhang, T.; Xu, Z.; Liu, G.; et al. Simultaneous Identification of EGFR, KRAS, ERBB2, and TP53 Mutations in Patients with Non-Small Cell Lung Cancer by Machine Learning-Derived Three-Dimensional Radiomics. *Cancers* **2021**, *13*, 1814. https://doi.org/10.3390/cancers13081814.
95. Jiang, Z.; Dong, Y.; Yang, L.; et al. CT-Based Hand-crafted Radiomic Signatures Can Predict PD-L1 Expression Levels in Non-small Cell Lung Cancer: A Two-Center Study. *J. Digit. Imaging* **2021**, *34*, 1073–1085. https://doi.org/10.1007/s10278-021-00484-9.
96. Wen, Q.; Yang, Z.; Dai, H.; et al. Radiomics Study for Predicting the Expression of PD-L1 and Tumor Mutation Burden in Non-Small Cell Lung Cancer Based on CT Images and Clinicopathological Features. *Front. Oncol.* **2021**, *11*, 620246. https://doi.org/10.3389/fonc.2021.620246.
97. Bracci, S.; Dolciami, M.; Trobiani, C.; et al. Quantitative CT texture analysis in predicting PD-L1 expression in locally advanced or metastatic NSCLC patients. *Radiol. Med.* **2021**, *126*, 1425–1433. https://doi.org/10.1007/s11547-021-01399-9.
98. Shiinoki, T.; Fujimoto, K.; Kawazoe, Y.; et al. Predicting programmed death-ligand 1 expression level in non-small cell lung cancer using a combination of peritumoral and intratumoral radiomic features on computed tomography. *Biomed. Phys. Eng. Express* **2022**, *8*, 025008. https://doi.org/10.1088/2057-1976/ac4d43.
99. Chen, Y.; Xu, T.; Jiang, C.; et al. CT-based radiomics signature to predict CD8+ tumor infiltrating lymphocytes in non-small-cell lung cancer. *Acta Radiol.* **2023**, *64*, 1390–1399. https://doi.org/10.1177/02841851221126596.
100. Sun, R.; Sundahl, N.; Hecht, M.; et al. Radiomics to predict outcomes and abscopal response of patients with cancer treated with immunotherapy combined with radiotherapy using a validated signature of CD8 cells. *J. Immunother. Cancer* **2020**, *8*, e001429. https://doi.org/10.1136/jitc-2020-001429.
101. Sun, Z.; Hu, S.; Ge, Y.; et al. Radiomics study for predicting the expression of PD-L1 in non-small cell lung cancer based on CT images and clinicopathologic features. *J. X-Ray Sci. Technol.* **2020**, *28*, 449–459. https://doi.org/10.3233/xst-200642.
102. Yoon, J.; Suh, Y.J.; Han, K.; et al. Utility of CT radiomics for prediction of PD-L1 expression in advanced lung adenocarcinomas. *Thorac. Cancer* **2020**, *11*, 993–1004. https://doi.org/10.1111/1759-7714.13352.
103. Liu, P.M.; Feng, B.; Shi, J.F.; et al. A deep-learning model using enhanced chest CT images to predict PD-L1 expression in non-small-cell lung cancer patients. *Clin. Radiol.* **2023**, *78*, e689–e697. https://doi.org/10.1016/j.crad.2023.05.010.
104. Fu, Y.; Zhang, H.; Xue, P.; et al. Qualitative analysis of PD-L1 expression in non-small-cell lung cancer based on chest CT radiomics. *Biomed. Signal Process. Control.* **2023**, *84*, 104815. https://doi.org/10.1016/j.bspc.2023.104815.
105. Montoya, C.; Spieler, B.; Welford, S.M.; et al. Predicting response to immunotherapy in non-small cell lung cancer- from bench to bedside. *Front. Oncol.* **2023**, *13*, 1225720. https://doi.org/10.3389/fonc.2023.1225720.
106. Iwatate, Y.; Hoshino, I.; Yokota, H.; et al. Radiogenomics for predicting p53 status, PD-L1 expression, and prognosis with machine learning in pancreatic cancer. *Br. J. Cancer* **2020**, *123*, 1253–1261. https://doi.org/10.1038/s41416-020-0997-1.
107. Park, C.; Jeong, D.Y.; Choi, Y.; et al. Tumor-infiltrating lymphocyte enrichment predicted by CT radiomics analysis is associated with clinical outcomes of non-small cell lung cancer patients receiving immune checkpoint inhibitors. *Front. Immunol.* **2023**, *13*, 1038089. https://doi.org/10.3389/fimmu.2022.1038089.
108. Chen, M.; Lu, H.; Copley, S.J.; et al. A Novel Radiogenomics Biomarker for Predicting Treatment Response and Pneumotoxicity From Programmed Cell Death Protein or Ligand-1 Inhibition Immunotherapy in NSCLC. *J. Thorac. Oncol.* **2023**, *18*, 718–730. https://doi.org/10.1016/j.jtho.2023.01.089.
109. Wu, S.; Zhan, W.; Liu, L.; et al. Pretreatment radiomic biomarker for immunotherapy responder prediction in stage IB–IV NSCLC (LCDigital-IO Study): A multicenter retrospective study. *J. Immunother. Cancer* **2023**, *11*, e007369. https://doi.org/10.1136/jitc-2023-007369.
110. Yolchuyeva, S.; Giacomazzi, E.; Tonneau, M.; et al. A Radiomics-Clinical Model Predicts Overall Survival of Non-Small Cell Lung Cancer Patients Treated with Immunotherapy: A Multicenter Study. *Cancers* **2023**, *15*, 3829. https://doi.org/10.3390/cancers15153829.
111. Yolchuyeva, S.; Ebrahimpour, L.; Tonneau, M.; et al. Multi-institutional prognostic modeling of survival outcomes in NSCLC patients treated with first-line immunotherapy using radiomics. *J. Transl. Med.* **2024**, *22*, 42. https://doi.org/10.1186/s12967-024-04854-z.

112. Wu, S.; Pan, J.; Zheng, Y.; et al. Integration of Machine Learning, Bioinformatics, and Experimental Validation to Identify Novel Diagnostic and Prognostic Biomarkers Associated with Succinylation in Lung Adenocarcinoma. *Drug Dev. Res.* **2025**, *86*, e70184. https://doi.org/10.1002/ddr.70184.
113. Zhang, J.; Zhao, X.; Zhao, Y.; et al. Value of pre-therapy ^{18}F-FDG PET/CT radiomics in predicting EGFR mutation status in patients with non-small cell lung cancer. *Eur. J. Nucl. Med. Mol. Imaging* **2020**, *47*, 1137–1146. https://doi.org/10.1007/s00259-019-04592-1.
114. Yang, B.; Ji, H.S.; Zhou, C.S.; et al. ^{18}F-fluorodeoxyglucose positron emission tomography/computed tomography-based radiomic features for prediction of epidermal growth factor receptor mutation status and prognosis in patients with lung adenocarcinoma. *Transl. Lung Cancer Res.* **2020**, *9*, 563–574. https://doi.org/10.21037/tlcr-19-592.
115. Shiri, I.; Amini, M.; Nazari, M.; et al. Impact of feature harmonization on radiogenomics analysis: Prediction of EGFR and KRAS mutations from non-small cell lung cancer PET/CT images. *Comput. Biol. Med.* **2022**, *142*, 105230. https://doi.org/10.1016/j.compbiomed.2022.105230.
116. Li, H.; Gao, C.; Sun, Y.; et al. Radiomics Analysis to Enhance Precise Identification of Epidermal Growth Factor Receptor Mutation Based on Positron Emission Tomography Images of Lung Cancer Patients. *J. Biomed. Nanotechnol.* **2021**, *17*, 691–702. https://doi.org/10.1166/jbn.2021.3056.
117. Wang, C.; Zhang, R.; Sun, X.; et al. Prediction of epidermal growth factor receptor mutation status by textural features in stage IV lung adenocarcinoma. *Memo-Mag. Eur. Med. Oncol.* **2024**, *17*, 100–106. https://doi.org/10.1007/s12254-024-00961-1.
118. Liu, Z.; Zhang, T.; Lin, L.; et al. Applications of radiomics-based analysis pipeline for predicting epidermal growth factor receptor mutation status. *Biomed. Eng. Online* **2023**, *22*, 17. Correction in: *Biomed. Eng. Online* **2023**, *22*, 32. https://doi.org/10.1186/s12938-022-01049-9.
119. Koyasu, S.; Nishio, M.; Isoda, H.; et al. Usefulness of gradient tree boosting for predicting histological subtype and EGFR mutation status of non-small cell lung cancer on ^{18}F FDG-PET/CT. *Ann. Nucl. Med.* **2020**, *34*, 49–57. https://doi.org/10.1007/s12149-019-01414-0.
120. Agüloğlu, N.; Aksu, A.; Akyol, M.; et al. Importance of pretreatment ^{18}F-FDG PET/CT texture analysis in predicting EGFR and ALK mutations in patients with non-small-cell lung cancer. *Nuklearmedizin* **2022**, *61*, 433–439. https://doi.org/10.1055/a-1868-4918.
121. Li, S.; Hu, Y.; Tian, C.; et al. Prediction of EGFR-TP53 genes co-mutations in patients with lung adenocarcinoma (LUAD) by ^{18}F-FDG PET/CT radiomics. *Clin. Transl. Oncol.* **2025**, *27*, 1506–1515. https://doi.org/10.1007/s12094-024-03685-0.
122. Zhang, M.; Bao, Y.; Rui, W.; et al. Performance of ^{18}F-FDG PET/CT Radiomics for Predicting EGFR Mutation Status in Patients with Non-Small Cell Lung Cancer. *Front. Oncol.* **2020**, *10*, 568857. https://doi.org/10.3389/fonc.2020.568857.
123. Aide, N.; Weyts, K.; Lasnon, C. Prediction of the Presence of Targetable Molecular Alteration(s) with Clinico-Metabolic 18 F-FDG PET Radiomics in Non-Asian Lung Adenocarcinoma Patients. *Diagnostics* **2022**, *12*, 2448. https://doi.org/10.3390/diagnostics12102448.
124. Li, S.; Li, Y.; Zhao, M.; et al. Combination of ^{18}F-Fluorodeoxyglucose PET/CT Radiomics and Clinical Features for Predicting Epidermal Growth Factor Receptor Mutations in Lung Adenocarcinoma. *Korean J. Radiol.* **2022**, *23*, 921–930. https://doi.org/10.3348/kjr.2022.0295.
125. Zhao, H.Y.; Su, Y.X.; Zhang, L.H.; et al. Prediction model based on ^{18}F-FDG PET/CT radiomic features and clinical factors of EGFR mutations in lung adenocarcinoma. *Neoplasma* **2022**, *69*, 233–241. https://doi.org/10.4149/neo_2021_201222n1388.
126. Gao, J.; Niu, R.; Shi, Y.; et al. The predictive value of [^{18}F]FDG PET/CT radiomics combined with clinical features for EGFR mutation status in different clinical staging of lung adenocarcinoma. *EJNMMI Res.* **2023**, *13*, 26. https://doi.org/10.1186/s13550-023-00977-4.
127. Liu, Q.; Sun, D.; Li, N.; et al. Predicting EGFR mutation subtypes in lung adenocarcinoma using ^{18}F-FDG PET/CT radiomic features. *Transl. Lung Cancer Res.* **2020**, *9*, 549–562. https://doi.org/10.21037/tlcr.2020.04.17.
128. Chang, C.; Zhou, S.; Yu, H.; et al. A clinically practical radiomics-clinical combined model based on PET/CT data and nomogram predicts EGFR mutation in lung adenocarcinoma. *Eur. Radiol.* **2021**, *31*, 6259–6268. https://doi.org/10.1007/s00330-020-07676-x.
129. Nair, J.K.R.; Saeed, U.A.; McDougall, C.C.; et al. Radiogenomic Models Using Machine Learning Techniques to Predict EGFR Mutations in Non-Small Cell Lung Cancer. *Can. Assoc. Radiol. J.* **2021**, *72*, 109–119. https://doi.org/10.1177/0846537119899526.
130. Tan, J.L.; Xia, L.; Sun, S.G.; et al. Prediction of EGFR mutation status in lung adenocarcinoma based on ^{18}F-FDG PET/CT radiomic features. *Am. J. Nucl. Med. Mol. Imaging* **2023**, *13*, 230–244.
131. Zhang, T.; Liu, Z.; Lin, L.; et al. Detection of the gene mutation of epidermal growth factor receptor in lung adenocarcinoma by radiomic features from a small amount of PET data. *Nucl. Med. Commun.* **2023**, *44*, 795–802. https://doi.org/10.1097/mnm.0000000000001718.

132. Ruan, D.; Fang, J.; Teng, X. Efficient ^{18}F-fluorodeoxyglucose positron emission tomography/computed tomography-based machine learning model for predicting epidermal growth factor receptor mutations in non-small cell lung cancer. *Q. J. Nucl. Med. Mol. Imaging* **2024**, *68*, 70–83. https://doi.org/10.23736/s1824-4785.22.03441-0.
133. Wang, Y.; Yang, G.; Gao, X.; et al. Subregion-specific ^{18}F-FDG PET-CT radiomics for the pre-treatment prediction of EGFR mutation status in solid lung adenocarcinoma. *Am. J. Nucl. Med. Mol. Imaging* **2024**, *14*, 134–143. https://doi.org/10.62347/ddrr4923.
134. Chang, C.; Sun, X.; Wang, G.; et al. A Machine Learning Model Based on PET/CT Radiomics and Clinical Characteristics Predicts ALK Rearrangement Status in Lung Adenocarcinoma. *Front. Oncol.* **2021**, *11*, 603882. https://doi.org/10.3389/fonc.2021.603882.
135. Wang, J.; Lv, X.; Huang, W.; et al. Establishment and Optimization of Radiomics Algorithms for Prediction of KRAS Gene Mutation by Integration of NSCLC Gene Mutation Mutual Exclusion Information. *Front. Pharmacol.* **2022**, *13*, 862581. https://doi.org/10.3389/fphar.2022.862581.
136. Zhang, R.; Shi, K.; Hohenforst-Schmidt, W.; et al. Ability of ^{18}F-FDG Positron Emission Tomography Radiomics and Machine Learning in Predicting KRAS Mutation Status in Therapy-Naive Lung Adenocarcinoma. *Cancers* **2023**, *15*, 3684. https://doi.org/10.3390/cancers15143684.
137. Hinzpeter, R.; Kulanthaivelu, R.; Kohan, A.; et al. Predictive [^{18}F]-FDG PET/CT-Based Radiogenomics Modelling of Driver Gene Mutations in Non-small Cell Lung Cancer. *Acad. Radiol.* **2024**, *31*, 5314–5323. https://doi.org/10.1016/j.acra.2024.06.038.
138. Li, J.; Ge, S.; Sang, S.; et al. Evaluation of PD-L1 Expression Level in Patients with Non-Small Cell Lung Cancer by ^{18}F-FDG PET/CT Radiomics and Clinicopathological Characteristics. *Front. Oncol.* **2021**, *11*, 789014. https://doi.org/10.3389/fonc.2021.789014.
139. Zhang, R.; Hohenforst-Schmidt, W.; Steppert, C.; et al. Standardized ^{18}F-FDG PET/CT radiomic features provide information on PD-L1 expression status in treatment-naïve patients with non-small cell lung cancer. *Nuklearmedizin* **2022**, *61*, 385–393. https://doi.org/10.1055/a-1816-6950.
140. Jiang, M.; Sun, D.; Guo, Y.; et al. Assessing PD-L1 Expression Level by Radiomic Features From PET/CT in Nonsmall Cell Lung Cancer Patients: An Initial Result. *Acad. Radiol.* **2020**, *27*, 171–179. https://doi.org/10.1016/j.acra.2019.04.016.
141. Kiss, F.J.; Járó, A.I.; Máthé, D.; et al. Predicting PD-L1 expression status in NSCLC using radiomic analysis of 18 F-FDG-PET/CT images. *Eur. J. Nucl. Med. Mol. Imaging* **2026**, *53*, 800–811. https://doi.org/10.1007/s00259-025-07453-2.
142. Ji, Y.; Cui, K.; Zhang, J.; et al. Noninvasive Prediction of Programmed Cell Death Protein-Ligand 1 Expression in Locally Advanced Non-small Cell Lung Cancer by ^{18}F-Fluorodeoxyglucose Positron Emission Tomography/Computed Tomography-Based Metabolic Habitats: A Multicenter Radiomic and Biological Study. *Ann. Surg. Oncol.* **2025**, *32*, 10094–10107. https://doi.org/10.1245/s10434-025-18139-2.
143. Lim, C.H.; Koh, Y.W.; Hyun, S.H.; et al. A Machine Learning Approach Using PET/CT-based Radiomics for Prediction of PD-L1 Expression in Non-small Cell Lung Cancer. *Anticancer Res.* **2022**, *42*, 5875–5884. https://doi.org/10.21873/anticanres.16096.
144. Wang, Y.B.; He, X.; Song, X.; et al. The radiomic biomarker in non-small cell lung cancer: ^{18}F-FDG PET/CT characterisation of programmed death-ligand 1 status. *Clin. Radiol.* **2023**, *78*, e732–e740. https://doi.org/10.1016/j.crad.2023.06.003.
145. Wang, Y.; Zhao, N.; Wu, Z.; et al. New insight on the correlation of metabolic status on ^{18}F-FDG PET/CT with immune marker expression in patients with non-small cell lung cancer. *Eur. J. Nucl. Med. Mol. Imaging* **2020**, *47*, 1127–1136. https://doi.org/10.1007/s00259-019-04500-7.
146. Wu, L.; Liu, J.; Wang, S.; et al. Negative Correlation Between ^{18}F-RGD Uptake via PET and Tumoral PD-L1 Expression in Non-Small Cell Lung Cancer. *Front. Endocrinol.* **2022**, *13*, 913631. https://doi.org/10.3389/fendo.2022.913631.
147. Wang, L.; Ruan, M.; Lei, B.; et al. The potential of ^{18}F-FDG PET/CT in predicting PDL1 expression status in pulmonary lesions of untreated stage IIIB-IV non-small-cell lung cancer. *Lung Cancer* **2020**, *150*, 44–52.
148. Zhou, J.; Zou, S.; Cheng, S.; et al. Correlation Between Dual-Time-Point FDG PET and Tumor Microenvironment Immune Types in Non-Small Cell Lung Cancer. *Front. Oncol.* **2021**, *11*, 559623. https://doi.org/10.3389/fonc.2021.559623.
149. Cui, Y.; Lin, Y.; Zhao, Z.; et al. Comprehensive ^{18}F-FDG PET-based radiomics in elevating the pathological response to neoadjuvant immunochemotherapy for resectable stage III non-small-cell lung cancer: A pilot study. *Front. Immunol.* **2022**, *13*, 994917. https://doi.org/10.3389/fimmu.2022.994917.
150. Yang, M.; Li, X.; Cai, C.; et al. [^{18}F]FDG PET-CT radiomics signature to predict pathological complete response to neoadjuvant chemoimmunotherapy in non-small cell lung cancer: A multicenter study. *Eur. Radiol.* **2024**, *34*, 4352–4363. https://doi.org/10.1007/s00330-023-10503-8.
151. Ahn, S.J.; Kwon, H.; Yang, J.J.; et al. Contrast-enhanced T1-weighted image radiomics of brain metastases may predict EGFR mutation status in primary lung cancer. *Sci. Rep.* **2020**, *10*, 8905. https://doi.org/10.1038/s41598-020-65470-7.

152. Meißner, A.K.; Gutsche, R.; Galldiks, N.; et al. Radiomics for the non-invasive prediction of PD-L1 expression in patients with brain metastases secondary to non-small cell lung cancer. *J. Neurooncol.* **2023**, *163*, 597–605. https://doi.org/10.1007/s11060-023-04367-7.
153. Hu, Y.; Geng, Y.; Wang, H.; et al. Improved Prediction of Epidermal Growth Factor Receptor Status by Combined Radiomics of Primary Nonsmall-Cell Lung Cancer and Distant Metastasis. *J. Comput. Assist. Tomogr.* **2024**, *48*, 780–788. https://doi.org/10.1097/rct.0000000000001591.
154. Zhang, G.; Man, Q.; Shang, L.; et al. Using Multi-phase CT Radiomics Features to Predict EGFR Mutation Status in Lung Adenocarcinoma Patients. *Acad. Radiol.* **2024**, *31*, 2591–2600. https://doi.org/10.1016/j.acra.2023.12.024.
155. Song, J.; Ding, C.; Huang, Q.; et al. Deep learning predicts epidermal growth factor receptor mutation subtypes in lung adenocarcinoma. *Med. Phys.* **2021**, *48*, 7891–7899. https://doi.org/10.1002/mp.15307.
156. Deng, K.; Wang, L.; Liu, Y.; et al. A deep learning-based system for survival benefit prediction of tyrosine kinase inhibitors and immune checkpoint inhibitors in stage IV non-small cell lung cancer patients: A multicenter, prognostic study. *EClinicalMedicine* **2022**, *51*, 101541. https://doi.org/10.1016/j.eclinm.2022.101541.
157. Xu, N.; Wang, J.; Dai, G.; et al. EfficientNet-Based System for Detecting EGFR-Mutant Status and Predicting Prognosis of Tyrosine Kinase Inhibitors in Patients with NSCLC. *J. Imaging Inform. Med.* **2024**, *37*, 1086–1099. https://doi.org/10.1007/s10278-024-01022-z.
158. Dong, Y.; Hou, L.; Yang, W.; et al. Multi-channel multi-task deep learning for predicting EGFR and KRAS mutations of non-small cell lung cancer on CT images. *Quant. Imaging Med. Surg.* **2021**, *11*, 2354–2375. https://doi.org/10.21037/qims-20-600.
159. Song, Z.; Liu, T.; Shi, L.; et al. The deep learning model combining CT image and clinicopathological information for predicting ALK fusion status and response to ALK-TKI therapy in non-small cell lung cancer patients. *Eur. J. Nucl. Med. Mol. Imaging* **2021**, *48*, 361–371. https://doi.org/10.1007/s00259-020-04986-6.
160. Xiao, Z.; Cai, H.; Wang, Y.; et al. Deep learning for predicting epidermal growth factor receptor mutations of non-small cell lung cancer on PET/CT images. *Quant. Imaging Med. Surg.* **2023**, *13*, 1286–1299. https://doi.org/10.21037/qims-22-760.
161. Zhang, B.; Qi, S.; Pan, X.; et al. Deep CNN Model Using CT Radiomics Feature Mapping Recognizes EGFR Gene Mutation Status of Lung Adenocarcinoma. *Front. Oncol.* **2021**, *10*, 598721. https://doi.org/10.3389/fonc.2020.598721.
162. Zhang, G.; Shang, L.; Cao, Y.; et al. Prediction of epidermal growth factor receptor (EGFR) mutation status in lung adenocarcinoma patients on computed tomography (CT) images using 3-dimensional (3D) convolutional neural network. *Quant. Imaging Med. Surg.* **2024**, *14*, 6048–6059. https://doi.org/10.21037/qims-24-33.
163. Shao, X.; Ge, X.; Gao, J.; et al. Transfer learning–based PET/CT three-dimensional convolutional neural network fusion of image and clinical information for prediction of EGFR mutation in lung adenocarcinoma. *BMC Med. Imaging* **2024**, *24*, 54. https://doi.org/10.1186/s12880-024-01232-5.
164. Yoon, H.J.; Choi, J.; Kim, E.; et al. Deep learning analysis to predict EGFR mutation status in lung adenocarcinoma manifesting as pure ground-glass opacity nodules on CT. *Front. Oncol.* **2022**, *12*, 951575. https://doi.org/10.3389/fonc.2022.951575.
165. Huang, X.; Sun, Y.; Tan, M.; et al. Three-Dimensional Convolutional Neural Network-Based Prediction of Epidermal Growth Factor Receptor Expression Status in Patients with Non-Small Cell Lung Cancer. *Front. Oncol.* **2022**, *12*, 772770. https://doi.org/10.3389/fonc.2022.772770.
166. Mahajan, A.; Kania, V.; Agarwal, U.; et al. Deep-Learning-Based Predictive Imaging Biomarker Model for EGFR Mutation Status in Non-Small Cell Lung Cancer from CT Imaging. *Cancers* **2024**, *16*, 1130. https://doi.org/10.3390/cancers16061130.
167. Yin, G.; Wang, Z.; Song, Y.; et al. Prediction of EGFR Mutation Status Based on ^{18}F-FDG PET/CT Imaging Using Deep Learning-Based Model in Lung Adenocarcinoma. *Front. Oncol.* **2021**, *11*, 709137. https://doi.org/10.3389/fonc.2021.709137.
168. Silva, F.; Pereira, T.; Morgado, J.; et al. *EGFR* Assessment in Lung Cancer CT Images: Analysis of Local and Holistic Regions of Interest Using Deep Unsupervised Transfer Learning. *IEEE Access* **2021**, *9*, 58667–58676. https://doi.org/10.1109/access.2021.3070701.
169. Tian, P.; He, B.; Mu, W.; et al. Assessing PD-L1 expression in non-small cell lung cancer and predicting responses to immune checkpoint inhibitors using deep learning on computed tomography images. *Theranostics* **2021**, *11*, 2098–2107. https://doi.org/10.7150/thno.48027.
170. He, B.; Dong, D.; She, Y.; et al. Predicting response to immunotherapy in advanced non-small-cell lung cancer using tumor mutational burden radiomic biomarker. *J. Immunother. Cancer* **2020**, *8*, e000550. https://doi.org/10.1136/jitc-2020-000550.
171. Yuan, L.; Wang, Q.; Sun, F.; et al. Deep learning and inflammatory markers predict early response to immunotherapy in unresectable NSCLC: A multicenter study. *Biomol. Biomed.* **2025**, *25*, 2252–2268. https://doi.org/10.17305/bb.2025.12324.
172. Zhu, Y.; Liu, Y.L.; Feng, Y.; et al. A CT-derived deep neural network predicts for programmed death ligand-1 expression status in advanced lung adenocarcinomas. *Ann. Transl. Med.* **2020**, *8*, 930. https://doi.org/10.21037/atm-19-4690.

173. Liang, C.; Zheng, M.; Zou, H.; et al. Deep learning-based image analysis predicts PD-L1 status from ^{18}F-FDG PET/CT images in non-small-cell lung cancer. *Front. Oncol.* **2024**, *14*, 1402994. https://doi.org/10.3389/fonc.2024.1402994.
174. Saad, M.B.; Hong, L.; Aminu, M.; et al. Predicting benefit from immune checkpoint inhibitors in patients with non-small-cell lung cancer by CT-based ensemble deep learning: A retrospective study. *Lancet Digit. Health* **2023**, *5*, e404–e420. Correction in: *Lancet Digit. Health* **2023**, *5*, e403. https://doi.org/10.1016/s2589-7500(23)00082-1.
175. Mu, W.; Jiang, L.; Shi, Y.; et al. Non-invasive measurement of PD-L1 status and prediction of immunotherapy response using deep learning of PET/CT images. *J. Immunother. Cancer* **2021**, *9*, e002118.
176. Huang, X.; Huang, X.; Xie, Y.; et al. Integrative habitat analysis and multi-instance deep learning for predictive model of PD-1/PD-L1 immunotherapy efficacy in NSCLC patients: A dual-center retrospective study. *BMC Med. Imaging* **2025**, *25*, 288. https://doi.org/10.1186/s12880-025-01828-5.
177. Pao, J.J.; Biggs, M.; Duncan, D.; et al. Predicting EGFR mutational status from pathology images using a real-world dataset. *Sci. Rep.* **2023**, *13*, 4404. https://doi.org/10.1038/s41598-023-31284-6.
178. Zhao, D.; Zhao, Y.; He, S.; et al. High accuracy epidermal growth factor receptor mutation prediction via histopathological deep learning. *BMC Pulm. Med.* **2023**, *23*, 244. https://doi.org/10.1186/s12890-023-02537-x.
179. Zanoletti, M.; Ugolini, F.; El Bachiri, L.; et al. EGFR Mutation Detection in Whole Slide Images of Non-Small Cell Lung Cancers Using a Two-Stage Deep Transfer Learning Approach. *Cancer Med.* **2025**, *14*, e71249. https://doi.org/10.1002/cam4.71249.
180. Zhang, W.; Wang, W.; Xu, Y.; et al. Prediction of Epidermal Growth Factor Receptor Mutation Subtypes in Non–Small Cell Lung Cancer from Hematoxylin and Eosin–Stained Slides Using Deep Learning. *Lab. Invest.* **2024**, *104*, 102094. https://doi.org/10.1016/j.labinv.2024.102094.
181. Terada, Y.; Takahashi, T.; Hayakawa, T.; et al. Artificial Intelligence–Powered Prediction of *ALK* Gene Rearrangement in Patients with Non–Small-Cell Lung Cancer. *JCO Clin. Cancer Inform.* **2022**, *6*, e2200070. Erratum in: *JCO Clin. Cancer Inform.* **2022**, *6*, e2200157. https://doi.org/10.1200/cci.22.00070.
182. Wang, X.; Zhao, J.; Marostica, E.; et al. A pathology foundation model for cancer diagnosis and prognosis prediction. *Nature* **2024**, *634*, 970–978. https://doi.org/10.1038/s41586-024-07894-z.
183. Cheng, G.; Zhang, F.; Xing, Y.; et al. Artificial Intelligence-Assisted Score Analysis for Predicting the Expression of the Immunotherapy Biomarker PD-L1 in Lung Cancer. *Front. Immunol.* **2022**, *13*, 893198. https://doi.org/10.3389/fimmu.2022.893198.
184. Wu, J.; Liu, C.; Liu, X.; et al. Artificial intelligence-assisted system for precision diagnosis of PD-L1 expression in non-small cell lung cancer. *Mod. Pathol.* **2022**, *35*, 403–411. https://doi.org/10.1038/s41379-021-00904-9.
185. Jain, M.S.; Massoud, T.F. Predicting tumour mutational burden from histopathological images using multiscale deep learning. *Nat. Mach. Intell.* **2020**, *2*, 356–362. https://doi.org/10.1038/s42256-020-0190-5.
186. Sadhwani, A.; Chang, H.W.; Behrooz, A.; et al. Comparative analysis of machine learning approaches to classify tumor mutation burden in lung adenocarcinoma using histopathology images. *Sci. Rep.* **2021**, *11*, 16605. https://doi.org/10.1038/s41598-021-95747-4.
187. Mayer, C.; Ofek, E.; Fridrich, D.E.; et al. Direct identification of ALK and ROS1 fusions in non-small cell lung cancer from hematoxylin and eosin-stained slides using deep learning algorithms. *Mod. Pathol.* **2022**, *35*, 1882–1887. https://doi.org/10.1038/s41379-022-01141-4.
188. Niu, Y.; Wang, L.; Zhang, X.; et al. Predicting Tumor Mutational Burden From Lung Adenocarcinoma Histopathological Images Using Deep Learning. *Front. Oncol.* **2022**, *12*, 927426. https://doi.org/10.3389/fonc.2022.927426.
189. Dammak, S.; Cecchini, M.J.; Breadner, D.; et al. Using deep learning to predict tumor mutational burden from scans of H&E-stained multicenter slides of lung squamous cell carcinoma. *J. Med. Imaging* **2023**, *10*, 017502. https://doi.org/10.1117/1.jmi.10.1.017502.
190. Ishii, S.; Takamatsu, M.; Ninomiya, H.; et al. Machine learning-based gene alteration prediction model for primary lung cancer using cytologic images. *Cancer Cytopathol.* **2022**, *130*, 812–823. https://doi.org/10.1002/cncy.22609.
191. Hondelink, L.M.; Hüyük, M.; Postmus, P.E.; et al. Development and validation of a supervised deep learning algorithm for automated whole-slide programmed death-ligand 1 tumour proportion score assessment in non-small cell lung cancer. *Histopathology* **2022**, *80*, 635–647. https://doi.org/10.1111/his.14571.
192. Choi, S.; Cho, S.I.; Ma, M.; et al. Artificial intelligence–powered programmed death ligand 1 analyser reduces interobserver variation in tumour proportion score for non–small cell lung cancer with better prediction of immunotherapy response. *Eur. J. Cancer* **2022**, *170*, 17–26. https://doi.org/10.1016/j.ejca.2022.04.011.
193. Liu, J.; Zheng, Q.; Mu, X.; et al. Automated tumor proportion score analysis for PD-L1 (22C3) expression in lung squamous cell carcinoma. *Sci. Rep.* **2021**, *11*, 15907. https://doi.org/10.1038/s41598-021-95372-1.
194. Zhao, Y.; Xiong, S.; Ren, Q.; et al. Deep learning using histological images for gene mutation prediction in lung cancer: A multicentre retrospective study. *Lancet Oncol.* **2025**, *26*, 136–146. https://doi.org/10.1016/s1470-2045(24)00599-0.

195. Wang, X.; Chen, P.; Ding, G.; et al. Dual-scale categorization based deep learning to evaluate programmed cell death ligand 1 expression in non-small cell lung cancer. *Medicine* **2021**, *100*, e25994. https://doi.org/10.1097/md.0000000000025994.
196. Ligero, M.; Serna, G.; El Nahhas, O.S.M.; et al. Weakly Supervised Deep Learning Predicts Immunotherapy Response in Solid Tumors Based on PD-L1 Expression. *Cancer Res. Commun.* **2024**, *4*, 92–102. https://doi.org/10.1158/2767-9764.crc-23-0287.
197. Kather, J.N.; Heij, L.R.; Grabsch, H.I.; et al. Pan-cancer image-based detection of clinically actionable genetic alterations. *Nat. Cancer* **2020**, *1*, 789–799. Correction in: *Nat. Cancer* **2020**, *1*, 1129. https://doi.org/10.1038/s43018-020-0087-6.
198. Lu, M.Y.; Chen, T.Y.; Williamson, D.F.K.; et al. AI-based pathology predicts origins for cancers of unknown primary. *Nature* **2021**, *594*, 106–110. https://doi.org/10.1038/s41586-021-03512-4.
199. Wang, Y.; Coudray, N.; Zhao, Y.; et al. HEAL: An automated deep learning framework for cancer histopathology image analysis. *Bioinformatics* **2021**, *37*, 4291–4295. https://doi.org/10.1093/bioinformatics/btab380.
200. Huang, Z.; Chen, L.; Lv, L.; et al. A new AI-assisted scoring system for PD-L1 expression in NSCLC. *Comput. Methods Programs Biomed.* **2022**, *221*, 106829. https://doi.org/10.1016/j.cmpb.2022.106829.
201. Campanella, G.; Kumar, N.; Nanda, S.; et al. Real-world deployment of a fine-tuned pathology foundation model for lung cancer biomarker detection. *Nat. Med.* **2025**, *31*, 3002–3010. https://doi.org/10.1038/s41591-025-03780-x.
202. Li, Y.; Lv, X.; Chen, C.; et al. A deep learning model integrating multisequence MRI to predict EGFR mutation subtype in brain metastases from non-small cell lung cancer. *Eur. Radiol. Exp.* **2024**, *8*, 2. https://doi.org/10.1186/s41747-023-00396-z.
203. You, S.; Fan, Y.; Yang, Z.; et al. Deep learning on brain metastasis for predicting EGFR genotype and EGFR-TKI therapy response in metastatic NSCLC: A multicenter study. *Front. Bioeng. Biotechnol.* **2025**, *13*, 1637095. https://doi.org/10.3389/fbioe.2025.1637095.
204. Cao, P.; Jia, X.; Wang, X.; et al. Deep learning radiomics for the prediction of epidermal growth factor receptor mutation status based on MRI in brain metastasis from lung adenocarcinoma patients. *BMC Cancer* **2025**, *25*, 443. https://doi.org/10.1186/s12885-025-13823-8.
205. Fang, Y.; Wang, M.; Song, Q.; et al. Tackling Tumor Heterogeneity Issue: Transformer-Based Multiple Instance Enhancement Learning for Predicting EGFR Mutation via CT Images. *IEEE Trans. Med. Imaging* **2025**, *44*, 4524–4535. https://doi.org/10.1109/TMI.2025.3578995.
206. Xiang, J.; Wang, X.; Zhang, X.; et al. A vision–language foundation model for precision oncology. *Nature* **2025**, *638*, 769–778. https://doi.org/10.1038/s41586-024-08378-w.
207. Shao, J.; Ma, J.; Zhang, S.; et al. Radiogenomic System for Non-Invasive Identification of Multiple Actionable Mutations and PD-L1 Expression in Non-Small Cell Lung Cancer Based on CT Images. *Cancers* **2022**, *14*, 4823. https://doi.org/10.3390/cancers14194823.
208. Song, J.; Wang, L.; Ng, N.N.; et al. Development and Validation of a Machine Learning Model to Explore Tyrosine Kinase Inhibitor Response in Patients with Stage IV *EGFR* Variant–Positive Non–Small Cell Lung Cancer. *JAMA Netw. Open* **2020**, *3*, e2030442. https://doi.org/10.1001/jamanetworkopen.2020.30442.
209. Zhao, S.; Li, W.; Liu, Z.; et al. End-to-End Prediction of EGFR Mutation Status with Denseformer. *IEEE J. Biomed. Health Inform.* **2024**, *28*, 54–65. https://doi.org/10.1109/jbhi.2023.3307295.
210. Gui, D.; Song, Q.; Song, B.; et al. AIR-Net: A novel multi-task learning method with auxiliary image reconstruction for predicting EGFR mutation status on CT images of NSCLC patients. *Comput. Biol. Med.* **2022**, *141*, 105157. https://doi.org/10.1016/j.compbiomed.2021.105157.
211. Feng, Y.; Song, F.; Zhang, P.; et al. Prediction of EGFR Mutation Status in Non–Small Cell Lung Cancer Based on Ensemble Learning. *Front. Pharmacol.* **2022**, *13*, 897597. https://doi.org/10.3389/fphar.2022.897597.
212. Chen, S.; Han, X.; Tian, G.; et al. Using stacked deep learning models based on PET/CT images and clinical data to predict EGFR mutations in lung cancer. *Front. Med.* **2022**, *9*, 1041034. https://doi.org/10.3389/fmed.2022.1041034.
213. Qin, R.; Wang, Z.; Qiao, K.; et al. Multi-Type Interdependent Feature Analysis Based on Hybrid Neural Networks for Computer-Aided Diagnosis of Epidermal Growth Factor Receptor Mutations. *IEEE Access* **2020**, *8*, 38517–38527. https://doi.org/10.1109/access.2020.2971281.
214. Prelaj, A.; Galli, E.G.; Miskovic, V.; et al. Real-world data to build explainable trustworthy artificial intelligence models for prediction of immunotherapy efficacy in NSCLC patients. *Front. Oncol.* **2023**, *12*, 1078822. https://doi.org/10.3389/fonc.2022.1078822.
215. Benfares, A.; Alami, B.; Boukansa, S.; et al. NSCLC EGFR Mutation Prediction via Random Forest Model: A Clinical–CT–Radiomics Integration Approach. *Adv. Respir. Med.* **2025**, *93*, 39. https://doi.org/10.3390/arm93050039.
216. Qin, X.; Wang, H.; Hu, X.; et al. Predictive models for patients with lung carcinomas to identify EGFR mutation status via an artificial neural network based on multiple clinical information. *J. Cancer Res. Clin. Oncol.* **2020**, *146*, 767–775. https://doi.org/10.1007/s00432-019-03103-x.

217. Wang, L.; Zhang, H.; Pan, C.; et al. Predicting Durable Responses to Immune Checkpoint Inhibitors in Non-Small-Cell Lung Cancer Using a Multi-Feature Model. *Front. Immunol.* **2022**, *13*, 829634. https://doi.org/10.3389/fimmu.2022.829634.
218. Yao, X.; Zhu, Y.; Huang, Z.; et al. Fusion of shallow and deep features from ^{18}F-FDG PET/CT for predicting EGFR-sensitizing mutations in non-small cell lung cancer. *Quant. Imaging Med. Surg.* **2024**, *14*, 5460–5472. https://doi.org/10.21037/qims-23-1028.
219. Peng, J.; Zhang, J.; Zou, D.; et al. Deep learning to estimate durable clinical benefit and prognosis from patients with non-small cell lung cancer treated with PD-1/PD-L1 blockade. *Front. Immunol.* **2022**, *13*, 960459. https://doi.org/10.3389/fimmu.2022.960459.
220. Zhang, X.; Zhang, G.; Qiu, X.; et al. Exploring non-invasive precision treatment in non-small cell lung cancer patients through deep learning radiomics across imaging features and molecular phenotypes. *Biomark. Res.* **2024**, *12*, 12. https://doi.org/10.1186/s40364-024-00561-5.
221. Hao, P.; Yu, Y.; Huang, C.T.; et al. Advancing EGFR mutation subtypes prediction in NSCLC by combining 3D pretrained ConvNeXt, radiomics, and clinical features. *Front. Oncol.* **2024**, *14*, 1464555. https://doi.org/10.3389/fonc.2024.1464555.
222. Gong, J.; Fu, F.; Ma, X.; et al. Hybrid deep multi-task learning radiomics approach for predicting EGFR mutation status of non-small cell lung cancer in CT images. *Phys. Med. Biol.* **2023**, *68*, 245021. https://doi.org/10.1088/1361-6560/ad0d43.
223. Wu, J.; Meng, H.; Zhou, L.; et al. Habitat radiomics and deep learning fusion nomogram to predict EGFR mutation status in stage I non-small cell lung cancer: A multicenter study. *Sci. Rep.* **2024**, *14*, 15877. https://doi.org/10.1038/s41598-024-66751-1.
224. Vanguri, R.S.; Luo, J.; Aukerman, A.T.; et al. Multimodal integration of radiology, pathology and genomics for prediction of response to PD-(L)1 blockade in patients with non-small cell lung cancer. *Nat. Cancer* **2022**, *3*, 1151–1164. https://doi.org/10.1038/s43018-022-00416-8.
225. Kim, S.; Lim, J.H.; Kim, C.H.; et al. Deep learning–radiomics integrated noninvasive detection of epidermal growth factor receptor mutations in non-small cell lung cancer patients. *Sci. Rep.* **2024**, *14*, 922. https://doi.org/10.1038/s41598-024-51630-6.
226. Huang, W.; Wang, J.; Wang, H.; et al. PET/CT Based EGFR Mutation Status Classification of NSCLC Using Deep Learning Features and Radiomics Features. *Front. Pharmacol.* **2022**, *13*, 898529. https://doi.org/10.3389/fphar.2022.898529.
227. Zuo, Y.; Liu, Q.; Li, N.; et al. Optimal ^{18}F-FDG PET/CT radiomics model development for predicting EGFR mutation status and prognosis in lung adenocarcinoma: A multicentric study. *Front. Oncol.* **2023**, *13*, 1173355. https://doi.org/10.3389/fonc.2023.1173355.
228. Zuo, Y.; Liu, Q.; Li, N.; et al. Explainable ^{18}F-FDG PET/CT radiomics model for predicting EGFR mutation status in lung adenocarcinoma: A two-center study. *J. Cancer Res. Clin. Oncol.* **2024**, *150*, 469. https://doi.org/10.1007/s00432-024-05998-7.
229. Lu, Y.; Liu, F.; Yu, Y.; et al. AI-enabled molecular phenotyping and prognostic predictions in lung cancer through multimodal clinical information integration. *Cell Rep. Med.* **2025**, *6*, 102216. https://doi.org/10.1016/j.xcrm.2025.102216.
230. Wang, C.; Ma, J.; Shao, J.; et al. Predicting EGFR and PD-L1 Status in NSCLC Patients Using Multitask AI System Based on CT Images. *Front. Immunol.* **2022**, *13*, 813072. https://doi.org/10.3389/fimmu.2022.813072.
231. Wang, X.Y.; Wu, S.H.; Ren, J.; et al. Predicting Gene Comutation of EGFR and TP53 by Radiomics and Deep Learning in Patients with Lung Adenocarcinomas. *J. Thorac. Imaging* **2025**, *40*, e0817. https://doi.org/10.1097/rti.0000000000000817.
232. Tan, X.; Li, Y.; Wang, S.; et al. Predicting EGFR mutation, ALK rearrangement, and uncommon EGFR mutation in NSCLC patients by driverless artificial intelligence: A cohort study. *Respir. Res.* **2022**, *23*, 132. https://doi.org/10.1186/s12931-022-02053-2.
233. Ji, Y.; Ge, R.; Meng, W.; et al. Enhanced prediction of gene mutation and risk stratification in non-small-cell lung cancer through dual-pathway fusion of radiomics and pathomics. *Front. Oncol.* **2025**, *15*, 1646851. https://doi.org/10.3389/fonc.2025.1646851.
234. Ai, X.; Jia, B.; He, Z.; et al. Noninvasive early identification of durable clinical benefit from immune checkpoint inhibition: A prospective multicenter study (NCT04566432). *Signal Transduct. Target. Ther.* **2024**, *9*, 350. https://doi.org/10.1038/s41392-024-02060-3.
235. Mitra, J.; Ghose, S.; Thawani, R. Clinically Explainable Prediction of Immunotherapy Response Integrating Radiomics and Clinico-Pathological Information in Non-Small Cell Lung Cancer. *Cancers* **2025**, *17*, 2679. https://doi.org/10.3390/cancers17162679.
236. Trivizakis, E.; Souglakos, J.; Karantanas, A.; et al. Deep Radiotranscriptomics of Non-Small Cell Lung Carcinoma for Assessing Molecular and Histology Subtypes with a Data-Driven Analysis. *Diagnostics* **2021**, *11*, 2383. https://doi.org/10.3390/diagnostics11122383.

237. Shao, J.; Ma, J.; Zhang, Q.; et al. Predicting gene mutation status via artificial intelligence technologies based on multimodal integration (MMI) to advance precision oncology. *Semin. Cancer Biol.* **2023**, *91*, 1–15 https://doi.org/10.1016/j.semcancer.2023.02.006.
238. Shao, J.; Ma, J.; Yu, Y.; et al. A multimodal integration pipeline for accurate diagnosis, pathogen identification, and prognosis prediction of pulmonary infections. *Innovation* **2024**, *5*, 100648. https://doi.org/10.1016/j.xinn.2024.100648.
239. Liu, Z.; Lin, G.; Yan, Z.; et al. Predictive mutation signature of immunotherapy benefits in NSCLC based on machine learning algorithms. *Front. Immunol.* **2022**, *13*, 989275. https://doi.org/10.3389/fimmu.2022.989275.
240. Shiri, I.; Maleki, H.; Hajianfar, G.; et al. Next-Generation Radiogenomics Sequencing for Prediction of EGFR and KRAS Mutation Status in NSCLC Patients Using Multimodal Imaging and Machine Learning Algorithms. *Mol. Imaging Biol.* **2020**, *22*, 1132–1148. https://doi.org/10.1007/s11307-020-01487-8.
241. Wang, B.; Bao, C.; Wang, X.; et al. Inter-equipment validation of PET-based radiomics for predicting EGFR mutation statuses in patients with non-small cell lung cancer. *Clin. Radiol.* **2024**, *79*, 571–578. https://doi.org/10.1016/j.crad.2023.12.030.
242. Yang, X.; Liu, M.; Ren, Y.; et al. Using contrast-enhanced CT and non-contrast-enhanced CT to predict EGFR mutation status in NSCLC patients—A radiomics nomogram analysis. *Eur. Radiol.* **2022**, *32*, 2693–2703. https://doi.org/10.1007/s00330-021-08366-y.
243. Liu, H.; Shu, P.; Zhao, L.; et al. Machine learning approaches for EGFR mutation status prediction in NSCLC: An updated systematic review. *Front. Oncol.* **2025**, *15*, 1576461. https://doi.org/10.3389/fonc.2025.1576461.
244. Li, B.; Su, J.; Liu, K.; et al. Deep learning radiomics model based on PET/CT predicts PD-L1 expression in non-small cell lung cancer. *Eur. J. Radiol. Open* **2024**, *12*, 100549. https://doi.org/10.1016/j.ejro.2024.100549.
245. Yamazaki, M.; Yagi, T.; Tominaga, M.; et al. Role of intratumoral and peritumoral CT radiomics for the prediction of EGFR gene mutation in primary lung cancer. *Br. J. Radiol.* **2022**, *95*, 20220374. https://doi.org/10.1259/bjr.20220374.
246. Cheng, Y.; Wang, H.; Yuan, W.; et al. Combined radiomics of primary tumour and bone metastasis improve the prediction of EGFR mutation status and response to EGFR-TKI therapy for NSCLC. *Phys. Med.* **2023**, *116*, 103177. https://doi.org/10.1016/j.ejmp.2023.103177.
247. Rinaldi, L.; Guerini Rocco, E.; Spitaleri, G.; et al. Association between Contrast-Enhanced Computed Tomography Radiomic Features, Genomic Alterations and Prognosis in Advanced Lung Adenocarcinoma Patients. *Cancers* **2023**, *15*, 4553. https://doi.org/10.3390/cancers15184553.
248. Yang, Y.; Yang, J.; Liang, Y.; et al. Identification and Validation of Efficacy of Immunological Therapy for Lung Cancer from Histopathological Images Based on Deep Learning. *Front. Genet.* **2021**, *12*, 642981. https://doi.org/10.3389/fgene.2021.642981.
249. Hashimoto, K.; Murakami, Y.; Omura, K.; et al. Prediction of Tumor PD-L1 Expression in Resectable Non-Small Cell Lung Cancer by Machine Learning Models Based on Clinical and Radiological Features: Performance Comparison with Preoperative Biopsy. *Clin. Lung Cancer* **2024**, *25*, e26–e34.e6. https://doi.org/10.1016/j.cllc.2023.08.010.
250. Chen, L.; Chen, L.; Ni, H.; et al. Prediction of CD3 T cells and CD8 T cells expression levels in non-small cell lung cancer based on radiomic features of CT images. *Front. Oncol.* **2023**, *13*, 1104316. https://doi.org/10.3389/fonc.2023.1104316.
251. Fuster-Matanzo, A.; Picó-Peris, A.; Bellvís-Bataller, F.; et al. Prediction of oncogene mutation status in non-small cell lung cancer: A systematic review and meta-analysis with a special focus on artificial intelligence-based methods. *Eur. Radiol.* **2026**, *36*, 2157–2185. https://doi.org/10.1007/s00330-025-11962-x.
252. Parra-Medina, R.; Guerron-Gomez, G.; Mendivelso-González, D.; et al. Deep learning in histopathology images for prediction of oncogenic driver molecular alterations in lung cancer: A systematic review and meta-analysis. *Transl. Lung Cancer Res.* **2025**, *14*, 1756–1769. https://doi.org/10.21037/tlcr-2024-1196.
253. Zheng, T.; Li, X.; Zhou, L.; et al. Predictive value of machine learning for PD-L1 expression in NSCLC: A systematic review and meta-analysis. *World J. Surg. Oncol.* **2025**, *23*, 199. https://doi.org/10.1186/s12957-025-03847-6.
254. Wang, T.W.; Hsu, M.S.; Lin, Y.H.; et al. Application of Radiomics in Prognosing Lung Cancer Treated with Epidermal Growth Factor Receptor Tyrosine Kinase Inhibitors: A Systematic Review and Meta-Analysis. *Cancers* **2023**, *15*, 3542. https://doi.org/10.3390/cancers15143542.
255. Singhal, K.; Azizi, S.; Tu, T.; et al. Large language models encode clinical knowledge. *Nature* **2023**, *620*, 172–180. Correction in: *Nature* **2023**, *620*, E19. https://doi.org/10.1038/s41586-023-06291-2.
256. Jee, J.; Fong, C.; Pichotta, K.; et al. Automated real-world data integration improves cancer outcome prediction. *Nature* **2024**, *636*, 728–736. https://doi.org/10.1038/s41586-024-08167-5.
257. Park, H.J.; Huh, J.Y.; Chae, G.; et al. Extraction of clinical data on major pulmonary diseases from unstructured radiologic reports using a large language model. *PLoS ONE* **2024**, *19*, e0314136. https://doi.org/10.1371/journal.pone.0314136.